U.S. Department
of Commerce

Volume 121
Number 4
October 2023

# Fishery Bulletin

Pacific Islands Fisheries
Science Center Library

Received on: 3/24

**U.S. Department of Commerce**

Gina M. Raimondo
Secretary

**National Oceanic and Atmospheric Administration**

Richard W. Spinrad
Administrator

**National Marine Fisheries Service**

Janet Coit
Assistant Administrator
for Fisheries

# Fishery Bulletin

**Scientific Editor**
José I. Castro
National Marine Fisheries Service, NOAA
263 13th Avenue South
Saint Petersburg, Florida 33701

**Managing Editor**
Kathryn Dennis
Scientific Publications Office
National Marine Fisheries Service, NOAA
1845 Wasp Boulevard, Building 176
Honolulu, Hawaii 96818

**Associate Editor**
Cara Mayo
Scientific Publications Office
National Marine Fisheries Service, NOAA
7600 Sand Point Way NE
Seattle, Washington 98115-0070

**Editorial Board**

| | |
|---|---|
| Henry L. Bart Jr. | Tulane University, New Orleans, Louisiana |
| Katherine E. Bemis | National Systematics Laboratory, Washington, DC |
| Matthew D. Campbell | National Marine Fisheries Service, Pascagoula, Mississippi |
| William B. Driggers III | National Marine Fisheries Service, Pascagoula, Mississippi |
| Gretchen L. Grammer | South Australian Research and Development Institute, Adelaide, Australia |
| Richard Langton | National Marine Fisheries Service, Walpole, Maine (retired) |
| J. Fernando Márquez-Farías | Universidad Autónoma de Sinaloa, Mazatlán, México |
| Richard S. McBride | National Marine Fisheries Service, Woods Hole, Massachusetts |
| Richard L. Merrick | National Marine Fisheries Service, Falmouth, Massachusetts (retired) |
| Richard D. Methot | National Marine Fisheries Service, Seattle, Washington |
| Lisa J. Natanson | National Marine Fisheries Service, Narragansett, Rhode Island (retired) |
| Mark S. Peterson | University of Southern Mississippi, Ocean Springs, Mississippi |
| André E. Punt | University of Washington, Seattle, Washington |
| Joseph M. Quattro | University of South Carolina, Columbia, South Carolina |
| John F. Walter III | National Marine Fisheries Service, Miami, Florida |

***Fishery Bulletin* website: https://spo.nmfs.noaa.gov/fb.htm**

*Fishery Bulletin* (ISSN 0090-0656) is published quarterly by the Scientific Publications Office, National Marine Fisheries Service, NOAA, 7600 Sand Point Way NE, Seattle, WA 98115-0070.

Although the contents of this publication have not been copyrighted and may be reprinted entirely, reference to source is appreciated.

The Secretary of Commerce has determined that the publication of this periodical is necessary according to law for the transaction of public business of this Department. Use of funds for printing of this periodical has been approved by the Director of the Office of Management and Budget.

**For Sale** by the Superintendent of Documents, U.S. Government Publishing Office, Washington, DC 20401. Subscription price per year: $32.00 domestic and $44.80 foreign. Cost per single issue: $19.00 domestic and $26.60 foreign. **See back for order form.**

*Fishery Bulletin* carries original research reports on investigations in fishery science, engineering, and economics. It began as the Bulletin of the United States Fish Commission in 1881; it became the Bulletin of the Bureau of Fisheries in 1904 and the *Fishery Bulletin* of the U.S. Fish and Wildlife Service in 1941. Separates were issued as documents through volume 46; the last document was no. 1103. Beginning with volume 47 in 1931 and continuing through volume 62 in 1963, each separate appeared as a numbered bulletin. A new system began in 1963, with volume 63, in which papers are bound together in a single issue. Beginning with volume 70, number 1, January 1972, *Fishery Bulletin* became a periodical, issued quarterly. In this form, it is available by subscription from the Superintendent of Documents, U.S. Government Publishing Office, Washington, DC 20401. It is also available free in limited numbers to libraries, research institutions, and state and federal agencies and in exchange for other scientific publications.

**U.S. Department of Commerce**
Seattle, Washington

**Volume 121**
**Number 4**
**October 2023**

# Fishery Bulletin

## Contents

### *Articles*

145–160 **Lisa J. Natanson, Camilla T. McCandless, and Nancy E. Kohler**

Distribution of the tiger shark (*Galeocerdo cuvier*) in the North Atlantic Ocean by season, sex, and life stage, based on tag and recapture data

161–171 **Jason E. Kahn, Christian H. Hager, D. Kyle Breault, and J. Carter Watterson**

Arrival and departure windows of Atlantic sturgeon (*Acipenser oxyrinchus oxyrinchus*) in Chesapeake Bay in Virginia

172–187 **Brittany D. Schwartzkopf, Emmanis Dorval, Dianna L. Porzio, Jonathan M. Walker, Kelsey C. James, and Brad E. Erisman**

Modeling somatic and otolith growth of the central subpopulation of northern anchovy (*Engraulis mordax*) by incorporating seasonality

188–198 **Benjamin Frey, Vyacheslav Lyubchich, Michelle Zapp Sluis, Nathaniel Miller, and David Secor**

Examining the periodicity of annular deposition of otolith microconstituents as a means of age validation

199–213 **Thomas E. Laidig and Diana L. Watters**

Distribution, abundance, and habitat associations of young of the year of rockfish species (*Sebastes* spp.) in deep waters along the central coast of California

214 **Acknowledgment of reviewers**

215–218 **Guidelines for authors**

The National Marine Fisheries Service (NMFS) does not approve, recommend, or endorse any proprietary product or proprietary material mentioned in this publication. No reference shall be made to NMFS, or to this publication furnished by NMFS, in any advertising or sales promotion that would indicate or imply that NMFS approves, recommends, or endorses any proprietary product or proprietary material mentioned herein or that has as its purpose an intent to cause directly or indirectly the advertised product to be used or purchased because of this NMFS publication.

The NMFS Scientific Publications Office is not responsible for the contents of the articles.

Digitized by the Internet Archive
in 2025

https://archive.org/details/fishery-bulletin_2023-10_121_4

National Marine Fisheries Service
NOAA

*Fishery Bulletin*
established in 1881

Spencer F. Baird
First U.S. Commissioner of Fisheries and founder of *Fishery Bulletin*

# Distribution of the tiger shark (*Galeocerdo cuvier*) in the North Atlantic Ocean by season, sex, and life stage, based on tag and recapture data

**Lisa J. Natanson (retired) (contact author)**
**Camilla T. McCandless**
**Nancy E. Kohler (retired)**

Email address for contact author: mangrules@yahoo.ca

Northeast Fisheries Science Center
National Marine Fisheries Service, NOAA
28 Tarzwell Drive
Narragansett, Rhode Island 02882

**Abstract**—Movements of the tiger shark (*Galeocerdo cuvier*) by life stage are largely unknown yet are necessary to determine essential fish habitat and sustainable fishery management practices. In an effort to elucidate distribution and movements of the tiger shark, we analyzed fishery-dependent and -independent tag (sample size [*n*]=10,516) and recapture (*n*=762) records for sharks caught in the North Atlantic Ocean during 1963–2018. Seasonal distribution of the tiger shark was examined by life stage—young of the year, juveniles (immature), and adults (mature)—and distribution patterns were used to identify potential nursery habitat. Tiger sharks were caught over a wide area from the Grand Banks of Newfoundland, Canada, south to Brazil and from coastal to offshore waters and into the eastern North Atlantic Ocean. Seasonal north–south movements were observed in all life stages, and 14 immature sharks were found to have migrated from the western to the eastern North Atlantic Ocean. A broad nursery area and a potential birthing area were identified on the continental shelf between Florida and Georgia on the basis of the repeated presence of neonates in summer across years and of the recapture of multiple tagged young-of-the-year sharks from the same location over a period of at least 2 years.

Manuscript submitted 18 June 2023.
Manuscript accepted 21 September 2023.
Fish. Bull. 121:145–160 (2023).
Online publication date: 11 October 2023.
doi: 10.7755/FB.121.4.1

The views and opinions expressed or implied in this article are those of the author (or authors) and do not necessarily reflect the position of the National Marine Fisheries Service, NOAA.

The tiger shark (*Galeocerdo cuvier*) is a wide-ranging, globally distributed predator found in tropical and warm temperate waters (Bigelow and Schroeder, 1948). Tiger sharks make extensive migrations in many parts of the world, and the range of this species is considered both coastal and oceanic (Heithaus et al., 2007; Ferreira et al., 2015). In the western North Atlantic Ocean (WNA), the tiger shark is known to undertake seasonal inshore–offshore movements in the Gulf of Mexico (GOM) and seasonal north–south movements along the East Coast of the United States (Lea et al., 2015; Ajemian et al., 2020). Evidence also exists for basin-wide migrations in the North Atlantic Ocean (Kohler et al., 1998; Kohler and Turner, 2019). Tiger sharks have been found in water temperatures ranging from 4.0°C to 34°C (Afonso and Hazin, 2015; Hammerschlag et al., 2022), but in the WNA they seem to prefer water temperatures between 26°C and 28°C, regardless of season (Hammerschlag et al., 2022). Because of its broad distribution, this species occurs in the waters of many countries and crosses numerous management boundaries. Therefore, understanding the movements of tiger sharks in general, and by life stage, is important to international management.

Tiger sharks are caught in commercial and recreational fisheries throughout the North Atlantic Ocean (Natanson et al., 1999; Domingo et al., 2016). The tiger shark is currently listed on the IUCN Red List of Threatened Species as near threatened globally (Ferreira and Simpfendorfer, 2019). However, in the North Atlantic Ocean, shark vulnerability to pelagic longline gear has been estimated to be low to moderate on the basis of an ecological risk assessment based on the species' productivity and susceptibility to the gear (Cortés et al., 2015). Furthermore, increases in tiger shark abundance in the WNA have been documented since the early 1990s, a trend attributable to the implementation of the National Marine Fisheries Service (NMFS) Shark Management Plan in 1993 (Carlson et al., 2012; Peterson et al., 2017).

Life history studies of tiger sharks have expanded in recent years. Results of the most recent study on growth dynamics, in which ages validated with bomb radiocarbon techniques were used, indicate a longevity of 27–29 years and an age at maturity of 10 years for both sexes (Kneebone et al., 2008). Updated reproductive parameters corroborated these estimates, indicating a size and age at median maturity of

258.9 cm in fork length (FL) and 9.5 years for males and of 261.4 cm FL and 11.6 years for females (Natanson et al., 2023). Tiger sharks are well known as generalist predators (Lowe et al., 1996), and they have a high trophic level indicative of a top predator (Cortés, 1999). They are considered an important component of the trophic structure for reef systems and other coastal habitats (Heithaus, 2001; Ruppert et al., 2013), and results of studies indicate that ontogenetic shifts in their diet may partly result from sharks of different sizes or sharks in different life stages occupying different habitats (Lowe et al., 1996; Aines et al., 2018).

Movement and migration information on the tiger shark is limited to discrete studies in which high-technology tagging methods were used with limited numbers of satellite or acoustic tags. The results of these studies indicate that seasonal migrations to higher latitudes are common and that, although there are resident individuals, migrations over long distances are also undertaken (Sulikowski et al., 2016; McClain et al., 2022). In some studies, longer migrations have been attributed to males (Lea et al., 2015), but more recent data indicate that they are undertaken by both sexes (McClain et al., 2022) and are likely related to foraging, especially in relation to turtle nesting sites (Fitzpatrick et al., 2012), temperature (Papastamatiou et al., 2013; Lea et al., 2018; Hammerschlag et al., 2022), or important habitats related to life stage (e.g., birthing and nursery areas) (Meyer et al., 2018). Data from these types of studies, however, are limited by the number of tagged individuals and a lack of representation by all life stages, and such data may not provide a complete picture of movements for the species (Meyer et al., 2018; Sequeira et al., 2019).

In this study, we used updated reproductive parameters (Natanson et al., 2023) in conjunction with conventional tagging data to examine the demographic characteristics of the population of tiger sharks in the North Atlantic Ocean. Specifically, we looked at potential variation in spatial and seasonal distributions and migrations by sex and life stage, young of the year (YOY), juveniles (immature), and adults (mature). We also examined locations of mature females and neonate individuals (<66.2*[1] cm FL) from March through August by using estimated time and size of birth (Castro, 2011) to identify possible areas of parturition and by using the distribution of YOY to identify potential nursery areas for the tiger shark. Information on movements by life stage can be used in management to understand essential fish habitat and to help define protected areas or other approaches to protect vulnerable portions of the population.

## Materials and methods

### Mark and recapture

Tag and recapture data from the NMFS Cooperative Shark Tagging Program (CSTP), for the period 1963–2018, were used with published maturity estimates (Natanson et al., 2023) to investigate distribution and movements of tiger sharks by sex and life stage. Tiger sharks were tagged by cooperating commercial and recreational fishermen, scientists, and fisheries observers. Tagging methods and quality control have remained consistent since the inception of the CSTP and are detailed in Casey and Kohler (1992) and Kohler and Turner (2019). Distances between release and recapture locations are expressed in straight-line nautical miles (nmi). Tag and recapture data were reported in FL, total length (TL), or weight (WT) and as measured or estimated. Lengths are presented in centimeters, and weights are provided in kilograms. All tagging and recapture data were converted to $FL_{OTB}$ (i.e., from the tip of the snout to the fork in the tail, over the body [OTB]) by using the I-MARK web application (Kohler and Turner, 2019) and conversions from Kohler et al. (1996). Published straight-line TL ($TL_{STR}$) data were converted to $FL_{OTB}$ (these converted values are indicated with asterisks) by using the conversion from Natanson et al. (2022):

$$TL_{STR} = 11.90 + 1.18(FL_{OTB}),$$

coefficient of determination $[r^2]$=0.996, $n$=605.

Unless otherwise noted, all lengths are presented in $FL_{OTB}$.

### Demographic structure

To investigate the spatial distribution of the population, tiger shark catch records of tagging and recapture events were divided into subsets by sex and life stage, where possible. Classification into stages was done by length. Sharks ≤106 cm FL were considered YOY (Natanson et al., 1999), sharks >106 cm FL and less than the median size at maturity by sex (258.9 and 261.4 cm FL, for males and females, respectively; Natanson et al., 2023) were classified as juveniles (immature), and sharks greater than or equal to the median size at maturity were classified as adults (mature). For sharks for which no sex was recorded, maturity status was determined by using the more conservative, larger, female size at maturity. Additionally, locations at which sharks ≤66.2 cm FL (neonates) were caught from May through August were examined as possible locations of birthing areas on the basis of an extension of the timing of parturition from Castro (2011) (June and July) to account for early and late parturition. The length at birth was based on the range (57.7*–66.2* cm FL) provided by Castro (2011) with the assumption that any free-living shark <66.2 cm FL had just been born. A chi-square test was used to determine if there was a significant difference between the sample sizes of females and males in the tagging data.

To visualize potential variation in the spatial distribution of the life stages of tiger sharks, catch locations by sex, life stage, and season were mapped by using R (vers. 4.1.3; R Core Team, 2022). Seasons were defined as winter (December–February), spring (March–May), summer (June–August), and fall (September–November). The

[1] An asterisk (*) after a size value denotes a fork length that has been converted from a total length.

distribution of catch records for neonates, adult females, and YOY were examined for patterns related to birthing and nursery areas.

## Results

### Tagging and recapture

Tiger sharks ($n$=10,516) were tagged in coastal waters throughout the continental shelf in the WNA from the Grand Banks of Newfoundland, Canada, south to Brazil and in offshore waters (past the 200-m depth contour) to 40°W (Table 1, Fig. 1). The majority of tags ($n$=9211) were deployed along the East Coast of the United States from Cape Hatteras, North Carolina, down and into the U.S. waters of the GOM. Sharks tagged were primarily captured on longline gear (80.8%) during commercial (32.7%) or scientific (33.2%) fishing operations or by fisheries observers (17.0%), followed by recreational anglers using rod and reel (17.0%). All industries fished in the same general locations, although spatial effort varied between them (Table 1, Fig. 1). Recreational anglers, in general, fished closer to shore, and commercial and scientific operations fished both inshore and offshore, particularly between northeastern Florida and north of Cape Hatteras (Table 1). Commercial effort was primarily focused on the east coast of Florida, and the bulk of the scientific effort was evenly distributed along the coast from Cape Hatteras to the Florida Keys. Observer coverage was highest from Cape Hatteras to the border of Florida and Georgia, and although recreational fishing was highest north of Cape Hatteras, it was fairly evenly distributed south of the cape and into the GOM but very limited in the Caribbean Sea and the Bahamas (Table 1).

Sharks were captured in all months of the year. Lengths of tagged tiger sharks encompassed the entire size range of the species (from birth to 391.0* cm FL; Bigelow and Schroeder, 1948), with a range of 40.1–457.2 cm FL for both sexes combined and a mean of 120.2 cm FL (standard deviation [SD] 51.1) and 134.7 cm FL (SD 60.4) for males and females, respectively (Fig. 2A). The lengths of 5 individuals were greater than the published maximum size, but because these lengths were estimated, none can be considered a definitive new maximum size; 3 of these sharks were females, and 2 of them were of unknown sex. Although caution should be exercised in taking these values as a new maximum size for tiger sharks, the sharks would be classified as mature, and, for that reason, these lengths were included in our analyses. Of those tagged sharks for which sex was reported, the proportions of females (57.3%) and males (42.7%) were significantly different from the expected ratio of 1:1 ($X^2(1, n=9419)=200.14$, $P<0.05$).

A total of 762 tiger shark recapture events were reported between 1967 and 2018 throughout the North Atlantic Ocean (Fig. 3), with an overall recapture rate of 7.2%. Of these, 35 individuals were recaptured multiple times (3 sharks were recaptured twice, and 2 sharks were recaptured 3 times). For 13 recaptured sharks, no information was turned in at tagging and their tag data could not be used for movement analysis. In all but 5 cases, sex was reported the same at both tagging and recapture. Sex was reported as unknown at recapture for 2 of those exceptions, and sex was reported unknown at tagging for the other 3 cases. Similar to the proportions

**Table 1**

The numbers of tagged tiger sharks (*Galeocerdo cuvier*) from the western North Atlantic Ocean caught between 1963 and 2018 by area tagged for each sex, life stage, and tagger industry. Also provided is the percentage of tagged fish that were mature for each sex. Tagged sharks were classified into 3 life stages: young of the year (YOY), juveniles (immature [IMM]), or adults (mature [MAT]). The tagger industries include commercial (COM) and scientific (SCI) fishing operations, fisheries observers (OBS), and recreational anglers (REC). The latitudinal borders of the tagging areas are as follows (in decimal degrees): north of Cape Hatteras (35.2500–45.5833°N), from Cape Hatteras to Florida (35.2499–30.7167°N), east coast of Florida (30.7168–25.3400°N), west coast of Florida (25.3401–30.2600°N), rest of the Gulf of Mexico (GOM, 302601–21.0333°N), Caribbean Sea (15.5667–21.3000°N), and the Bahamas and adjacent waters (13.0000–25.0833°N). The total number of sharks tagged includes those of unknown sex or maturity and 2 fish caught outside the location parameters.

| | | Females | | | | Males | | | | Tagger industry | | | |
|---|---|---|---|---|---|---|---|---|---|---|---|---|---|
| Area | Total no. tagged | YOY | IMM | MAT | % MAT | YOY | IMM | MAT | % MAT | COM | SCI | OBS | REC |
| North of Cape Hatteras | 1318 | 141 | 398 | 23 | 4.1 | 81 | 209 | 22 | 7.0 | 160 | 164 | 131 | 859 |
| Cape Hatteras to Florida | 3066 | 787 | 727 | 73 | 4.6 | 668 | 506 | 39 | 3.2 | 298 | 1424 | 1062 | 282 |
| Florida East Coast | 4692 | 1258 | 1125 | 95 | 3.8 | 1226 | 762 | 35 | 1.7 | 2808 | 1422 | 273 | 185 |
| Florida West Coast | 677 | 94 | 225 | 23 | 6.7 | 102 | 143 | 8 | 3.2 | 80 | 109 | 270 | 217 |
| Rest of GOM | 419 | 33 | 182 | 9 | 4.0 | 26 | 87 | 10 | 8.1 | 25 | 109 | 49 | 232 |
| Caribbean Sea | 113 | 3 | 41 | 11 | 20.0 | 4 | 28 | 5 | 13.5 | 44 | 64 | 1 | 4 |
| Bahamas and adjacent waters | 229 | 1 | 112 | 27 | 19.3 | 2 | 36 | 20 | 34.5 | 29 | 194 | 0 | 6 |
| Total | 10,516 | 2317 | 2810 | 262 | 4.9 | 2109 | 1771 | 139 | 3.5 | 3444 | 3486 | 1786 | 1785 |

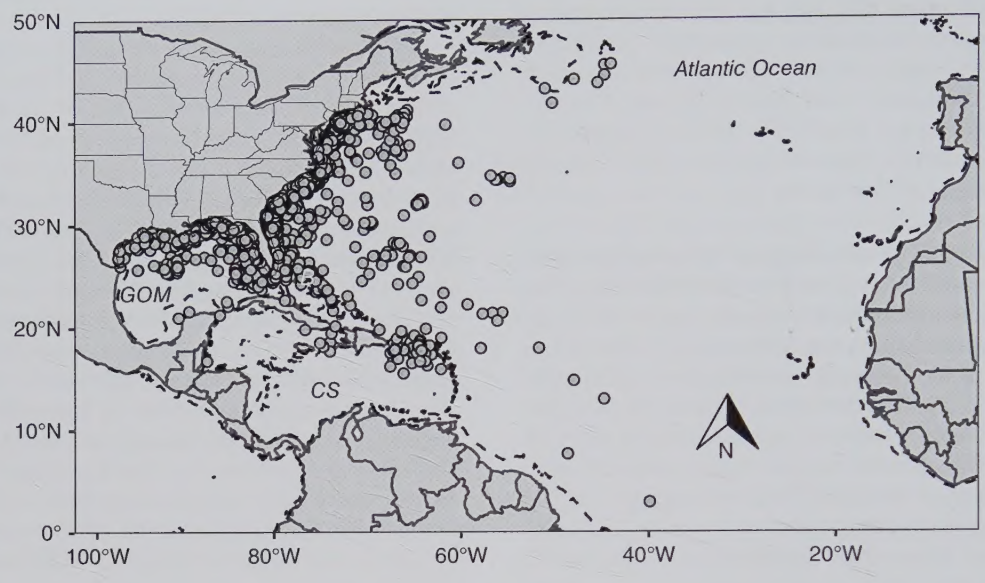


**Figure 1**

Map showing the distribution of all tiger sharks (*Galeocerdo cuvier*) tagged in the western North Atlantic Ocean by participants in the Cooperative Shark Tagging Program of the National Marine Fisheries Service between 1963 and 2018. Circles indicate locations where sharks were tagged. The dashed black line indicates the 200-m contour. GOM=Gulf of Mexico; CS=Caribbean Sea.

of tagged sharks, recaptured females (56.2%) outnumbered recaptured males (43.8%) for sharks for which sex was reported at recapture ($n$=714). Sizes of recaptured tiger sharks ranged from 66.0 to 373.0 cm FL with a mean of 142.8 cm FL (SD 50.4) and 154.7 cm FL (SD 56.6) for males and females, respectively (Fig. 2B), nearly representing the entire size range of this species. Commercial fishermen (69.3%) recaptured the majority of tiger sharks, followed by recreational anglers (18.0%), biologists (5.8%), fisheries observers (4.5%), unknown (2.4%), and educators (<1%). The majority of sharks recaptured were caught on longline gear (75.7%) during commercial fishing operations.

The range of overall time at liberty for tiger sharks was 0.0–13.4 years with a mean of 1.0 year (SD 1.4). Most sharks were at liberty less than a year (71.8%). Time at liberty varied depending on life stage, with mature males having a higher mean time at liberty (5.7 years [SD 3.9]) than the means for males at all other maturity stages (Table 2). Distance between tagging and recapture locations ranged from 0 to 3643 nmi with a mean of 243.2 nmi (SD 449.5). Although mean distance between tagging and recapture locations was higher for mature sharks of both sexes, immature fish had higher maximum distances (Table 2).

Recapture locations were concentrated close to the coast between Long Island, New York, and Florida, into the U.S. portion of the GOM. Additional recapture events occurred along the coast of Mexico in the GOM into the Caribbean Sea and south to Brazil. North of Long Island, sharks were recaptured farther offshore. The northernmost recapture was on the Grand Banks of Newfoundland, and the easternmost recapture was in the coastal waters of Guinea-Bissau, a country in West Africa (Fig. 3).

Tiger sharks transited throughout the WNA, including the GOM and Caribbean Sea (Fig. 3). A total of 37 sharks crossed between these water bodies. The majority of these individuals moved from the main body of the Atlantic Ocean into either the GOM ($n$=11) or the Caribbean Sea ($n$=14). Movement was also seen from the GOM into both the main body of the Atlantic Ocean ($n$=5) and the Caribbean Sea ($n$=5) and from the Caribbean Sea into both the main body of the Atlantic Ocean ($n$=1) and the GOM ($n$=1).

A total of 116 sharks, of both sexes, traveled more than 500 nmi; of these, 115 individuals had length data at tagging and 109 individuals had length data at both tagging and recapture. The majority of tiger sharks that travelled over 500 nmi were immature (82%, 84% including YOY), reflecting the prevalence of this life stage in the tagging data (Table 2). Even though adults account for only 5% of the total recapture events, this life stage had the greatest percentage of recaptured sharks that travelled over 500 nmi. (Table 2). Of those sharks that travelled >500 nmi, 23 individuals were tagged when YOY, 88 sharks were tagged when immature, and 4 fish were tagged when mature. Six fish were immature at tagging and mature at recapture. Two female tiger sharks recaptured in 1995 had traveled from the East Coast (off Frying Pan Shoals in North Carolina and off St. Augustine, Florida) across the middle of the Atlantic Ocean (45°W). One of these females, immature at both tagging and recapture, traveled to 41.5°W and was recaptured after 571 d at liberty. The other female was a YOY at tagging and still immature when recaptured

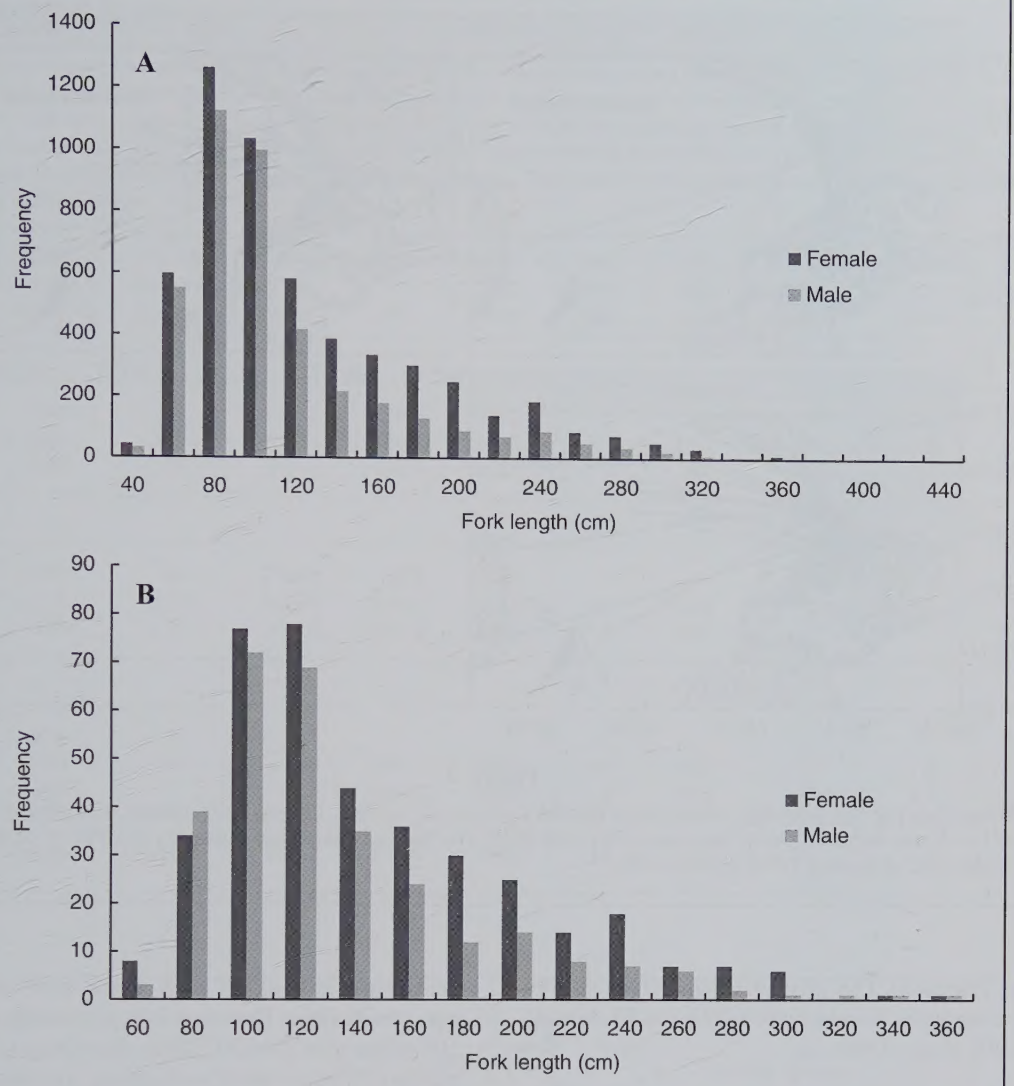


**Figure 2**

Size–frequency histograms for (**A**) tagged and (**B**) recaptured tiger sharks (*Galeocerdo cuvier*) from the North Atlantic Ocean for the period between 1963 and 2018.

off the coast of Guinea-Bissau at 17.5°W; the transit of this shark remains the longest distance traveled to date for a tiger shark in the CSTP (3643 nmi; Kohler and Turner, 2019) (Fig. 4). Since 1995, an additional 12 individuals that had been tagged in the coastal waters of the WNA have been reported to have been recaptured in the eastern North Atlantic (ENA). These sharks were all immature at tagging and recapture and consisted of 6 females, 5 males, and 1 individual of unknown sex (Fig. 4).

All of the 35 tiger sharks that were recaptured multiple times were immature at tagging and final recapture (Table 3). Twenty-two (63%) of these sharks were originally tagged as YOY. Multiple mark-recapture records indicate that individual tiger sharks tagged and recaptured as YOY, and up to 124 cm FL, were recaptured in the vicinity of their tagging location for up to 3 months and/or returned to the area where they were tagged for up to 2 years (Table 3). The continental shelf off northern Florida was used by YOY each month of the year. Several of the immature sharks also made long-distance movements; for example, a 91-cm-FL male was tagged off northern Florida in November, recaptured there the following May, and recaptured again in December nearly 1400 nmi away in the Caribbean Sea off Venezuela (Table 3). A 134-cm-FL female was tagged and recaptured off North Carolina in September of the same year and was recaptured again 2 years later east of the Mid-Atlantic Ridge (>2300 nmi away). Only 1 shark was recaptured multiple times in the GOM, a 156-cm-FL female at tagging that used the northeastern GOM over

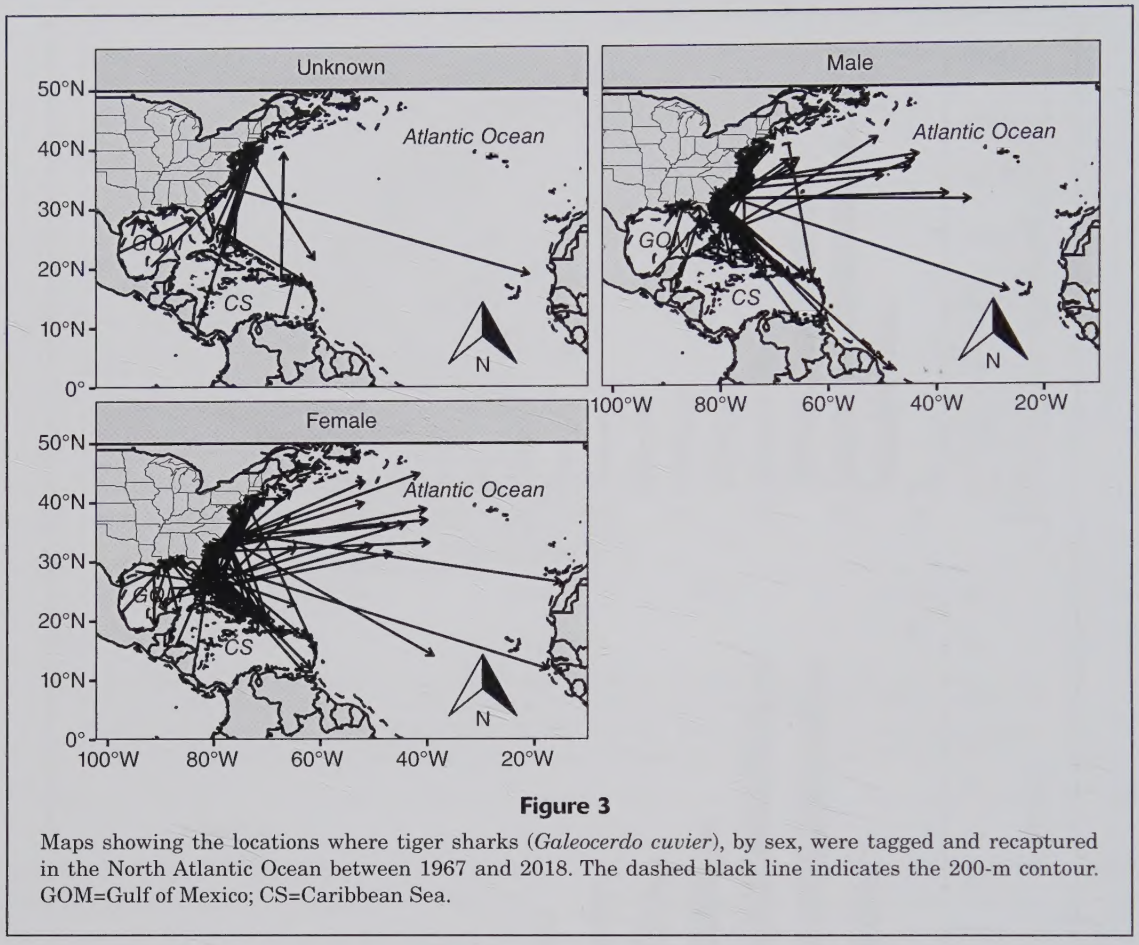


**Figure 3**

Maps showing the locations where tiger sharks (*Galeocerdo cuvier*), by sex, were tagged and recaptured in the North Atlantic Ocean between 1967 and 2018. The dashed black line indicates the 200-m contour. GOM=Gulf of Mexico; CS=Caribbean Sea.

multiple years (Table 3). The largest tagged tiger sharks with multiple recapture events were a 214-cm-FL female and a 223-cm-FL male (Table 3).

### Demographic structure

Females with length information ($n$=5797), based on combined tag and recapture data, ranged in size from 48.0 to 457.2 cm FL. Of these, 284 females were classified as mature. Males with length information ($n$=4336) ranged in size from 41.8 to 373.0 cm FL. Of these, 153 males were considered mature. Sharks of unknown sex with length data ($n$=1132) ranged in size from 40.1 to 457.2 cm FL. Of these, 107 individuals were classified as mature. All of these samples were used in combined sex analyses.

**Life stage—immature** Across both sexes, 95.2% of the specimens ($n$=11,221, tagged and recaptured combined) were classified as a juvenile tiger shark ($n$=9654, including YOY); of these, immature females (56.9%) outnumbered immature males (43.1%) overall and in all seasons. Individuals of both sexes were found in the same general areas, although 2 immature males were caught off Brazil, the southernmost extent of where our data were collected, 311.6 nmi farther south than any female was caught (Figs. 5 and 6). Immature animals of both sexes were caught in all seasons from Cape Hatteras into the GOM and down in the Bahamas and the Caribbean Sea (Suppl. Figs. 1A and 2A) (online only). In winter and spring, immature individuals of both sexes were found concentrated in these areas, but in summer and fall, immature sharks ranged farther north and east, with females traveling up to Nova Scotia, Canada, and males moving up to Massachusetts.

**Life stage—mature** Adult females ($n$=284) outnumbered adult males ($n$=151) in all seasons, except in summer, although the largest difference was in spring. Mature fish of both sexes overlapped the range of immature fish; however, mature females had a slightly different seasonal distribution than mature males (Suppl. Figs. 1B and 2B) (online only). In fall, mature males were found up to Cape Hatteras, and mature females were found as far north as Long Island and slightly offshore. In winter, mature females were found as far north as North Carolina, and mature males were found only in the GOM and south. In spring and summer, mature fish of both sexes shared approximately the same range.

**Life stage—young of the year** The majority of YOY ($n$=4606) were encountered between the U.S. waters of the GOM and Long Island, although they were found as

**Table 2**

Summary of tag and recapture data by life stage for tiger sharks (*Galeocerdo cuvier*) from the western North Atlantic Ocean caught between 1963 and 2018. Tagged sharks were classified into 3 life stages: young of the year (YOY), juveniles (immature), or adults (mature). Mean distances traveled and times at liberty are provided with standard deviations (SDs) and maximum values. Other values include the number and percentage of tagged fish that traveled >500 nautical miles (nmi) and the number of tagged fish that crossed from the western to the eastern North Atlantic Ocean. The asterisk (*) indicates that this shark was tagged as a YOY and recaptured as a juvenile.

| Life stage | No. of sharks tagged | No. of recapture events | Distance travelled (nmi) | | | No. >500 nmi | % >500 nmi | No. that crossed Atlantic | Time at liberty (years) | | |
|---|---|---|---|---|---|---|---|---|---|---|---|
| | | | Mean | SD | Max | | | | Mean | SD | Max |
| Females | | | | | | | | | | | |
| YOY | 2317 | 64 | 72.7 | 176.6 | 1282 | 2 | 3.1 | 1* | 0.3 | 0.2 | 0.8 |
| Juveniles | 2810 | 300 | 266.4 | 480.1 | 3643 | 56 | 18.7 | 7 | 1.0 | 1.3 | 8.2 |
| Adults | 262 | 22 | 300.0 | 424.7 | 1556 | 5 | 22.7 | 0 | 2.2 | 2.1 | 8.0 |
| Males | | | | | | | | | | | |
| YOY | 2109 | 61 | 60.2 | 88.1 | 494 | 0 | | 0 | 0.2 | 0.2 | 1.3 |
| Juveniles | 1772 | 222 | 234.9 | 442.4 | 3018 | 30 | 13.5 | 5 | 0.8 | 1.0 | 6.0 |
| Adults | 138 | 12 | 525.3 | 533.6 | 1690 | 5 | 41.7 | 0 | 5.7 | 3.9 | 13.4 |
| Unknown | | | | | | | | | | | |
| YOY | 214 | 0 | | | | 0 | | 0 | | | |
| Juveniles | 769 | 42 | 431.6 | 630.4 | 3089 | 9 | 21.4 | 1 | 1.0 | 1.0 | 4.4 |
| Adults | 102 | 5 | 781.4 | 615.0 | 1623 | 3 | 60.0 | 0 | 3.1 | 2.8 | 7.5 |
| Total | 10,493 | 728 | 243.2 | 449.5 | 3643 | 116 | 15.9 | 14 | 1.0 | 1.4 | 13.4 |

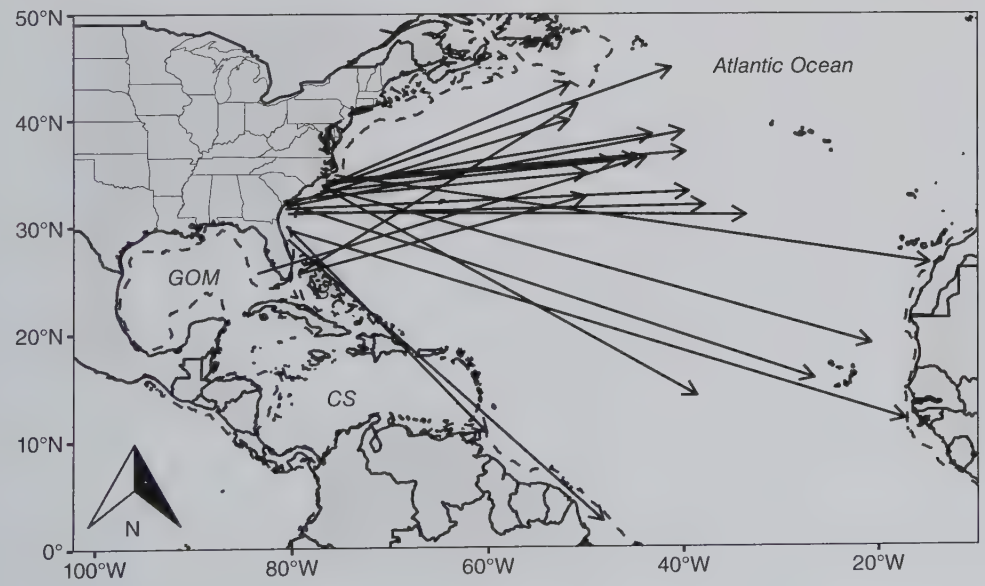


**Figure 4**

Map showing the locations where immature tiger sharks (*Galeocerdo cuvier*) that traveled east of longitude 60°W were tagged and recaptured in the North Atlantic Ocean between 1963 and 2018. The dashed black line indicates the 200-m contour. GOM=Gulf of Mexico; CS=Caribbean Sea.

## Table 3

List of tagged tiger sharks (*Galeocerdo cuvier*) that were recaptured multiple times, by tagging location and month and by size in fork length (FL), sex, and estimated age at tagging calculated by using conversions from Kneebone et al. (2008). Records of sharks tagged and caught in the North Atlantic Ocean during 1963–2018 were used in this study. The letter *X* marks the month the shark was tagged and the following months in which it was recaptured. If there is no superscript character after the *X*, the tagging and recapture events occurred in the same location. A superscript numeral *2* denotes that the shark was recaptured in the same month as it was tagged or that it was recaptured twice in the same month. If the superscript *2* follows a superscript letter, both recapture events in that month occurred at the same location. The superscript letters *N*, *V*, *J*, *M*, *Z*, *C*, *F*, *S*, and *R* denote the following recapture locations, respectively: off North Carolina, Virginia, New Jersey, Maryland, Venezuela in the Caribbean Sea, northern Cuba, Florida's western panhandle, Florida's southern Atlantic coast, and east of the Mid-Atlantic Ridge. The asterisk (*) identifies a tiger shark that was recaptured 6 years following the tagging year in June, approximately 260 nautical miles north-northwest of Bermuda.

| Size | | Age | Year 1 | | | | | | | | | | | | Year 2 | | | | | | | | | | | | Year 3 | | | | | | | | | | | | Year 4 | | | | | | | |
|---|---|---|---|---|---|---|---|---|---|---|---|---|---|---|---|---|---|---|---|---|---|---|---|---|---|---|---|---|---|---|---|---|---|---|---|---|---|---|---|---|---|---|---|---|---|
| (cm FL) | Sex | (years) | J | F | M | A | M | J | J | A | S | O | N | D | J | F | M | A | M | J | J | A | S | O | N | D | J | F | M | A | M | J | J | A | S | O | N | D | J | F | M | A | M | J | J | A | S |
| New Jersey | | | | | | | | | | | | | | | | | | | | | | | | | | | | | | | | | | | | | | | | | | | | | | | |
| 107 | M | 1.4 | | | | | | X | $X^N$ | | | $X^N$ | | | | | | | | | | | | | | | | | | | | | | | | | | | | | | | | | | | |
| Maryland | | | | | | | | | | | | | | | | | | | | | | | | | | | | | | | | | | | | | | | | | | | | | | | |
| 108 | M | 1.4 | | | | | | | X | | | | | | | | | | | | | | | | | $X^N$ | | | | | $X^N$ | | | | | | | | | | | | | | | |
| 155 | M | 3.3 | | | | | | | | | | X | | | | | | | $X^V$ | | | | | | | | | | | | | | | $X^J$ | | | | | | | | | | | | | |
| North Carolina | | | | | | | | | | | | | | | | | | | | | | | | | | | | | | | | | | | | | | | | | | | | | | | |
| 134 | F | 2.3 | | | | | | | | | $X^2$ | | | | | | | | | | | | | | | | | | | | | | | | | | | | | | | | | | | |
| 147 | – | 2.9 | X | | X | | | | | | $X^M$ | | | | | | | | | | | | | | | | | | | | | | | | | | | | | | | | | | | |
| South Carolina | | | | | | | | | | | | | | | | | | | | | | | | | | | | | | | | | | | | | | | | | | | | | | | |
| 120 | M | 1.9 | X | | | | | | $X^{N2}$ | | | | | | | | | | | | | | | | | | | | | | | | | | | | | | | | | | | | | |
| Northern Florida Atlantic coast | | | | | | | | | | | | | | | | | | | | | | | | | | | | | | | | | | | | | | | | | | | | | | | |
| 72 | F | 0.3 | | | | | | | | | X | | | | | | | | | | $X^2$ | | | | | | | | | | | | | | | | | | | | | | | | | |
| 76 | M | 0.4 | | | | | | | | | X | | X | | | | | | | | | | | | | | | | | | | | | | | | | | | | | | | | | |
| 77 | M | 0.4 | | | | | | | | | | | X | | | | | | | | X | | X | | | | | | | | | | | | | | | | | | | | | | | |
| 79 | M | 0.5 | | | | X | | X | | | | | | | | | | | | | | | | | | X | | | | | | | | | | | | | | | | | | | |
| 85 | M | 0.7 | | | | | | | | | | | X | | | | | | | | X | | | | | | | | | $X^N$ | | | | | | | | | | | | | | | |
| 85 | F | 0.7 | | | | | | | | | | | X | | X | | | | | | X | | | | | X | | | | | | | | | | | | | | | | | | | |
| 86 | F | 0.7 | | | | | | | | | | | | X | | | | | | | X | | | | | | | | | | | | | | | | | | | | | | | | | |
| 87 | F | 0.7 | | | | | | | | | | | | X | | | | | | | | X | X | | | | | | | | | | | | | | | | | | | | | | | |
| 87 | F | 0.7 | X | | | | | | | | X | X | | | | | | | | | | | | | | | | | | | | | | | | | | | | | | | | | | |
| 90 | M | 0.8 | | | | | | | | | | | X | | | | | | | | | | X | | | | | | | | | | | | | | | | | | | | | | | |

(*Continued on next page*)

**Table 3** (*continued*)

| Size (cm FL) | Sex | Age (years) | Year 1 | | | | | | | | | | | | Year 2 | | | | | | | | | | | | Year 3 | | | | | | | | | | | | Year 4 | | | | | | |
|---|---|---|---|---|---|---|---|---|---|---|---|---|---|---|---|---|---|---|---|---|---|---|---|---|---|---|---|---|---|---|---|---|---|---|---|---|---|---|---|---|---|---|---|---|
| | | | J | F | M | A | M | J | J | A | S | O | N | D | J | F | M | A | M | J | J | A | S | O | N | D | J | F | M | A | M | J | J | A | S | O | N | D | J | F | M | A | M | J | J | A | S |
| Northern Florida Atlantic coast | | | | | | | | | | | | | | | | | | | | | | | | | | | | | | | | | | | | | | | | | | | | | | | |
| 91 | M | 0.9 | | | | | | | | | | | X | | | | | | | X | | | | | | $X^{Z}$ | | | | | | | | | | | | | | | | | | | | |
| 93 | M | 0.9 | | | | | | | | | | | X | | X | | | | | X | | | | | | | | | | | | | | | | | | | | | | | | | | |
| 94* | M | 1.0 | | | | X | | X | | | | | | | | | | | | | | | | | | | | | | | | | | | | | | | | | | | | | | |
| 96 | M | 1.0 | X | | | | | $X^{2}$ | | | | | | | | | | | | | | | | | | | | | | | | | | | | | | | | | | | | | | |
| 97 | F | 1.1 | | | | X | | | $X^{2}$ | | | | | | | | | | | | | | | | | | | | | | | | | | | | | | | | | | | | | |
| 98 | F | 1.1 | | | | | | X | X | X | | | | | | | | | | | | | | | | | | | | | | | | | | | | | | | | | | | $X^{C}$ |
| 99 | F | 1.1 | | | | | | | X | | | | X | | X | | | | | | | | | | | | | | | | | | | | | | | | | | | | | | |
| 100 | F | 1.2 | | | X | X | | | | | | | | | | | | | | | | | X | | | | | | | | | | | | | | | | | | | | | | |
| 102 | F | 1.2 | | | | | $X^{2}$ | | | X | | | | | | | | | | | | | | | | | | | | | | | | | | | | | | | | | | | | |
| 103 | F | 1.3 | | | | | | $X^{2}$ | | | | X | | | | | | | | | | | | | | | | | | | | | | | | | | | | | | | | | | |
| 103 | F | 1.3 | | | | | | | X | | | | | X | | | | | | | | $X^{J}$ | | | | | | | | | | | | | | | | | | | | | | | | |
| 104 | F | 1.3 | | | X | | | | | | | X | X | | | | | | | | | | | | | | | | | | | | | | | | | | | | | | | | |
| 109 | F | 1.5 | | | | | | | | X | X | | | | | | | | | | | | | | | | | | | | | | | | | | | | | | | | | | |
| 110 | M | 1.5 | | X | X | X | | | | | | | | | | | | | | | | | | | | | | | | | | | | | | | | | | | | | | |
| 114 | M | 1.6 | | | | | | | | | | | X | | | | X | | | | | | | | | | $X^{N}$ | | | | | | | | | | | | | | | | | | |
| 124 | F | 2.0 | | | | | | | | | X | | | | | | | | | | | X | X | | | | | | | | | | | | | | | | | | | | | | |
| Bimini Islands | | | | | | | | | | | | | | | | | | | | | | | | | | | | | | | | | | | | | | | | | | | | | | |
| 214 | F | 6.1 | | | | $X^{2}$ | | X | | | | | | | | | | | | | | | | | | | | | | | | | | | | | | | | | | | | | |
| 223 | F | 6.7 | | | | | X | | | | | | | | | | | | $X^{S2}$ | | | | | | | | | | | | | | | | | | | | | | | | | | |
| Alabama | | | | | | | | | | | | | | | | | | | | | | | | | | | | | | | | | | | | | | | | | | | | | | |
| 156 | M | 3.3 | | | | | | | | | | | X | | | | | | | | | X | | | | | | | | | | | | | | | | | | | | | | | $X^{F}$ |

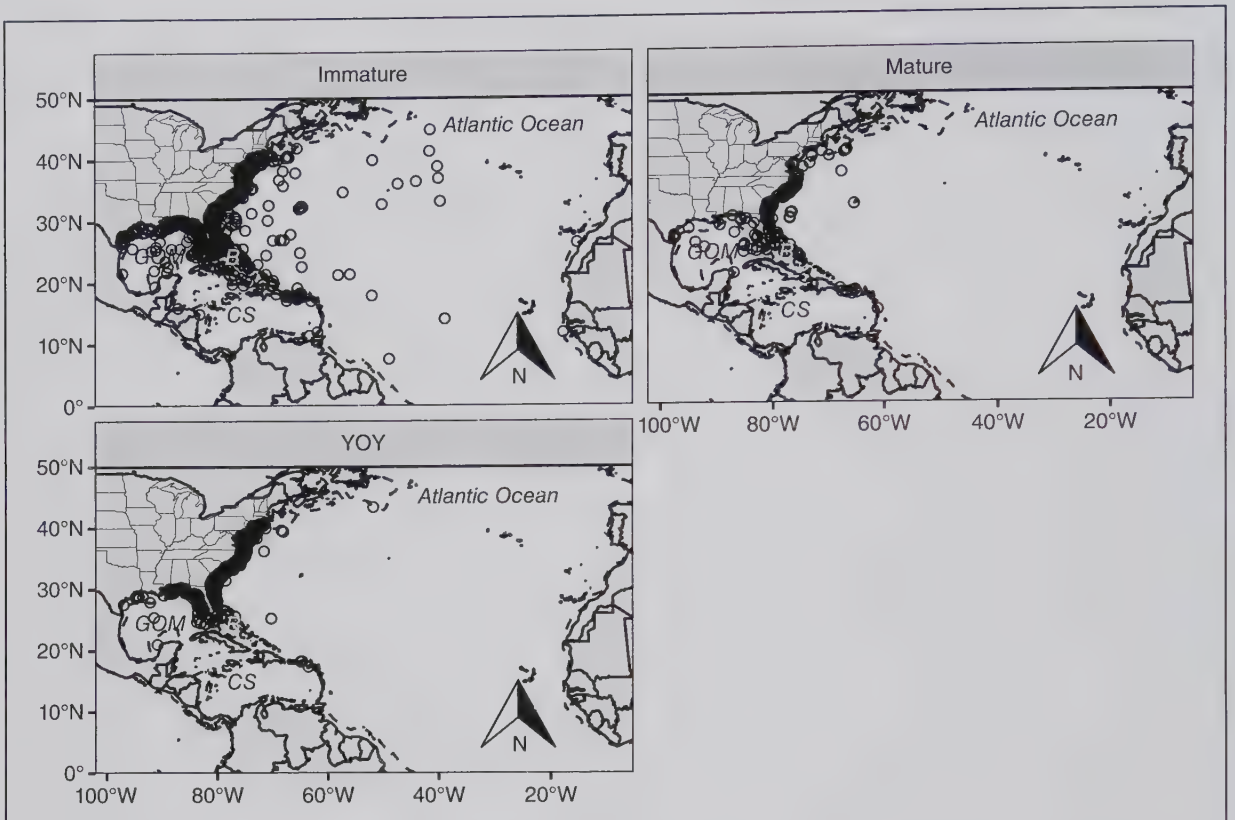


**Figure 5**

Maps showing the distribution of female tiger sharks (*Galeocerdo cuvier*) tagged and recaptured in the western North Atlantic Ocean between 1974 and 2018, by life stage, young of the year (YOY), juveniles (immature), and adults (mature). The dashed black line indicates the 200-m contour. GOM=Gulf of Mexico; CS=Caribbean Sea.

far north as the Grand Banks of Newfoundland ($n$=1) and as far east as Georges Bank ($n$=3) (Figs. 5 and 6). In spring, YOY were tightly clustered from the east coast of Florida up to Cape Hatteras and from off the west coast of Florida to the Florida Panhandle (Suppl. Figs. 1C and 2C) (online only). In summer, YOY were up the coast from Cape Hatteras, as far north as Massachusetts, and were found south in the GOM, but by fall, they appeared to be retreating south and, by winter, the majority were between Cape Hatteras and the tip of Florida, similar to the distribution of YOY in spring (Suppl. Figs. 1C and 2C) (online only). The majority of YOY (82.0%, $n$=3777) were caught between 29°N and 34°N, with a concentration (65.6%, $n$=3023) at 29–31°N. In the GOM, YOY ($n$=273) were found primarily along the coast between 80.3°W and 97.0°W, although one was captured in Mexico, and in winter, individuals of both sexes were found farther offshore (Figs. 5 and 6, Suppl. Figs. 1C and 2C [online only]).

**Neonates and mature females** In May–August, 225 neonates were caught from off eastern Florida up through New York. Although neonates were caught in all 4 months, the majority were caught in July (55.5%) and August (32.9%), and 86.2% of them were caught between Florida and Georgia (between 29°N and 32°N) (Suppl. Fig. 3) (online only). Mature females were primarily caught in May (50.4%) and were less concentrated in distribution than neonates; the majority of the mature female sharks in May (66.1%) were evenly distributed between 29.6°N and 36.8°N (Suppl. Fig. 4) (online only). Of those females caught in May, 24.2% were caught in the area of highest neonate abundance, and 43.5% of those females caught in June were caught in that area. In July and August, the portion of mature females caught in the area of neonate abundance decreased (to 21.4% and 20.0%, respectively). In these latter months, mature females were more spread out and distributed as far north as 40.9°N. No neonates were found in the northeast Caribbean Sea. Not enough samples were obtained from the GOM for neonate inquiry.

## Discussion

The results of our analysis of 55 years of tag and recapture data advance our knowledge of the distribution and habitat use by life stage of tiger sharks in the North Atlantic Ocean. Conventional tagging relies on cooperation from commercial and recreational fishing industries, whether they participate as taggers or simply capture tagged sharks. Therefore, results include fishery-dependent data,

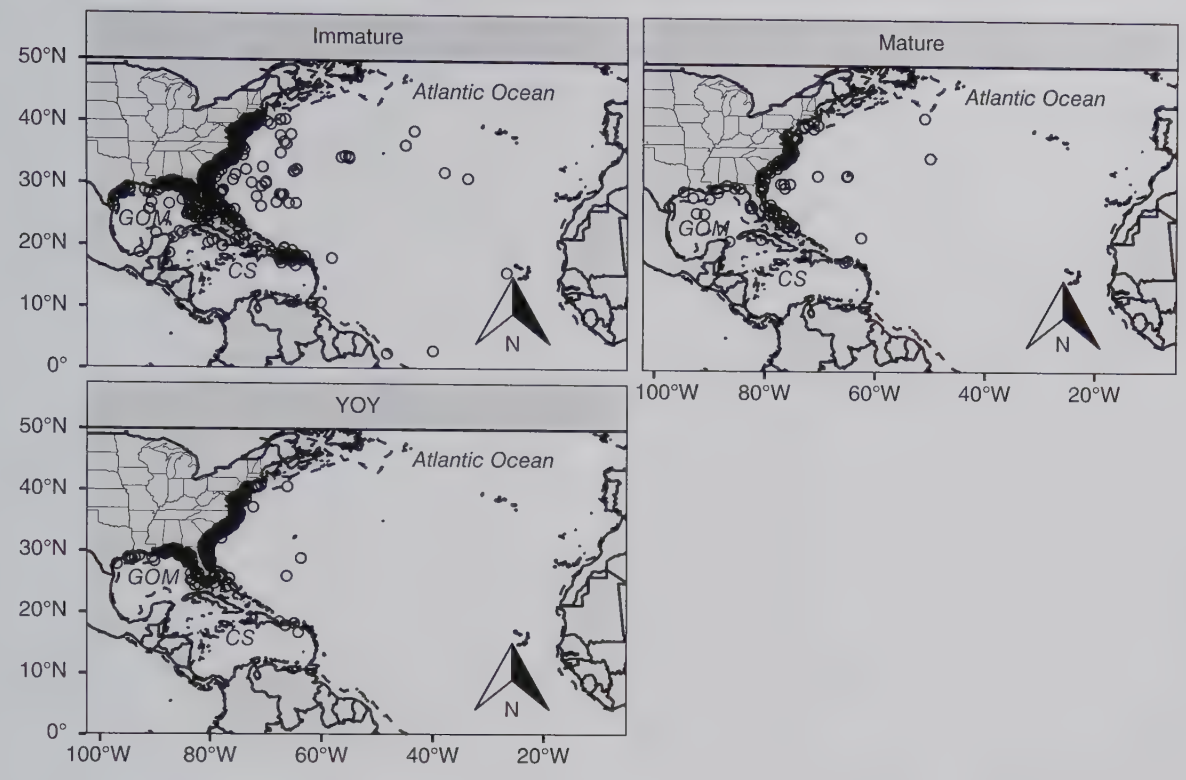


**Figure 6**

Maps showing the distribution of male tiger sharks (*Galeocerdo cuvier*) tagged and recaptured in the western North Atlantic Ocean between 1963 and 2018, by life stage, young of the year (YOY), juveniles (immature), and adults (mature). The dashed black line indicates the 200-m contour. GOM=Gulf of Mexico; CS=Caribbean Sea.

and the number of tagging and recapture events in an area may reflect fishing effort rather than fish distribution. Additionally, the CSTP is based in the United States, likely leading to a higher proportion of recapture events occurring in U.S. waters of the Atlantic Ocean, the GOM, and the Caribbean Sea. In this study, the tagging and recapture data that were analyzed are a compilation of fishery-dependent (from commercial and recreational fisheries) and fishery-independent (from research trips and surveys) sources. Differences in type and location of fishery, gear selectivity, and fishing method can influence the size and distribution of the individuals caught. For example, most of the fishing for all gears and industries occurred close to shore, leading to a higher likelihood of encountering immature sharks (Fig. 1) (Natanson et al., 2023). These same limitations have been noted in other studies on migratory sharks (Mucientes et al., 2009; Heupel et al., 2018; Natanson et al., 2020). Because the large amounts of data on such sharks are inaccessible when using other methods, the use of fishery-dependent methods will remain an important source of data.

Because fishery-dependent data could bias results if fishing occurred in areas of concentrated juveniles, or of single-sex groups, and because the inclusion of fishery-independent data from scientific surveys and comparisons to published data from the use of fishery-independent methods (i.e., electronic tagging) have their own inherent biases, it is necessary to use multiple sampling methods and gear types to mitigate much of such biases. It is also important to note that some of the fishery-independent data were obtained by using sampling of fixed stations, possibly contributing some bias due to site selection that may not result in sampling across the entire habitat (McClelland and Sass, 2012). The ability to use data from both fishery-dependent and -independent sources allowed us to have a broader geographic range and, as a result, a broader biological range (the entire size range for each sex) for examining this species (Natanson et al., 2023).

We observed substantial geographic overlap in the distribution of individuals of all life stages and of both sexes of the tiger shark. In particular, all life stages and both sexes spent considerable time between Cape Hatteras and northeastern Florida. The majority of our data are from immature sharks caught at depths less than 200 m. Driggers et al. (2008, fig. 3) found YOY and juvenile sharks in this same area as well. Our data also indicate that tiger sharks have some degree of seasonal north–south migration, a finding that corresponds with results of other studies that indicate similar migrations in the Atlantic Ocean (Lea et al., 2015; Ajemian et al., 2020) and that indicate that tiger sharks are capable of both making extensive migrations and having periods of

residency (Sulikowski et al., 2016; McClain et al., 2022). Mature tiger sharks of both sexes were primarily caught in the GOM in winter, off the east coast of Florida and off North Carolina in spring, and ranged from the GOM to New England in summer. In fall, most catches of adults were off the coast from the east coast of Florida to North Carolina, although adult females were found as far north as Long Island. The observation of adult tiger sharks seasonally in the GOM is consistent with reports of mature tiger sharks in the GOM in spring and summer (Springer 1938, 1940; Baughman and Springer, 1950; Clark and von Schmidt, 1965; Dodrill, 1977).

Timing and location of mating cannot be determined with our data. Mature males and females overlap throughout the majority of their range in all seasons, except for in winter when overlap is limited and a low sample size for mature males in winter may bias this result. Results of previous studies indicate that a mating season occurs in spring in the GOM and the Caribbean Sea (Baughman and Springer, 1950; Clark and von Schmidt, 1965; Rivera-López, 1970). The Bahamas, in the vicinity of Tiger Beach, have been proposed as a mating area for tiger sharks in the Atlantic Ocean, on the basis of mating scars found on females in winter (Sulikowski et al., 2016). Lea et al. (2015) tracked mature males and found they routinely returned to this area in winter and suggested mating as a possible driver. Our data do indicate overlap of mature males and females in this region of the Bahamas during winter. Additionally, our data indicate some overlap in the GOM off the panhandle and west coast of Florida near Apalachicola and Englewood, respectively, in the spring, but no overlap in the Caribbean Sea during spring.

Pregnant females with embryos in various stages of development have been observed off the west coast of Florida in spring and early summer (Springer, 1938, 1940; Baughman and Springer, 1950; Clark and von Schmidt, 1965; Dodrill, 1977) and off southwest Puerto Rico in the Caribbean Sea (Rivera-López, 1970). Data from the CSTP indicate the presence of YOY in this area; however, there is no evidence of neonates, indicating that these YOY may move into these areas from the GOM or from the main body of the Atlantic Ocean after parturition. Sulikowski et al. (2016) suggested that the area off Tiger Beach may be a gestation area, given the consistent number of large females with an extended residency and observations of pregnant females. Smukall et al. (2022) reported captures of near-term and recently postpartum females, verified by ultrasonography, near the Bimini Islands in the Bahamas during late spring and summer. Additionally, Smukall et al. (2022) reported frequent catches of young-of-the-year tiger sharks, including neonate-size individuals, but acoustic data indicate limited residency, potentially meaning that YOY moved out of the area soon after parturition.

Because near-term pregnant females are found in the GOM and Atlantic Ocean, it is probable that they birth, and possibly gestate, in their respective water bodies, although we do not have direct data from the GOM to corroborate it for that area. Our data indicate that the highest concentration of neonates between March and August overlap the locations of mature females in the waters off the East Coast of the United States at this time (Springer, 1938; Clark and von Schmidt, 1965). The presence of postpartum females between New Jersey and southern New England during June–August indicates a northward movement of mature females after birthing (Natanson et al., 2023).

Seasonal north–south migrations were undertaken by tiger sharks in the YOY, juvenile, and adult stages. The YOY concentrate between the east coast of Florida and Cape Hatteras throughout the year, expanding north in summer and fall (Suppl. Figs. 1C and 2C) (online only). Natanson et al. (1999) reported concentrated catches of neonate and YOY tiger sharks on the continental shelf between 29°N and 33°N. Driggers et al. (2008), using data on catch per unit of effort of neonates, expanded this region to 27–35°N, with the area of 31–33°N as the most important. The majority of YOY (82.0%) in this study were caught between 29°N and 34°N, with a concentration between 29°N and 31°N (65.6%). In contrast, Driggers et al. (2008) found the highest concentration of YOY tiger sharks at 32°N in waters off the East Coast. The differences in these areas of high concentration for YOY between our study and Driggers et al. (2008) may be a result of timing and type of sampling. Data from this study were collected year-round and are a combination of 55 years of fishery-dependent and -independent (fixed-station and random-stratified surveys and targeted research sampling) data, and the data from Driggers et al. (2008) are temporally discrete (August–September) and based on 13 years of a single fishery-independent survey (with a random-stratified design). Additionally, the concentrations may shift depending on optimal environmental conditions for each stage in a given year.

Shark nursery areas can be detected by using the presence of gravid females with near-term embryos, neonates, and small juveniles for viviparous species (Castro, 1993). Although presence data can be used to detect nursery habitat, isolated events do not provide information on the importance of this habitat in supporting juvenile shark populations (McCandless, 2007). Monitoring through long-term fishery-independent surveys, conventional mark-recapture work, and acoustic telemetry studies can help develop a better picture of how nursery habitat is used (McCandless, 2007). With fishery managers in mind, Heupel et al. (2007) developed a quantitative definition for identifying important shark nursery areas by using 3 criteria for neonates and YOY: 1) these juveniles are more commonly encountered in the area than other areas, 2) they have a tendency to remain in or return to the area for extended periods, and 3) the area is repeatedly used across years.

On the basis of these criteria, the tagging and recapture data used in our study indicate that the area from off the east coast of Florida north of Cape Canaveral to off Jekyll Island in Georgia (between 29°N and 31°N) provides nursery habitat for tiger sharks. Data from multiple recapture events indicate that this area has concentrations of neonate- and YOY-size sharks, that these sharks spend several months there following parturition that occurs within

the area or following migration to the area, and that these sharks repeatedly use this area across years. Expanding this region to Cape Island, South Carolina (33°N), incorporates data from Driggers et al. (2008) indicating the importance of this region for both neonates and YOY. Our data on neonates, YOY, and multiple recaptured immature tiger sharks, combined with data from Driggers et al. (2008) and McClain et al. (2022), support the existence of separate, broad birthing areas and nursery habitats in the GOM and in waters off the East Coast (Heupel et al., 2007; Driggers et al., 2008). Knowledge of defined areas of concentration informs management decisions regarding refinement of essential fish habitat and spatial management and conservation goals to protect the vulnerable life stages of this species (Heupel et al., 2007, 2018; Kinney and Simpfendorfer, 2009). The area of concentration for YOY in this study encompasses the range where neonates were concentrated.

This report is the first to document that immature tiger sharks undertook long-distance movements from the western to the eastern Atlantic Ocean. These data indicate movements of tiger sharks that are much broader and of longer distances and taken at smaller sizes than previously known for this species. Although results from other studies indicate that adult males and females and subadult (no longer a juvenile but not yet an adult) females undertake long-distance movements (Hammerschlag et al., 2012; Lea et al., 2015; Ajemian et al., 2020), the outcomes of many studies indicate that juvenile tiger sharks cannot undertake long-distance migrations because of inefficient swimming in the more anguilliform body of the young tiger shark (Lea et al., 2015, 2018; Aines et al., 2018) or because of the effect of environmental factors on body size (i.e., small sharks are less tolerant of low sea-surface temperatures) (Lea et al., 2018).

Our data indicate that YOY use coastal waters of the United States fairly continuously from Louisiana to Long Island, depending on the season, and are found offshore and north to New England in summer. Individual tiger sharks of both sexes tagged as YOY traveled >500 nmi, indicating that this life stage is capable of movements of longer distances than previously thought. For example, one YOY, was tagged in February and recaptured 6 months later southeast of Newfoundland, having traveled nearly 1300 nmi. Another was tagged in November and recaptured after 1 year in the Caribbean Sea off Venezuela, having traveled nearly 1400 nmi. By the juvenile stage, the range of tiger sharks becomes Atlantic basin-wide. The coastal range extends from New England down and into the Caribbean Sea. The north–south migration along the Atlantic coast of the northeastern United States taken by immature fish is complicated by offshore and transatlantic movements. These sharks move north in summer past New England to the east; some remain in coastal waters, and others venture offshore presumably with the Gulf Stream and as far north as the Grand Banks of Newfoundland. This northward offshore movement with the Gulf Stream has been documented for adult males (Lea et al., 2015, 2018) and for adult and subadult females (Hammerschlag et al., 2012) by using satellite tracking data, and results of our study indicate that immature tiger sharks of both sexes also follow this pattern. Additionally, our data indicate movement of immature tiger sharks, including YOY, into and out of the Caribbean Sea from both the main body of the Atlantic Ocean and the GOM.

It has been suggested that ontogenetic movements into more oceanic habitats are possibly related to foraging (Lowe et al., 1996; Lea et al., 2015), and more recently McClain et al. (2022) suggested a reproductive component to migration. On the basis of their electronic tagging data, Lea et al. (2018) further suggested an ontogenetic shift in foraging strategy and diet that leads to longer migrations by adult males. Although a foraging component may certainly drive these migrations, our data indicate that immature tiger sharks make extensive migrations throughout the Atlantic Ocean, refuting the ontogenetic component of the basis for longer distance migration. Long migrations are evident even for young juveniles; for example, the transatlantic migration of over 3600 nmi of a tiger shark tagged as a YOY and recaptured 2 years later.

In conjunction with the data we present on juveniles crossing the Atlantic Ocean, and data from other studies, we suggest that a northeasterly track could be the route that these sharks take to the eastern Atlantic Ocean. Following the major current system in the North Atlantic Ocean, this track starts with the Gulf Stream, moving north and east with the North Atlantic Drift and then south to the Canary Current before following the North Equatorial Current back to the WNA as has been previously postulated for the migration of the blue shark (Casey, 1985). Afonso et al. (2017) suggested an equatorial route for juvenile tiger sharks linking the eastern and western Atlantic Ocean. Additionally, Domingo et al. (2016), using observer data, documented that tiger sharks in the North Atlantic Ocean were more broadly distributed than previously thought. A limited number of mature sharks of both sexes ($n$=10; 2 males, 7 females, and 1 individual of unknown sex) in this study made movements greater than 500 nmi within the WNA, although none crossed the North Atlantic basin. Although mature individuals have not yet been documented to travel across the North Atlantic basin, they have been repeatedly shown to have the ability to travel the long distances required for this movement (Hammerschlag et al., 2012; Ferreira et al., 2015; Lea et al., 2015). The lower percentage of mature sharks in our sample may also be a factor in this result. Much of the data are limited to immature sharks crossing the North Atlantic basin, but these movements and distributions strongly indicate that there is only one population in the North Atlantic Ocean.

Conventional tags are significantly less costly than electronic tags; therefore, more individuals of a species can be tagged with them at various times, locations, and life stages. Additionally, long-term studies with increased numbers of recapture events can enhance the body of knowledge. Sample size is important in interpreting results from tagging studies, and an increase in sample size allows for a larger range and scope of questions that

can be answered (Sequeira et al., 2019). When examining tagging data for population trends and movements, an increased number of tags makes it possible to see variation in movements between individuals, life stages, or sexes (Sequeira et al., 2019); it is therefore important to tag individuals of all sizes and sexes to obtain a complete overview of the movements of a species. Additionally, the duration of tag deployment and the location of release of tagged fish can influence movements for certain shark species (Rooker et al., 2019). It is apparent from studies of a variety of species, including the tiger shark, that individuals can be resident or migratory for given periods of time and stages of maturity.

Despite the number of tiger sharks tagged in the CSTP, it took 34 years and 5832 tiger sharks to be tagged before the first tiger shark tagged in the WNA was recaptured in the ENA. It is certainly doubtful that we have seen all possible scenarios, particularly with mature sharks. These recapture events are important not only in that the tiger shark can cross the North Atlantic Ocean, therefore indicating potential mixing within the population, but in that immature sharks are capable of this movement. Pooling all tagging data on the tiger shark in the WNA creates a better picture of the movements of this species than examining those studies individually. For example, Lea et al. (2015, 2018) stated that only mature males make long-distance migrations and that movements into and out of the Caribbean Sea were not observed; however, with the addition of Hammerschlag et al. (2012), Rooker et al. (2019), and Ajemian et al. (2020), it is apparent that females also travel long distances and exchange between these water bodies. Combining data from conventional and electronic tagging studies can provide a far more robust, comprehensive picture of the movements of a species and of the drivers for those movements than the representation formed when using data from just one type of tagging, leading to advancements in management measures (Hammerschlag et al., 2022) to better support sustainable fisheries.

## Conclusions

We examined seasonal movement patterns of the tiger shark on the basis of sex and life stage and have added to the literature describing seasonal north–south movements of the tiger shark. Additionally, our data indicate that immature tiger sharks tagged in the WNA make long-distance migrations to the ENA. We propose that there is a potential route that runs up the coast of North America in the WNA and crosses over to the ENA, revealing potential mixing within the population not indicated by data from electronic tagging to date. We also identified a broad nursery area and potential birthing grounds off the East Coast of the United States. Tagged tiger sharks crossed multiple international jurisdictions, indicating that management measures need to have a basin-wide scale. The results of this project highlight the need for the use of more long-term, conventional tagging along with electronic tagging to fully understand the movements of shark species and to adequately implement management strategies.

## Resumen

Los movimientos del tiburón tigre (*Galeocerdo cuvier*) durante las etapas de su vida, son en gran medida desconocidos. Sin embargo, es necesario conocerlos para determinar su hábitat esencial y las prácticas sostenibles de manejo pesquero. En un esfuerzo por dilucidar la distribución y los movimientos del tiburón tigre, analizamos datos de marcaje dependientes e independientes de la pesquería (tamaño de la muestra [*n*]=10,516) y registros de recaptura (n=762) de tiburones tigre capturados en el océano Atlántico norte entre 1963 y 2018. Se examinó la distribución estacional del tiburón tigre por etapa de vida—juveniles del año, juveniles (inmaduros) y adultos (maduros)—y se utilizaron patrones de distribución para identificar posibles hábitats de cría nza. Se capturaron tiburones tigre en una amplia zona desde los Grandes Bancos de Terranova (Canadá) hacia el sur, en Brasil y desde la costa hasta alta mar y hacia el este del océano Atlántico Norte. Se observaron movimientos estacionales de norte a sur en todas las etapas de la vida, y se descubrió que 14 tiburones inmaduros habían migrado del océano Atlántico Norte occidental al oriental. Se identificó una amplia zona de crianza y una posible zona de nacimiento en la plataforma continental entre Florida y Georgia con base en recurrencia de neonatos en verano a lo largo de los años y en la recaptura de múltiples tiburones tigre juveniles del año marcados en el mismo lugar durante un periodo de al menos 2 años.

## Acknowledgments

We thank the many CSTP volunteers for contributing data over the years. We also thank the past and present members of the Apex Predators Program of the NOAA Northeast Fisheries Science Center, particularly K. Zewinski for help in verifying tag and recapture data and M. Passerotti for reviewing the manuscript. We also appreciate all the people who helped get us literature references during the pandemic: N. Hammerschlag, N. Whitney, J. Kneebone, and J. Castro.

## Literature cited

Aines, A. C., J. K. Carlson, A. Boustany, A. Mathers, and N. E. Kohler.
2018. Feeding habits of the tiger shark, *Galeocerdo cuvier*, in the northwest Atlantic Ocean and Gulf of Mexico. Environ. Biol. Fishes 101:403–415.

Afonso, A. S., and F. H. V. Hazin.
2015. Vertical movement patterns and ontogenetic niche expansion in the tiger shark, *Galeocerdo cuvier*. PLoS ONE 10(1):e116720.

Afonso, A. S., F. H. V. Hazin, R. R. Barreto, F. M. Santana, and R. P. Lessa.
2012. Extraordinary growth in tiger sharks *Galeocerdo cuvier* from the South Atlantic Ocean. J. Fish Biol. 81:2080–208.

Afonso, A. S., R. Garla, and F. H. V. Hazin.
2017. Tiger sharks can connect equatorial habitats and fisheries across the Atlantic Ocean basin. PLoS ONE 12(9):e0184763.

Ajemian, M. J., J. M. Drymon, N. Hammerschlag, R. J. D. Wells, G. Street, B. Falterman, J. A. McKinney, W. B. Driggers III, E. R. Hoffmayer, C. Fischer, et al.
2020. Movement patterns and habitat use of tiger sharks (*Galeocerdo cuvier*) across ontogeny in the Gulf of Mexico. PLoS ONE 15(7):e0234868.

Baughman, J. L., and S. Springer.
1950. Biological and economic notes on the sharks of the Gulf of Mexico, with reference to those of Texas, and with a key for their identification. Am. Midland Nat. 44:96–152.

Bigelow, H. B., and W. C. Schroeder.
1948. Sharks. *In* Fishes of the western North Atlantic. Part 1: lancelets, cyclostomes, sharks (J. Tee-Van, C.M. Breder, S.F. Hildebrand, A.E. Parr, and W.C. Schroeder, eds.), p. 59–546. Sears Found. Mar. Res., Yale Univ. Press, New Haven, CT.

Carlson, J. K., L. F. Hale, A., Morgan, and G. Burgess.
2012. Relative abundance and size of coastal sharks derived from commercial shark longline catch and effort data. J. Fish Biol. 80:1749–1764.

Casey, J. G.
1985. Transatlantic migrations of the blue shark: a case history of cooperative shark tagging. *In* Proceedings of the First World Angling Conference; Cap d'Agde, 12–18 September 1984 (R. H. Stroud, ed.). p. 253–268. Int. Game Fish Assoc., Ft. Lauderdale, FL.

Casey, J. G., and N. E. Kohler.
1992. Tagging studies on the shortfin mako shark (*Isurus oxyrinchus*) in the western North Atlantic. Aust. J. Freshw. Res. 43:45–60.

Castro, J. I.
1993. The shark nursery of Bulls Bay, South Carolina, with a review of the shark nurseries of the southeastern coast of the United States. Environ. Biol. Fishes 38:37–48.
2011. The sharks of North America, 640 p. Oxford Univ. Press, New York.

Clark, E., and K. von Schmidt.
1965. Sharks of the central Gulf Coast of Florida. Bull. Mar. Sci. 15:13–83.

Cortés, E.
1999. Standardized diet compositions and trophic levels of sharks. ICES J. Mar. Sci. 56:707–717.

Cortés, E., A. Domingo, P. Miller, R. Forselledo, F. Mas, F. Arocha, S. Campana, R. Coelho, C. Da Silva, F. H. V. Hazin, et al.
2015. Expanded ecological risk assessment of pelagic sharks caught in Atlantic pelagic longline fisheries. Collect. Vol. Sci. Pap. ICCAT 71(6):2637–2688.

Dodrill, J. W.
1977. A hook and line survey of the sharks found within five hundred meters of shore along Melbourne Beach, Brevard County, Florida. M.S. thesis, 304 p. Fla. Inst. Tech., Melbourne, FL.

Domingo, A., R. Coelho, E. Cortes, B. Garcia-Cortes, F. Mas, J. Mejuto, P. Miller, A. Ramos-Cartelle, M. N. Santos, and K. Yokawa.
2016. Is the tiger shark *Galeocerdo cuvier* a coastal species? Expanding its distribution range in the Atlantic Ocean using at-sea observer data. J. Fish Biol. 88:1123–1128.

Driggers, W. B., III, G. W. Ingram Jr., M. A. Grace, C. T. Gledhill, T. A. Henwood, C. N. Horton, and C. M. Jones.
2008. Pupping areas and mortality rates of young tiger sharks *Galeocerdo cuvier* in the western North Atlantic Ocean. Aquat. Biol. 2: 161–170.

Ferreira, L. C., and C. Simpfendorfer.
2019. *Galeocerdo cuvier*. The IUCN Red List of Threatened Species 2019: e.T39378A2913541. [Available from website.]

Ferreira, L. C., M. Thums, J. J. Meeuwig, G. M. S. Vianna, J. Stevens, R. McAuley, and M. G. Meekan.
2015. Crossing latitudes—long-distance tracking of an apex predator. PLoS ONE 10(2):e0116916.

Fitzpatrick, R., M. Thums, I. Bell, M. G. Meekan, J. D. Stevens, and A. Barnett.
2012. A comparison of the seasonal movements of tiger sharks and green turtles provides insight into their predator-prey relationship. PLoS ONE 7(12):e51927.

Hammerschlag, N., A. J. Gallagher, J. Wester, J. Luo, and J. S. Ault.
2012. Don't bite the hand that feeds: assessing ecological impacts of provisioning ecotourism on an apex marine predator. Funct. Ecol. 26:567–576.

Hammerschlag, N., L. H. McDonnell, M. J. Rider, G. M. Street, E. L. Hazen, L. J. Natanson, C. T. McCandless, M. R. Boudreau, A. J. Gallagher, M. L. Pinsky, et al.
2022. Ocean warming alters the distributional range, migratory timing, and spatial protections of an apex predator, the tiger shark (*Galeocerdo cuvier*). Global Change Biol. 28:1990–2005.

Heithaus, M. R.
2001. The biology of tiger sharks, *Galeocerdo cuvier*, in Shark Bay, Western Australia: sex ratio, size distribution, diet, and seasonal changes in catch rates. Environ. Biol. Fishes 61:25–36.

Heithaus, M. R., A. J. Wirsing, L. M. Dill, and L. I. Heithaus.
2007. Long-term movements of tiger sharks satellite-tagged in Shark Bay, Western Australia. Mar. Biol. 151: 1455–1461.

Heupel, M. R., J. K. Carlson, and C. A. Simpfendorfer.
2007. Shark nursery areas: concepts, definition, characterization and assumptions. Mar. Ecol. Prog. Ser. 337: 287–297.

Heupel, M. R., S. Kanno, A. P. B. Martins, and C. A. Simpfendorfer.
2018. Advances in understanding the roles and benefits of nursery areas for elasmobranch populations. Mar. Freshw. Res. 70:897–907.

Kinney, M. J., and C. A. Simpfendorfer.
2009. Reassessing the value of nursery areas to shark conservation and management. Conserv. Lett. 2:53–60.

Kneebone J., L. J. Natanson, A. H. Andrews, and W. H. Howell.
2008. Using bomb radiocarbon analyses to validate age and growth estimates for the tiger shark, *Galeocerdo cuvier*, in the western North Atlantic. Mar. Biol. 154: 423–434.

Kohler, N. E., and P. A. Turner.
2019. Distributions and movements of Atlantic shark species: a 52-year retrospective atlas of mark and recapture data. Mar. Fish. Rev. 81(2)1–93.

Kohler, N. E., J. G. Casey, and P. A. Turner.
1996. Length-length and length-weight relationships for 13 shark species from the western North Atlantic. NOAA Tech. Memo. NMFS-NE-110, 22 p.
1998. NMFS Cooperative Shark Tagging Program, 1962–1993: an atlas of shark tag and recapture data. Mar. Fish. Rev. 60(2)1–87.

Lea, J. S. E., B. M. Wetherbee, N. Queiroz, N. Bernie, C. Aming, L. L. Sousa, G. R. Mucientes, N. E. Humphries, G. M. Harvey, D. W. Sims, et al.
2015. Repeated, long-distance migrations by a philopatric predator targeting highly contrasting ecosystems. Sci. Rep. 5:11202.

Lea, J. S. E., B. M. Wetherbee, L. L. Sousa, C. Aming, N. Burnie, N. E. Humphries, N. Queiroz, G. M. Harvey, D. W. Sims, and M. S. Shivji.
2018. Ontogenetic partial migration is associated with environmental drivers and influences fisheries interactions in a marine predator. ICES J. Mar. Sci. 75:1383–1392.

Lowe, C. G., B. M. Wetherbee, G. L. Crow, and A. L. Tester.
1996. Ontogenetic dietary shifts and feeding behavior of the tiger shark, *Galercerdo cuvier*, in Hawaiian waters. Environ. Biol. Fishes 47:203–211.

McCandless, C. T.
2007. Preface. Am. Fish. Soc. Symp. 50:vii–ix.

McClain, M. A., N. Hammerschlag, A. J. Gallagher, J. M. Drymon, J., R. D. Grubbs, T. L. Guttridge, M. J. Smukall, B. S. Frazier, and T. S. Daly-Engel.
2022. Age-dependent dispersal and relatedness in tiger sharks (*Galeocerdo cuvier*). Front. Mar. Sci.

McClelland, M. A., and G. G. Sass.
2012. Assessing fish collections from random and fixed site sampling methods on the Illinois River. J. Freshw. Ecol. 27:325–333.

Meyer, C. G., J. M. Anderson, D. M. Coffey, M. R. Hutchinson, M. A. Royer, and K. N. Holland.
2018. Habitat geography around Hawaii's oceanic islands influences tiger shark (*Galeocerdo cuvier*) spatial behaviour and shark bite risk at ocean recreation sites. Sci. Rep. 8:4945.

Mucientes, G. R., N. Queiroz, L. L. Sousa, P. Tarroso, and D. W. Sims.
2009. Sexual segregation of pelagic sharks and the potential threat from fisheries. Biol. Lett. 5:156–159.

Natanson, L. J., J. G. Casey, N. E. Kohler, and T. Colket IV.
1999. Growth of the tiger shark, *Galeocerdo cuvier*, in the western North Atlantic based on tag returns and length frequencies; and a note on the effects of tagging. Fish. Bull. 97:944–953.

Natanson, L. J., M. Winton, H. Bowlby, W. Joyce, B. Deacy, R. Coelho, and D. Rosa.
2020. Updated reproductive parameters for the shortfin mako (*Isurus oxyrinchus*) in the North Atlantic Ocean with inferences of distribution by sex and reproductive stage. Fish. Bull. 118:21–36.

Natanson, L. J., W. B Driggers III, C. T. McCandless, and N. E. Kohler.
2023. Updated reproductive parameters for the tiger shark (*Galeocerdo cuvier*) in the western North Atlantic Ocean. Fish Bull. 121:84–95.

Natanson, L. J., C. T. McCandless, M. S. Passerotti, C. N. Belcher, H. Bowlby, W. B. Driggers III, B. S. Frazier, J. Gelsleichter, S. J. B. Gulak, J. M. Hendon, et al.
2022. Morphometric conversions for 33 shark species from the western North Atlantic Ocean. Mar. Fish. Rev. 84(3–4):1–65.

Papastamatiou, Y. P., C. G. Meyer, F. Carvalho, J. J. Dale, M. R. Hutchinson, and K. N. Holland.
2013. Telemetry and random-walk models reveal complex patterns of partial migration in a large marine predator. Ecology 94:2595–2606.

Peterson, C. D., C. N. Belcher, D. M. Bethea, W. B. Driggers III, B. S Frazier, and R. J. Latour.
2017. Preliminary recovery of coastal sharks in the southeast United States. Fish Fish. 18:845–859.

R Core Team.
2022. R: a language and environment for statistical computing. R Foundation for Statistical Computing, Vienna, Austria. [Available from website, accessed March 2022.]

Rivera-López, J.
1970. Studies on the biology of the nurse shark, *Ginglymostoma cirratum* Bonneterre, and the tiger shark, *Galeocerdo cuvieri* Peron and Le Sueur. M.S. thesis, 80 p. Univ. Puerto Rico, Mayaguez, Puerto Rico.

Rooker, J. R., M. A. Dance, R. J. D. Wells, M. J. Ajemian, B. A. Block, M. R. Castleton, J. M. Drymon, B. J. Falterman, J. S. Franks, N. Hammerschlag, et al.
2019. Population connectivity of pelagic megafauna in the Cuba-Mexico-United States triangle. Sci. Rep. 9:1663.

Ruppert, J. L. W., M. J. Travers, L. L. Smith, M. J. Fortin, and M. G. Meekan.
2013. Caught in the middle: combined impacts of shark removal and coral loss on the fish communities of coral reefs. PLoS ONE 8(9):e74648.

Sequeira, A. M. M., M. R. Heupel, M.-A. Lea, V. M. Eguíluz, C. M. Duarte, M. G. Meekan, M. Thums, H. J. Calich, R. H. Carmichael, D. P. Costa, et al.
2019. The importance of sample size in marine megafauna tagging studies. Ecol. Appl. 29:e01947.

Smukall, M. J., A. C. Seitz, F. Dhellemmes, M. P. M. van Zinnicq Bergmann, V. Heim, S. H. Gruber, and T. L. Guttridge.
2022. Residency, site fidelity, and regional movement of tiger sharks (*Galeocerdo cuvier*) at a pupping location in the Bahamas. Sustainability 14:10017.

Springer, S.
1938. Notes on the sharks of Florida. Proc. Fla. Acad. Sci. 3:9–41.
1940. The sex ratio and seasonal distribution of some Florida sharks. Copeia 1940(3):188–194.

Sulikowski, J. A., C. R. Wheeler, A. J. Gallagher, B. K. Prohaska, J. A. Langan, and N. Hammerschlag.
2016. Seasonal and life-stage variation in the reproductive ecology of a marine apex predator, the tiger shark *Galeocerdo cuvier*, at a protected female-dominated site. Aquat. Biol. 24:175–184.

National Marine Fisheries Service
NOAA

*Fishery Bulletin*
established in 1881

Spencer F. Baird
First U.S. Commissioner of Fisheries and founder of *Fishery Bulletin*

# Arrival and departure windows of Atlantic sturgeon (*Acipenser oxyrinchus oxyrinchus*) in Chesapeake Bay in Virginia

**Jason E. Kahn (contact author)**[1]
**Christian H. Hager**[2]
**D. Kyle Breault**[2]
**J. Carter Watterson**[3]

Email address for contact author: jason.kahn@noaa.gov

[1] Office of Protected Resources
National Marine Fisheries Service, NOAA
1315 East-West Highway, Building SSMC3
Silver Spring, Maryland 20910-3282

[2] Chesapeake Scientific LLC
100 Sixpence Court
Williamsburg, Virginia 23185

[3] Naval Facilities Engineering Systems Command
U.S. Department of the Navy
1322 Patterson Avenue
Washington Navy Yard
Washington, District of Columbia 20374

**Abstract**—The Atlantic sturgeon (*Acipenser oxyrinchus oxyrinchus*) has been listed under the Endangered Species Act since 2012, with the Chesapeake Bay distinct population segment listed as endangered. We tracked the timing of occupancy and movement in Chesapeake Bay of adult Atlantic sturgeon from the York River to best identify when Atlantic sturgeon are likely to interact with anthropogenic threats. We monitored 84 adult (40 male and 44 female) Atlantic sturgeon from August 2013 through January 2020 by using acoustic telemetry. Both spawning and non-spawning fish regularly utilized Chesapeake Bay, with females and males arriving as early as 27 February (when the mean water temperature was 7.7°C) and 4 March (6.5°C) and departing as late as 24 January (6.3°C) and 27 January (6.5°C), respectively. Peak occupation of the bay by Atlantic sturgeon occurred from 1 April to 31 August and again from 15 October to 1 December. Females of above average size (>1880 mm in fork length) spent significantly longer in the bay (>113 d) than smaller females and all males before spawning; therefore, the females capable of producing the most eggs were disproportionately exposed to anthropogenic threats. Although changes in arrival and departure dates are not statistically significant, during the 7 years of this study, both males and females generally arrived earlier and departed later each year than the previous year, increasing residency in Chesapeake Bay by a month in that time.

Manuscript submitted 19 January 2023.
Manuscript accepted 26 October 2023.
Fish. Bull. 121:161–171 (2023).
Online publication date: 16 November 2023.
doi: 10.7755/FB.121.4.2

The views and opinions expressed or implied in this article are those of the author (or authors) and do not necessarily reflect the position of the National Marine Fisheries Service, NOAA.

The National Marine Fisheries Service listed 5 distinct population segments (DPSs) of Atlantic sturgeon (*Acipenser oxyrinchus oxyrinchus*) under the Endangered Species Act in 2012 (Federal Register, 2012a 2012b). Since this listing, new spawning populations have been discovered (Hager et al., 2014; Balazik et al., 2017; Farrae et al., 2017; Savoy et al., 2017). It now appears that some rivers support 2 genetically different spawning populations and that rivers identified within the geographic area of a DPS may have a seasonal spawning group of sturgeon that are more closely related to sturgeon spawning in other rivers outside of the area of that DPS (White et al., 2021). Of the 5 DPSs in the United States, the Gulf of Maine DPS was listed as threatened under the Endangered Species Act, and the New York Bight, Chesapeake Bay, Carolina, and South Atlantic DPSs were listed as endangered. At the time of listing, the Chesapeake Bay DPS had one known spawning population: the population in the James River, which at the time had been confirmed to spawn after summer as temperatures decline (Balazik et al., 2012a). Like the York River, the James River is located in Virginia. Since the listing in 2012, adult Atlantic sturgeon have been confirmed to spawn in the York River (Hager et al., 2014); spawning is likely occurring in the Nanticoke River, located on the Delmarva Peninsula, and possibly in the Rappahannock River, located in eastern Virginia (ASMFC, 2017). Results of genetic analyses of the populations in the James and York Rivers indicate that these 2 populations are significantly differentiated (White et al., 2021).

Atlantic sturgeon are long-lived, wide-ranging, late-maturing, iteroparous, anadromous fish that spawn intermittently (Smith, 1985; Bemis and Kynard, 1997; Dadswell, 2006; NMFS, 2007; Peterson et al., 2008; Hager et al., 2020). Adult and migratory juvenile Atlantic sturgeon spend significant portions of each year along the East Coast for feeding, growing, overwintering, and migrating (Dovel and Berggren, 1983; Smith, 1985; Bain, 1997; Stevenson, 1997; Wirgin et al., 2015). These individuals undertake seasonal migrations to utilize inshore and offshore habitat (Ingram et al., 2019).

In Chesapeake Bay, there have been no peer-reviewed reports of the timing or windows of occupancy of Atlantic sturgeon. The objective of this study was to identify that timing and the movement of adult Atlantic sturgeon within Chesapeake Bay. We evaluated the migrations of males and females separately in terms of seasons, years, calendar days, photoperiod, and temperatures. Understanding the periods of occupancy is essential for the National Marine Fisheries Service to protect and ultimately recover this endangered species.

## Materials and methods

We identified the entrance to Chesapeake Bay as an invisible line from Fort Story, Virginia, to Fisherman's Island National Wildlife Refuge near Cape Charles, Virginia, because this location was the most restricted point at the mouth of the bay (Fig. 1). We determined that a fish had left Chesapeake Bay if it was detected on receivers beyond the boundary denoted by this line or if it entered the mouth of the James, York, or Rappahannock River (Fig. 1). At locations where passive acoustic receivers (VR2W, Innovasea Systems Inc.[1], Boston, MA) were deployed to detect fish implanted with acoustic tags, water temperatures were collected with HOBO U12-015 data loggers (Onset Computer Corp., Bourne, MA) zip tied to the acoustic receivers or from the First Landing (near Cape Henry, Virginia) and York Spit (at the mouth of the York River near Perrin, Virginia) monitoring locations of the NOAA Chesapeake Bay Interpretive Buoy System (data available from website, accessed January 2022).

Atlantic sturgeon were captured, implanted with acoustic transmitters (or tags), and released while on spawning runs in the Pamunkey and Mattaponi Rivers, the 2 main tributaries to the York River. For our analysis, individuals were considered to be on spawning runs if they met a 2-part test: 1) the fish moved a minimum of 20 km above the saltwater interface, and 2) it spent at least 2 weeks in fresh water (Kahn et al., 2019; Hager et al., 2020; Kahn et al., 2021). All tagged Atlantic sturgeon were in the adult size range (1250–2272 mm in fork length [FL]; Grunwald et al., 2008; Waldman et al., 2019; Kahn et al., 2019, 2021) and were captured in upstream freshwater locations on confirmed spawning grounds (Kahn et al., 2019; Hager et al., 2020).

Atlantic sturgeon were captured by using gill nets made of mesh with stretch measures of 23–36 cm from late July through mid-October during 2013–2019 (see Kahn et al., 2019) in the Pamunkey and Mattaponi Rivers. Our research methods followed the permit requirements

[1] Mention of trade names or commercial companies is for identification purposes only and does not imply endorsement by the National Marine Fisheries Service, NOAA.

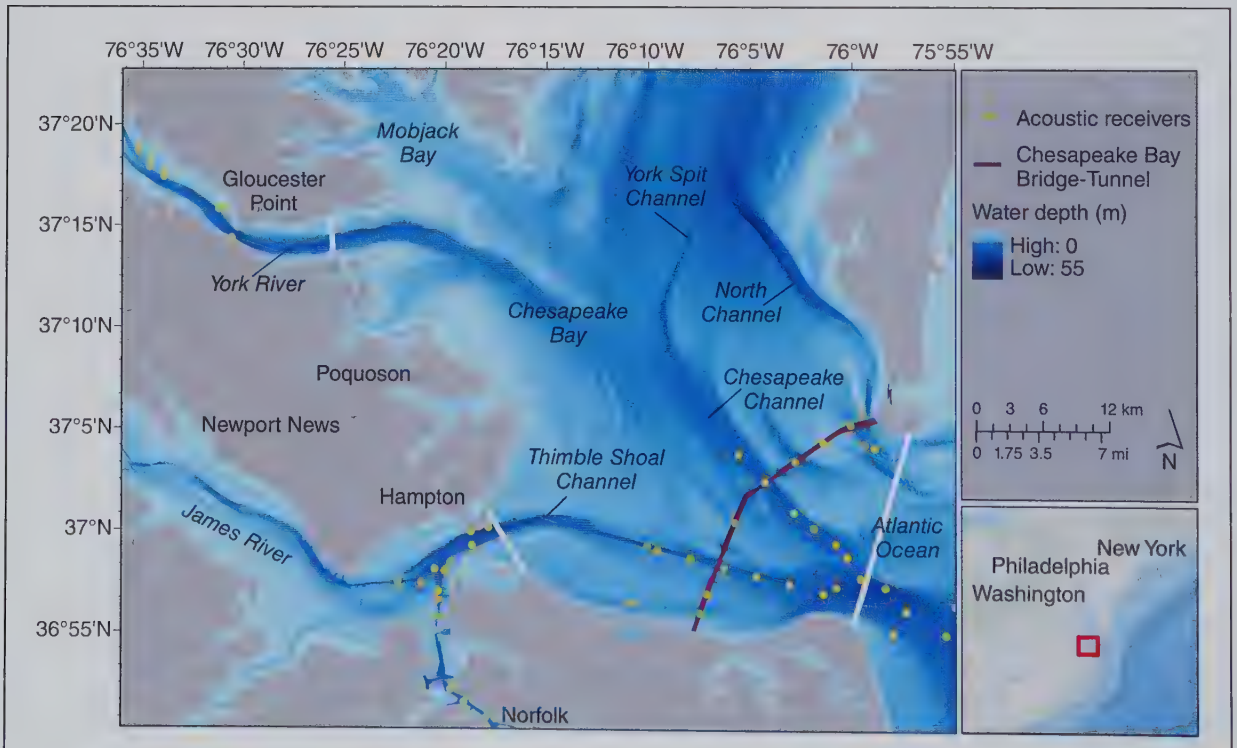


**Figure 1**

Map of the mouth of Chesapeake Bay showing the locations of passive acoustic receivers and the boundaries (white lines) identified to define the extent of Chesapeake Bay for documenting arrival, departure, and residency of tagged Atlantic sturgeon (*Acipenser oxyrinchus oxyrinchus*) in the bay. Fish were monitored with acoustic telemetry from August 2013 through January 2020.

and protocols of the Endangered Species Act (Kahn and Mohead, 2010).

Results of the genetic analysis of a previous study (White et al., 2021) indicate that fish from the York River are distinct from fish from other populations along the East Coast. However, some of the fish implanted with transmitters by our team and used in this study were fish natal to the James, Hudson, and Savannah Rivers, as well as to Albemarle Sound (Kazyak et al., 2021). Therefore, the occupancy timing presented herein is weighted toward adults of the population of the York River but is representative of movements of fish natal to 3 different DPSs.

The sex of individuals was determined by applying pressure to the ventral surface, moving from the anterior to posterior ends, ending at the vent. This technique typically produced milt from males (>90% of the time), and females on occasion produced eggs (<20% of the time). Gravid females were usually confirmed to be female when transmitters were implanted. Sex was routinely confirmed upon recapture (Kahn et al., 2021). Ultimately, sex was confirmed for every fish tagged and recaptured in this study.

During this study, 84 adult Atlantic sturgeon (40 males and 44 females) were implanted with V16P-4H, V16P-6x, or V16-6x acoustic transmitters (Innovasea Systems Inc.), with each tag weighing no more than 17.3 g. Transmitters produced a 69 kHz signal every 70–150 s and had a minimum life span of 6 years (11 transmitters) and a maximum life span of 10 years (73 transmitters). Transmitters were placed into incisions of 3–4 cm that were made most often between the 3rd and 4th ventral scutes anterior to the anal fins. The incisions were closed by using Vicryl dissolvable sutures (Ethicon Inc., Raritan, NJ).

The implanted transmitters were passively detected from August 2013 through January 2020. No females were tagged with acoustic transmitters in 2013; therefore, emigrations in 2013 and immigrations in 2014 were recorded for only males. Through January 2020, 100 acoustic receivers in the York River system, Chesapeake Bay, and Atlantic Ocean remained in place (Fig. 1). They were serviced and their data was downloaded either monthly or every other month depending on their location. Receivers in rivers, Chesapeake Bay, and nearshore waters of the Atlantic Ocean were downward-facing and deployed within 6 m of the surface, and offshore receivers were anchored to the seafloor and recovered with an acoustic release.

When monitoring movements of Atlantic sturgeon, we assumed acoustic transmitters were in fish that were behaving normally. We also performed range tests by using stationary transmitters and receivers at variable distances in Chesapeake Bay near the mouth of the James River. We used transmitters of the same size for the monitoring in this study and for the range tests to minimize error, but detection distances can also be affected by environmental conditions, such as tides and sea state (Mathies et al., 2014). A single stationary transmitter with a 10-s ping rate was deployed, and receivers were deployed every 100 m away from this transmitter. When receivers were placed at a depth of approximately 10 m, the distance at which over 90% of signals from the test transmitter were detected under optimal conditions was 1.3 km; in contrast, for receivers deployed at depths less than 2 m under rough conditions, this detection rate extended out only 200 m. Under various conditions over a 1-week period, receivers within 700 m of the transmitter detected at least 90% of transmissions. For the purposes of understanding when Atlantic sturgeon were present in Chesapeake Bay, we defined presence as multiple detections on 1 receiver or detections on 2 neighboring receivers on the same day. Therefore, any variability in detection distance would lead to underestimation of the timing of arrival and departure. Generally, we expected to detect fish within 700 m of a receiver.

Atlantic sturgeon belonging to the spawning population in the York River spawn only during the fall (August–October) of each year (Kahn et al., 2019; Hager et al., 2020). The times of first arrival to Chesapeake Bay from the Atlantic Ocean, of departure from Chesapeake Bay into tributary river systems, of entry into Chesapeake Bay from those same systems, and of departure from Chesapeake Bay to the Atlantic Ocean were recorded for each transmitter implanted in a fish as ordinal dates and as photoperiod in hours, minutes, and seconds from sunrise to sunset. We report the timing of these movements for each sex but considered mean, median, and timing for different proportions of transmitters (10%, 20%, etc.). In any given year, the general pattern of migration followed a normal distribution once it began; therefore, we report the earliest arrival and latest departure because 1) not all fish in the population are tagged with acoustic transmitters and not all tagged fish were acoustically detected, meaning that the timing is an approximation of actual first arrival or last departure, and 2) the purpose of this analysis was to identify periods of presence and absence from Chesapeake Bay. However, results from analyses of statistical differences are presented as mean values. We recorded the temperature from the nearest source (HOBO data logger, acoustic receiver, or buoy).

Most individuals left Chesapeake Bay in the summer by initiating a spawning run. Non-spawning fish generally remained near the mouth of the bay and were consistently detected throughout the summer, and spawning fish moved farther into the bay and had periods during which they were not detected as they moved through the areas without receiver coverage (Fig. 1). We conservatively calculated residency times in the bay from the date of first detection to the date of last detection, such that data for an animal detected leaving the mouth of the York River in the fall and not detected again were aggregated with data for other tagged fish leaving the river and used to calculate an average date of entry into the bay from the river, but we did not use that single data point to estimate bay residency. However, the dates of first or last detection, when used to calculate residency, were not necessarily representative of the beginning or end of occupancy because receiver coverage was incomplete. These periods of presence in Chesapeake Bay were analyzed by sex, by length and sex (because adult Atlantic sturgeon are sexually dimorphic), and by year.

Each Atlantic sturgeon was classified as either above or below the average length for its sex. Measurements were made by using a 2.44-m PVC T-board with a 3-m tailor's tape measure. The mean lengths of males and females were 1518 and 1880 mm FL (Kahn et al., 2019). Because fish generally grew through time, when adults were recaptured, they occasionally had moved from below average to above average length. For example, Fish 13-015, a male, was captured 6 times during the 7 years of this study (in 2013–2017 and 2019), ranging in size from 1490 to 1548 mm FL. This individual was categorized as *below average* the first 2 years and *above average* the last 5 years. In the event that a fish was not captured in the year of the analysis, its most recent measured length was used for categorization.

Differences in arrival and departure times (ordinal dates) and temperature were assessed by using analysis of variance in statistical software R (vers. 4.2.2; R Core Team, 2022). The significance level was 0.05. When significant differences were identified, Tukey's honestly significant difference test was used to identify significantly different variables. Data were organized in a table identifying sex, size category, year, bay entry, river entry, river departure and arrival, bay departure, photoperiod for each day of arrival and departure, and days spent in the bay before and after each spawning period for each tagged individual. Because photoperiod and day are correlated, only day of the year is discussed for ease in identifying when Atlantic sturgeon were present.

Sampling was conducted under permits from the Virginia Marine Resources Commission, the Virginia Department of Wildlife Resources (formerly the Virginia Department of Game and Inland Fisheries), and the National Marine Fisheries Service (permit nos, 16547 and 19642).

## Results

Both spawning and non-spawning fish regularly utilized Chesapeake Bay, starting as the water began to warm in the spring and ending as it cooled in the fall. The earliest arrival of a tagged Atlantic sturgeon in Chesapeake Bay from the Atlantic Ocean was detected on 27 February for females and on 4 March for males, corresponding to daily mean water temperatures of 7.3°C and 6.5°C at the locations of first detection upon entry, respectively. Males and females generally did not arrive until water temperatures were above 6°C, except for 3 females, who arrived in water as cool as 2.9°C. The latest date of arrival of a fish implanted with an acoustic tag to the bay from the ocean, with the exception of the arrival of a male outlier on 22 August, was recorded on 17 July for males and on 11 July for females, corresponding to daily mean water temperatures of 27.9°C and 26.0°C at their locations of first detection upon entry, respectively. In all years, at least 1 Atlantic sturgeon remained in the bay after its arrival, even during the spawning event, until departure back to the ocean. The latest departure (last detection) from the bay to the ocean after spawning was recorded on 24 January for females and on 27 January for males, corresponding to daily mean water temperatures of 6.3°C and 6.5°C at the locations of last detection, respectively. Atlantic sturgeon generally left Chesapeake Bay for the ocean when water temperatures were approaching a minimum of 6°C, with the exception of a large male that left for the ocean when the daily mean water temperature at its location of last detection was 3.4°C.

The majority of fish were detected moving through Chesapeake Bay on spawning runs. Spawning males were detected in the bay during 78.7% (244 detections of the 310 times males are known to have moved through the bay to reach the river when they were detected) of their spawning runs, and spawning females were detected during 81.2% (108 detections of the 133 times females were known to be present) of theirs. Non-spawning fish did not always return to Chesapeake Bay, but when they did males were detected during 67.7% (23 detections of the 34 times males were known to be present) of their non-spawning years and females detected during 55.0% (61 detections of the 111 times females were known to be present) of theirs. The detection rate between years varied (Table 1), but the locations of the passive acoustic receivers we used to monitor migrations did not.

Males and females were detected in Chesapeake Bay during January or February 1.5% (5 of 344 males) and 1.2% (3 of 244 females) of the time, as both their arrival and departure between the bay and the ocean pushed into winter. There were no significant interannual differences in date of entry to the bay from the ocean in the spring or in date of departure from the bay to the ocean in the fall for males or females (Table 2). However, only 5 of 77 (6.5%) returning fish (male or female) were detected in the bay before 1 April in 2014 (0 fish), in 2015 (1 fish, when the mean daily temperature near the detection location was 10.2°C), and in 2016 (4 fish, when temperatures were 11–12.6°C), but in 2018 and 2019, the first fish were detected entering the bay in February.

Further illustrating this shift in arrival times, in 2018 and 2019, 30.8% of all adults (33 of 107 fish) had entered the bay by 10 April. The first detections in February of 2018 and 2019 were of the same female that arrived when the mean temperature in the bay was 2.9°C and 7.3°C. Likewise, in each of 2013, 2014, 2015, and 2016, cumulatively only 3 fish (of 161 individuals, 1.9%) were detected still out-migrating through the bay toward the ocean during December but, by 2019, 10 fish (of 47 individuals, 21.3%) were detected in the bay in December, with 2 fish remaining in the bay until January. Of those fish detected in December 2019 and January 2020, 9 individuals were tagged with acoustic transmitters in 2013 and 2014, with the other fish tagged with acoustic transmitters in 2015; therefore, the increase in sturgeon presence in December and January following the 2019 spawning season was not just a case of more Atlantic sturgeon being tagged with acoustic transmitters in later years. This apparent extension of the use of Chesapeake Bay was not significant, and only males had any significant differences in interannual behavior (Table 2).

**Table 1**

Numbers of Atlantic sturgeon (*Acipenser oxyrinchus oxyrinchus*) of each sex tagged and the numbers and proportions of males and females that were detected within Chesapeake Bay at some point during a season, either before (pre) or after (post) spawning from 2013 through 2019. Atlantic sturgeon typically do not spawn every year; therefore, values are provided for both spawning and non-spawning fish. NA=not applicable because no tagged male or female Atlantic sturgeon were detected during the specified season.

| | | Spawning | | | | | | Non-spawning | | | | | |
|---|---|---|---|---|---|---|---|---|---|---|---|---|---|
| | | Males | | | Females | | | Males | | | Females | | |
| | | | Detected in bay | | | Detected in bay | | | Detected in bay | | | Detected in bay | |
| Year | Season | No. tagged | No. | % | No. tagged | No. | % | No. tagged | No. | % | No. tagged | No. | % |
| 2013 | Post | 12 | 10 | 0.83 | NA | NA | – | NA | NA | – | NA | NA | – |
| 2014 | Pre | 9 | 8 | 0.89 | NA | NA | – | 3 | 1 | 0.33 | NA | NA | – |
| | Post | 27 | 24 | 0.89 | 9 | 8 | 0.89 | 3 | 0 | 0.00 | NA | NA | – |
| 2015 | Pre | 24 | 23 | 0.96 | 2 | 2 | 1.00 | 4 | 4 | 1.00 | 6 | 4 | 0.67 |
| | Post | 24 | 13 | 0.54 | 4 | 3 | 0.75 | 4 | 3 | 0.75 | 6 | 2 | 0.33 |
| 2016 | Pre | 22 | 21 | 0.96 | 5 | 4 | 0.80 | 3 | 2 | 0.66 | 7 | 4 | 0.57 |
| | Post | 22 | 16 | 0.73 | 12 | 10 | 0.83 | 6 | 2 | 0.33 | 6 | 1 | 0.17 |
| 2017 | Pre | 28 | 25 | 0.89 | 4 | 4 | 1.00 | 3 | 3 | 1.00 | 13 | 11 | 0.85 |
| | Post | 29 | 21 | 0.72 | 17 | 15 | 0.88 | 2 | 2 | 1.00 | 13 | 7 | 0.54 |
| 2018 | Pre | 27 | 26 | 0.96 | 11 | 11 | 1.00 | 2 | 2 | 1.00 | 19 | 14 | 0.74 |
| | Post | 27 | 14 | 0.52 | 14 | 10 | 0.71 | 2 | 2 | 1.00 | 19 | 7 | 0.37 |
| 2019 | Pre | 28 | 24 | 0.86 | 22 | 18 | 0.82 | 1 | 1 | 1.00 | 11 | 8 | 0.73 |
| | Post | 31 | 19 | 0.61 | 33 | 23 | 0.70 | 1 | 1 | 1.00 | 11 | 3 | 0.27 |

The average date of arrival to Chesapeake Bay from the Atlantic Ocean for females was 12 April and for males was 22 April ($P$=0.005), correlating to mean temperatures at the locations of first detection upon entry into the bay of 11.8°C and 13.5°C ($P$=0.01), respectively. Fish of both sexes spent prolonged periods in Chesapeake Bay from entry to initiating a spawning run but took a quicker, more direct route out of the bay after spawning (Fig. 2). Females spent an average of 96.98 d (range: 27–184 d) in the bay before spawning, compared with 82.86 d (range: 3–160 d) for males ($P$=0.051). Males entered their spawning river from the bay on average on 13 July (when the mean temperature in the bay was 25.6°C; range: 11 April–3 September), and females entered on average on 15 July (24.8°C; range: 30 March–7 October). Females, on average, left the York River and reentered the bay on 24 October (19.4°C; range: 17 September–19 December), and males reentered on 25 October (18.8°C; range: 19 September–21 January). Males left the bay for the ocean after spawning on 13 November (15.4°C; range: 25 September–27 January), on average, and the average departure date for females was 9 November (16.6°C; range: 3 October–24 January). Arrival and departure dates relative to average length are provided in Table 3.

After spawning, males spent on average 20.51 d (range: 1–89 d) in Chesapeake Bay, compared with 14.79 d (range: 1–72 d) for females, as they out-migrated ($P$=0.022, for males versus females; $P$=0.11, when considering relative length of each sex). Results from assessment by period, either before or after spawning, indicate that females spent significantly longer in Chesapeake Bay only during the prespawning period in 2015 ($P$=0.02) and 2016 ($P$=0.038), spending 129.00 d (range: 116–142 d) and 115.30 d (range: 74–155 d) in the bay when males spent an average of 72.89 d (range: 26–134 d) and 71.92 d (range: 5–144 d) there. Differences between size groups and sexes were detected for bay entry day, river entry day, river entry temperature, and prespawning days (Table 4).

## Discussion

The Atlantic sturgeon is an endangered species in Chesapeake Bay, and the best mitigation to promote its conservation is limiting potentially harmful interactions by identifying the times Atlantic sturgeon are present in Chesapeake Bay and by planning potentially harmful activities accordingly. Females were recorded in the bay during prespawning periods from 27 February to 7 October. Males entered the bay as early as 4 March and stayed during the spring and summer until as late as 3 September. With the lone exception of the spawning initiation on 7 October, the departure of Atlantic sturgeon from Chesapeake Bay to rivers and reentry into Chesapeake Bay from rivers did not overlap. In every year of this study, females were in the bay from 28 March to 26 November, and males were in the bay from 3 April to 23 November (Fig. 2). Females entered Chesapeake Bay from the Atlantic Ocean earlier than males, with the smallest

**Table 2**

Comparison of annual averages of the days of arrival and departure of tagged Atlantic sturgeon (*Acipenser oxyrinchus oxyrinchus*) into or out of Chesapeake Bay or a river, temperatures in the bay and river at arrival and departure, and number of days tagged fish spent in the bay before and after spawning, by sex. Atlantic sturgeon were monitored with acoustic telemetry from August 2013 through January 2020. Letters denote statistically significant differences ($P \leq 0.05$), with values having like letters not being significantly different from those within the compared group. Arrival and departure days are given as days of the year.

| | Males before spawning | | | | |
|---|---|---|---|---|---|
| Year | Bay entry day | River entry day | Bay entry temp (°C) | River entry temp (°C) | No. of days in bay |
| 2015 | 115.85 | 189.10$^{ab}$ | 14.9 | 25.6$^{ab}$ | 72.89$^{a}$ |
| 2016 | 115.11 | 187.15$^{a}$ | 13.8 | 24.9$^{ab}$ | 71.92$^{a}$ |
| 2017 | 104.00 | 186.22$^{a}$ | 12.5 | 24.5$^{a}$ | 83.21$^{ab}$ |
| 2018 | 114.85 | 194.09$^{ab}$ | 12.4 | 26.1$^{ab}$ | 81.58$^{ab}$ |
| 2019 | 107.41 | 212.09$^{b}$ | 13.7 | 26.7$^{b}$ | 106.46$^{b}$ |
| | Males after spawning | | | | |
| Year | River exit day | Bay exit day | River exit temp (°C) | Bay exit temp (°C) | No. of days in bay |
| 2014 | 289.00$^{a}$ | 309.14 | 20.1$^{a}$ | 15.4 | 20.75 |
| 2015 | 296.25$^{abc}$ | 311.00 | 18.1$^{ab}$ | 17.0 | 20.06 |
| 2016 | 300.45$^{bc}$ | 322.36 | 18.2$^{ab}$ | 14.9 | 21.09 |
| 2017 | 295.53$^{ab}$ | 320.00 | 20.2$^{a}$ | 15.0 | 27.59 |
| 2018 | 300.66$^{bc}$ | 319.72 | 18.6$^{ab}$ | 13.6 | 19.44 |
| 2019 | 306.44$^{c}$ | 319.70 | 17.1$^{b}$ | 14.9 | 12.27 |
| | Females before spawning | | | | |
| Year | Bay entry day | River entry day | Bay entry temp (°C) | River entry temp (°C) | No. of days in bay |
| 2015 | 104.67 | 222.00 | 13.2 | 27.7 | 129.00 |
| 2016 | 104.14 | 197.20 | 13.1 | 22.9 | 115.25 |
| 2017 | 88.47 | 176.25 | 9.4 | 24.2 | 86.50 |
| 2018 | 108.16 | 202.82 | 10.9 | 26.8 | 89.18 |
| 2019 | 103.15 | 192.59 | 13.1 | 23.0 | 96.47 |
| | Females after spawning | | | | |
| Year | River exit day | Bay exit day | River exit temp (°C) | Bay exit temp (°C) | No. of days in bay |
| 2014 | 297.25 | 313.71 | 18.0 | 14.5 | 14.71 |
| 2015 | 287.67 | 310.67 | 19.9 | 17.0 | 20.50 |
| 2016 | 289.67 | 307.18 | 20.8 | 16.9 | 18.70 |
| 2017 | 295.28 | 310.41 | 20.1 | 17.2 | 16.69 |
| 2018 | 292.93 | 311.35 | 21.4 | 16.7 | 12.00 |
| 2019 | 302.85 | 317.96 | 18.0 | 15.2 | 12.13 |

females returning the earliest (Table 4). When spawning, females of below average size (<1880 mm FL) entered the York River the earliest, all males entered roughly at a similar intermediary time, and then significantly later, females of above average size moved into the river (Table 4). The largest females with the most reproductive potential (Mitchell et al. 2020) spent significantly more time each summer in the bay (over 113 d on average) than smaller females or all males. Therefore, the threats faced by Atlantic sturgeon in Chesapeake Bay are disproportionately affecting the largest females of the population, those most critical to the recovery of this population of Atlantic sturgeon.

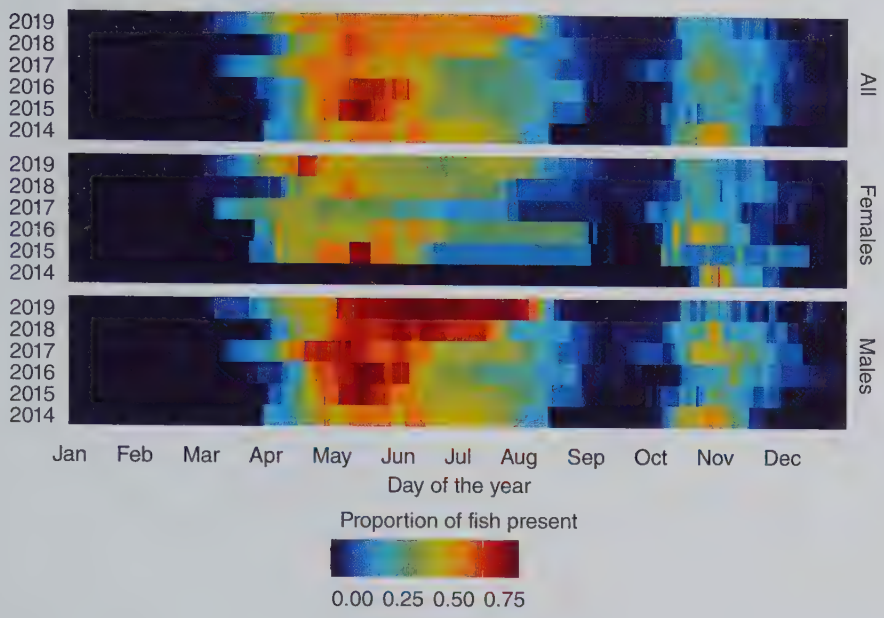


**Figure 2**

Proportion of all tagged Atlantic sturgeon (*Acipenser oxyrinchus oxyrinchus*) present in Chesapeake Bay during the periods before and after spawning from August 2013 through January 2020. Presence of females and males are also shown separately. No females were tagged or available for detection until the fall of 2014. Passive acoustic telemetry was used to monitor tagged fish.

One of the threats in Chesapeake Bay is vessel strike, with the tendency of Atlantic sturgeon to drift along with water flow (Poletto et al., 2014) making them particularly vulnerable to being pulled through the propellers of vessels (Brown and Murphy, 2010; Balazik et al., 2012b; Demetras et al., 2020). In modeling efforts, this suction of propellers is great enough to pull a whale up from a depth equivalent to 2 full ship drafts and into contact with propellers (Silber et al., 2010). When fish are pulled up to propellers, there is a direct linear relationship between length and probability of being struck such that smaller fish have a better chance than longer fish of moving through without contacting a blade. We recommend that vessel operation and movement be timed to avoid, to the extent possible, the periods from 1 April through 31 August and from 15 October through 1 December. Although this timing would avoid interactions with most tagged adult individuals, adult presence between 2013 and 2019, at its extremes, was documented between 27 February and 24 January; therefore, Atlantic sturgeon will face threats in Chesapeake Bay even if those protection periods are established.

Adult Atlantic sturgeon use Chesapeake Bay seasonally, as has been reported for this species in other systems (Dovel and Berggren, 1983; Smith, 1985; Bain, 1997; Dunton et al., 2010; Ingram and Peterson, 2016; Ingram et al., 2019). Atlantic sturgeon overwinter in the Atlantic Ocean, and they move into Chesapeake Bay as waters begin to warm. Males and females generally do not arrive until water temperatures are above 6°C. In general, both males and females have been arriving to the bay earlier and earlier each year (Table 2, Fig. 2). This trend of earlier arrival times is consistent with temperature data (from buoys of the Chesapeake Bay Interpretive Buoy System) that indicate that the warming of Chesapeake Bay begins earlier each year, affecting migratory timing and species distributions in the bay and other areas along the Atlantic coast of the United States (Richardson et al., 2018; Crear et al., 2020; Pinsky et al., 2020). Our observations support the conclusion of Ingram et al. (2019) that use of offshore habitat was influenced primarily by inshore drivers.

Departure of tagged fish from Chesapeake Bay and back into the Atlantic Ocean occurred relatively quickly after spawning (Table 4). On average, females took approximately 2 weeks and males took approximately 3 weeks to move through the bay to the ocean. Females generally left the York River after spawning, and males remained until all females had left. Because the timing of the spawning season of Atlantic sturgeon is driven by temperature and photoperiod (Hager et al., 2020), male out-migration into the bay was significantly later in 2016 and 2018, and the late movement from river to bay became even more extreme in 2019 (Table 2). Despite the change in the day that males reentered the bay from rivers, there was no corresponding change in the day males left the bay for the ocean. Given that nearly every male spawns every year (Hager et al., 2020), acoustic

**Table 3**

Range of ordinal dates of occupancy in Chesapeake Bay for each size class of Atlantic sturgeon (*Acipenser oxyrinchus oxyrinchus*) monitored with acoustic telemetry from August 2013 through January 2020, by sex and season, before (pre) and after (post) spawning. The size classes are below or above average size, which was 1518 and 1880 mm in fork length [FL] for males and females, respectively. The year 2016 was a leap year. A day of the year exceeds 365 or 366 for a particular year because at least 1 fish from that size class remained in Chesapeake Bay into the following calendar year. NA=not available because no females of that size class were detected in that year.

| | | Below average (mm FL) | Above average (mm FL) |
|---|---|---|---|
| Year | Season | Males | |
| 2013 | Post | 276–327 | 275–312 |
| 2014 | Pre | 106–224 | 91–225 |
| | Post | 280–327 | 271–326 |
| 2015 | Pre | 101–242 | 93–239 |
| | Post | 279–333 | 271–370 |
| 2016 | Pre | 69–241 | 91–240 |
| | Post | 283–392 | 285–359 |
| 2017 | Pre | 71–245 | 67–243 |
| | Post | 262–369 | 276–356 |
| 2018 | Pre | 91–246 | 91–243 |
| | Post | 287–335 | 279–374 |
| 2019 | Pre | 85–239 | 63–230 |
| | Post | 284–351 | 285–373 |
| | | Below average (mm FL) | Above average (mm FL) |
| Year | Season | Females | |
| 2013 | Post | NA | NA |
| 2014 | Pre | NA | NA |
| | Post | 293–326 | 278 |
| 2015 | Pre | 85–200 | 103–244 |
| | Post | 278–349 | 273–287 |
| 2016 | Pre | 87–247 | 88–242 |
| | Post | 275–330 | 284–309 |
| 2017 | Pre | 68–210 | 90–205 |
| | Post | 270–347 | 260–320 |
| 2018 | Pre | 59–243 | 87–235 |
| | Post | 277–335 | 282–374 |
| 2019 | Pre | 58–252 | 64–280 |
| | Post | 272–365 | 270–389 |

detections of tagged males in Chesapeake Bay in the fall were generally a result of them leaving the York River. However, because fewer than half of all females spawn each year, detections of tagged females from September until they left the bay for the ocean were not necessarily a result of them leaving a river. Atlantic sturgeon continued to leave the bay at similar temperatures each year regardless of spawning status, size, or sex (Tables 2 and 4), indicating that the cue for exiting the bay is either day or temperature and not simply a rapid migration from spawning river to ocean once spawning is complete.

## Conclusions

Atlantic sturgeon face the greatest risk of interacting with anthropogenic threats when in estuarine and fresh water. Virginia and Maryland both support a variety of fisheries in Chesapeake Bay that have bycatch of Atlantic sturgeon (Welsh et al., 2002; Stein et al., 2004; ASSRT, 2007; Trice[2]). Water quality in Chesapeake Bay has improved somewhat in the past 50 years, but large areas are still hypoxic or anoxic (Scavia et al., 2021; Tian et al., 2022). Vessel strikes are the most frequently observed source of mortality of Atlantic sturgeon in Chesapeake Bay (in records of Atlantic sturgeon salvaged and reported under National Marine Fisheries Service permit no. 21858), despite very low reporting rates (Brown and Murphy, 2010; Balazik et al., 2012b; Fox et al.[3]).

The results of our research indicate that Atlantic sturgeon use Chesapeake Bay primarily when water temperatures exceed 6°C. When Chesapeake Bay is cooler, Atlantic sturgeon in coastal waters off mid-Atlantic states seek thermal refuge in offshore waters (Ingram et al., 2019; Rothermel et al., 2020; Hager and Breault[4]). The amount of the year during which water temperatures are higher than 6°C in Chesapeake Bay is increasing relatively rapidly. When this study began in 2013, the period of offshore overwintering by Atlantic sturgeon was 2–4 months, but the length of that period has fallen to approximately 35 d in 2019. Waters along the Atlantic coast of the United States are expected to continue warming through the 21st century (IPCC, 2023), affecting the timing of arrivals and departures of Atlantic sturgeon into and from Chesapeake Bay. As waters in Chesapeake Bay provide more days of hospitable temperatures for Atlantic sturgeon, we anticipate and have observed a corresponding increase in their use of Chesapeake Bay, particularly by the largest females (>1880 mm FL), who currently spend significantly longer in Chesapeake Bay than fish of any other sizes (Table 4). All adult Atlantic sturgeon in Chesapeake Bay are subject to the threats of vessel strike, poor water quality, and bycatch. Vessel strikes appear to pose the greatest threat

[2] Trice, G. E., IV. 2014. Observing striped bass and Atlantic sturgeon bycatch in a striped bass fishery using raised footlines in the Chesapeake Bay, 9 p. Fishery Resource Grant FRG 2014-02. Va. Inst. Mar. Sci., William Mary, Gloucester Point, Va. [Available from website.]

[3] Fox, D. A., E. A. Hale, and J. A. Sweka. 2020. Examination of Atlantic sturgeon vessel strikes in the Delaware River estuary, 36 p. Final report for NMFS award no. NA16NMF4720357. [Available from Agric. Annex Rm. 123, Del. State Univ., 1200 N. DuPont Hwy., Dover, DE 19901.]

[4] Hager, C., and D. K. Breault. 2023. Spatiotemporal distributions of species detected within Virginia's offshore lease areas. Volume 2: The Virginia Wind Energy Lease Area A-0483, 141 p. Report to Bureau of Ocean Energy Management for contract no. 140M0122P0023. [Available from Chesapeake Scientific LLC, 100 Sixpence Ct., Williamsburg, VA 23185.]

**Table 4**

Comparison of average seasonal residency in Chesapeake Bay and its rivers for tagged Atlantic sturgeon (*Acipenser oxyrinchus oxyrinchus*) monitored with acoustic telemetry from August 2013 through January 2020, by sex and size class. Average days of arrival in the bay and then in a river, days of departure from that river and then from the bay, temperatures in the bay and river at entry and exit, and number of days tagged fish spent in the bay each season, before and after spawning, are provided. The size classes are below or above average size (BA or AA), which was 1518 and 1880 mm in fork length for males and females, respectively. Letters denote statistically significant differences ($P \leq 0.05$), with values having like letters not being significantly different from values in each column for arrivals and departures separately. Days of entry and exit are given as days of the year.

| | | Before spawning | | | | |
|---|---|---|---|---|---|---|
| Sex | Size class | Bay entry day | River entry day | Bay entry temp (°C) | River entry temp (°C) | No. of days |
| Female | AA | $104.77^{ab}$ | $218.88^{b}$ | 12.22 | $27.02^{b}$ | $113.61^{a}$ |
| | BA | $100.51^{a}$ | $179.35^{a}$ | 11.46 | $23.18^{a}$ | $83.36^{b}$ |
| Male | AA | $111.56^{b}$ | $196.09^{c}$ | 13.78 | $26.10^{b}$ | $86.15^{b}$ |
| | BA | $112.18^{b}$ | $191.04^{ac}$ | 13.13 | $24.82^{a}$ | $77.45^{b}$ |
| | | After spawning | | | | |
| Sex | Size class | River exit day | Bay exit day | River exit temp (°C) | Bay exit temp (°C) | No. of days |
| Female | AA | 294.33 | 311.31 | 20.25 | 16.69 | 14.84 |
| | BA | 298.07 | 313.44 | 18.86 | 16.01 | 14.76 |
| Male | AA | 297.19 | 316.04 | 18.96 | 15.08 | 21.44 |
| | BA | 298.60 | 316.92 | 18.46 | 15.42 | 19.04 |

to populations of this species, and the larger the fish, the less likely it is to pass through a propeller without being struck, disproportionately threatening large females who also have the greatest fecundity. The U.S. Congress established the Endangered Species Act to require federal agencies and encourage states to protect endangered species like the Atlantic sturgeon. The data provided herein should allow managers to establish appropriate avoidance periods to protect Atlantic sturgeon and prevent the extirpation of populations of Chesapeake Bay.

## Resumen

El esturión del Atlántico (*Acipenser oxyrinchus oxyrinchus*) está incluido la Ley de Especies Amenazadas desde 2012, con una fracción de la población de la bahía de Chesapeake listada como en peligro. Rastreamos los lapsos de ocupación y movimiento de esturiones adultos en la bahía de Chesapeake del Atlántico procedentes del río York para identificar cuándo es probable que el esturión del Atlántico interactúe con las amenazas antropogénicas. Monitoreamos 84 esturiones del Atlántico adultos (40 machos y 44 hembras) desde agosto de 2013 hasta enero de 2020 mediante telemetría acústica. Tanto los peces desovantes como los no-desovantes utilizaron regularmente la bahía de Chesapeake, con hembras y machos llegando desde el 27 de febrero (cuando la temperatura media del agua fue de 7.7°C) y el 4 de marzo (6.5°C) y partiendo el 24 de enero (6.3°C) y el 27 de enero (6.5°C), respectivamente. La mayor ocupación en la bahía por el esturión del Atlántico fue del 1 de abril al 31 de agosto y de nuevo del 15 de octubre al 1 de diciembre. Antes de desovar, las hembras de tamaño mayor al promedio (>1880 mm de longitud furcal) pasaron significativamente más tiempo en la bahía (>113 d) que las hembras más pequeñas y todos los machos. Por lo tanto, las hembras capaces de producir la mayor cantidad de huevos estuvieron desproporcionadamente expuestas a las amenazas antropogénicas. Aunque los cambios en las fechas de llegada y salida no son estadísticamente significativos, durante los 7 años de este estudio, tanto los machos como las hembras generalmente llegaron antes y se marcharon más tarde cada año que el anterior, aumentando en un mes la residencia en la Bahía de Chesapeake.

## Acknowledgments

This research was made possible by technicians of Chesapeake Scientific LLC, the Pamunkey Indian Tribe, personnel of the U.S. Fish and Wildlife Service, National Marine Fisheries Service and U.S. Navy, and, for river access,

W. Tyler. Funding was provided by the U.S. Navy (contract nos. N62470-10-D-3011, N62470-15-D-8006, and N62470-09-D-2003) and the National Marine Fisheries Service (contract no. NA18NMF4720076, through the Tribal Grant Program).

## Literature cited

ASMFC (Atlantic States Marine Fisheries Commission).
2017. 2017 Atlantic sturgeon benchmark stock assessment and peer review report, 374 p. ASMFC, Arlington, VA. [Available from website.]

ASSRT (Atlantic Sturgeon Status Review Team).
2007. Status review of Atlantic sturgeon (*Acipenser oxyrinchus oxyrinchus*), 174 p. Report to the Northeast Regional Office, National Marine Fisheries Service. [Available from website.]

Bain, M. B.
1997. Atlantic and shortnose sturgeons of the Hudson River: common and divergent life history attributes. Environ. Biol. Fishes 48:347–358.

Balazik, M. T., G. C. Garman, J. P. Van Eenennaam, J. Mohler, and L. C. Woods III.
2012a. Empirical evidence of fall spawning of Atlantic sturgeon in the James River, Virginia. Trans. Am. Fish. Soc. 141:1465–1471.

Balazik, M. T., K. J. Reine, A. J. Spells, C. A. Fredrickson, M. L. Fine, G. C. Garman, and S. P. McIninch.
2012b. The potential for vessel interactions with adult Atlantic sturgeon in the James River, Virginia. North Am. J. Fish. Manage. 32:1062–1069.

Balazik, M. T., D. J. Farrae, T. L. Darden, and G. C. Garman.
2017. Genetic differentiation of spring-spawning and fall-spawning male Atlantic sturgeon in the James River, Virginia. PLoS ONE 12(7):e0179661.

Bemis, W. E., and B. Kynard.
1997. Sturgeon rivers: an introduction to acipenseriform biogeography and life history. Environ. Biol. Fishes 48:167–183.

Brown, J. J., and G. W. Murphy.
2010. Atlantic sturgeon vessel-strike mortalities in the Delaware Estuary. Fisheries 35:72–83.

Crear, D. P., B. E. Watkins, M. A. M. Friedrichs, P. St-Laurent, and K. C. Weng.
2020. Estimating shifts in phenology and habitat use of cobia in Chesapeake Bay under climate change. Front. Mar. Sci. 7:579135.

Dadswell, M.
2006. A review of the status of Atlantic Sturgeon in Canada, with comparisons to populations in the United States and Europe. Fisheries 31:218–229.

Demetras, N. J., B. A. Helwig, and A. S. McHuron.
2020. Reported vessel strike as a source of mortality of White Sturgeon in San Francisco Bay. Cal. Fish Wild. J. 106:59–65.

Dovel, W. L., and T. J. Berggren.
1983. Atlantic sturgeon of the Hudson River estuary, New York. N. Engl. Fish Game J. 30:140–172.

Dunton, K. J., A. Jordaan, K. A. McKown, D. O. Conover, and M. G. Frisk.
2010. Abundance and distribution of Atlantic sturgeon (*Acipenser oxyrinchus*) within the Northwest Atlantic Ocean, determined from five fishery-independent surveys. Fish. Bull. 108:450–465.

Farrae, D. J., W. C. Post, and T. L. Darden.
2017. Genetic characterization of Atlantic sturgeon, *Acipenser oxyrinchus oxyrinchus*, in the Edisto River, South Carolina and identification of genetically discrete fall and spring spawning. Conserv. Genet. 18:813–823.

Grunwald, C., L. Maceda, J. Waldman, J. Stabile, and I. Wirgin.
2008. Conservation of Atlantic sturgeon *Acipenser oxyrinchus oxyrinchus*: delineation of stock structure and distinct population segments. Conserv. Genet. 9:1111–1124.

Federal Register.
2012a. Endangered and threatened wildlife and plants; threatened and endangered status for distinct population segments of Atlantic sturgeon in the Northeast Region. Fed. Regist. 77:5880–5912. [Available from website.]
2012b. Endangered and threatened wildlife and plants; final listing determinations for two distinct population segments of Atlantic sturgeon (*Acipenser oxyrinchus oxyrinchus*) in the Southeast. Fed. Regist. 77:5914–5982. [Available from website.]

Hager, C., J. Kahn, C. Watterson, J. Russo, and K. Hartman.
2014. Evidence of Atlantic Sturgeon (*Acipenser oxyrinchus*) spawning in the York River system. Trans. Am. Fish. Soc. 143:1217–1219.

Hager, C. H., J. C. Watterson, and J. E. Kahn.
2020. Spawning drivers and frequency of endangered Atlantic Sturgeon in the York River system. Trans. Am. Fish. Soc. 149:474–485.

Ingram, E. C., and D. L. Peterson.
2016. Annual spawning migrations of adult Atlantic sturgeon in the Altamaha River, Georgia. Mar. Coast. Fish. 8:595–606.

Ingram, E. C., R. M. Cerrato, K. J. Dunton, and M. G. Frisk.
2019. Endangered Atlanitc Sturgeon in the New York Wind Energy Area: implications of future development in an offshore wind energy site. Sci. Rep. 9:12432.

IPCC (Intergovernmental Panel on Climate Change).
2023. Climate change 2023: synthesis report. Contribution of working groups I, II and III to the sixth assessment report of the Intergovernmental Panel on Climate Change, 184 p. IPCC, Geneva, Switzerland. [Available from website.]

Kahn, J., and M. Mohead.
2010. A protocol for use of shortnose, Atlantic, Gulf, and green sturgeons. NOAA Tech. Memo. NMFS-OPR-45, 62 p.

Kahn, J. E., C. Hager, J. C. Watterson, N. Mathies, and K. J. Hartman.
2019. Comparing abundance estimates from closed population mark-recapture models of endangered adult Atlantic sturgeon. Endanger. Species Res. 39:63–76.

Kahn, J. E., J. C. Watterson, C. H. Hager, N. Mathies, and K. J. Hartman.
2021. Calculating adult sex ratios from observed breeding sex ratios for wide-ranging, intermittently breeding species. Ecosphere 12(5):e03504.

Kahnle, A. W., K. A. Hattala, and K. McKown.
2007. Status of Atlantic sturgeon of the Hudson River estuary, New York, USA. Am. Fish. Soc. Symp. 56:347–363.

Kazyak, D. C., S. L. White, B. A. Lubinski, R. Johnson, and M. Eackles.
2021. Stock composition of Atlantic sturgeon (*Acipenser oxyrinchus oxyrinchus*) encountered in marine and estuarine environments on the U.S, Atlantic Coast. Conserv. Genet. 22:767–781.

Mathies, N. H., M. B. Ogburn, G. McFall, and S. Fangman.
2014. Environmental interference factors affecting detection range in acoustic telemetry studies using fixed receiver arrays. Mar. Ecol. Prog. Ser. 495:27–38.

Mitchell, S. M. J., M. J. Dadswell, C. Ceapa, and M. J. W. Stokesbury.
2020. Fecundity of Atlantic sturgeon (*Acipenser oxyrinchus* Mitchill, 1815) captured by the commercial fishery in the Saint John River, New Brunswick, Canada. J. Appl. Ichthyol. 36:142–150.

Peterson, D. L., P. Schueller, R. DeVries, J. Fleming, C. Grunwald, and I. Wirgin.
2008. Annual run size and genetic characteristics of Atlantic Sturgeon in the Altamaha River, Georgia. Trans. Am. Fish. Soc. 137:393–401.

Pinsky, M. L., R. L. Selden, and Z. J. Kitchel.
2020. Climate-driven shifts in marine species ranges: scaling from organisms to communities. Annu. Rev. Mar. Sci. 12:153–179.

Poletto, J. B., D. E. Cocherell, N. Ho, J. J. Cech Jr., A. P. Klimley, and N. A. Fangue.
2014. Juvenile green sturgeon (*Acipenser medirostris*) and white sturgeon (*Acipenser transmontanus*) behavior near water-diversion fish screens: experiments in a laboratory swimming flume. Can. J. Fish. Aquat. Sci. 71:1030–1038.

R Core Team.
2014. R: a language and environment for statistical computing. R Foundation for Statistical Computing, Vienna, Austria. [Available from website, accessed December 2022.]

Richardson, J. P., J. S. Lefcheck, and R. J. Orth.
2018. Warming temperatures alter the relative abundance and distribution of two co-occurring foundational seagrasses in Chesapeake Bay, USA. Mar. Ecol. Prog. Ser. 599:65–74.

Rothermel, E. R., M. T. Balazik, J. E. Best, M. W. Breece, D. A. Fox, B. I. Gahagan, D. E. Haulsee, A. L. Higgs, M. H. P. O'Brien, M. J. Oliver, et al.
2020. Comparative migration ecology of striped bass and Atlantic sturgeon in the US Southern mid-Atlantic bight [sic] flyway. PLoS ONE 15(6):e0234442.

Savoy, T., L. Maceda, N. K. Roy, D. Peterson, and I. Wirgin.
2017. Evidence of natural reproduction of Atlantic sturgeon in the Connecticut River from unlikely sources. PLoS ONE 12(4):e0175085.

Scavia, D., I. Bertani, J. M. Testa, A. J. Bever, J. D. Blomquist, M. A. M. Friedrichs, L. C. Linker, B. D. Michael, R. R. Murphy, and G. W. Shenk.
2021. Advancing estuarine ecological forecasts: seasonal hypoxia in Chesapeake Bay. Ecol. Appl. 31(6):e02384.

Silber, G. K., J. Slutsky, and S. Bettridge.
2010. Hydrodynamics of a ship/whale collision. J. Exp. Mar. Biol. Ecol. 391:10–19.

Smith, T. I. J.
1985. The fishery, biology, and management of Atlantic sturgeon, *Acipenser oxyrhynchus*, in North America. Environ. Biol. Fishes 14:61–72.

Stein, A. B., K. D. Friedland, and M. Sutherland.
2004. Atlantic sturgeon marine distribution and habitat use along the northeastern coast of the United States. Trans. Am. Fish. Soc. 133:527–537.

Stevenson, J. T.
1997. Life history characteristics of Atlantic sturgeon (*Acipenser oxyrinchus*) in the Hudson River and a model for fishery management. M.S. thesis, 222 p. Univ. Maryland, College Park, MD.

Tian, R., C. F. Cerco, G. Bhatt, L. C. Linker, and G. W. Shenk.
2022. Mechanisms controlling climate warming impact on the occurrence of hypoxia in Chesapeake Bay. J. Am. Water Resour. Assoc. 58:855–875.

Waldman, J., S. E. Alter, D. Peterson, L. Maceda, N. Roy, and I. Wirgin.
2019. Contemporary and historical effective population sizes of Atlantic sturgeon *Acipenser oxyrinchus oxyrinchus*. Conserv. Genet. 20:167–184.

Welsh, S. A., S. M. Eyler, M. F. Mangold, and A. J. Spells.
2002. Capture locations and growth rates of Atlantic Sturgeon in the Chesapeake Bay. Am. Fish. Soc. Symp. 28:183–194.

White, S. L., D. C. Kazyak, T. L. Darden, D. J. Farrae, B. A. Lubinski, R. L. Johnson, M. S. Eakles, M. T. Balazik, H. M. Brundage III, A. G. Fox, et al.
2021. Establishment of a microsatellite genetic baseline for North American Atlantic sturgeon (*Acipenser o. oxyrinchus*) and range-wide analysis of population genetics. Conserv. Genet. 22:977–992.

Wirgin, I., M. W. Breece, D. A. Fox, L. Maceda, K. W. Wark, and T. King.
2015. Origin of Atlantic Sturgeon collected off the Delaware coast during spring months. North Am. J. Fish. Manage. 35:20–30.

National Marine
Fisheries Service
NOAA

*Fishery Bulletin*
established in 1881

Spencer F. Baird
First U.S. Commissioner
of Fisheries and founder
of *Fishery Bulletin*

# Modeling somatic and otolith growth of the central subpopulation of northern anchovy (*Engraulis mordax*) by incorporating seasonality

**Brittany D. Schwartzkopf (contact author)**[1]
**Emmanis Dorval**[1,2]
**Dianna L. Porzio**[3]
**Jonathan M. Walker**[1,4]
**Kelsey C. James**[1]
**Brad E. Erisman**[1]

Email address for contact author: brittany.schwartzkopf@noaa.gov

[1] Fisheries Resources Division
Southwest Fisheries Science Center
National Marine Fisheries Service, NOAA
8901 La Jolla Shores Drive
La Jolla, California 92037

[2] Lynker
(under contract with NOAA Southwest Fisheries Science Center)
202 Church Street SE #536
Leesburg, Virginia 20175

[3] Marine Region
California Department of Fish and Wildlife
2451 Signal Street, AltaSea Berth 59
San Pedro, California 90731

[4] Cooperative Institute for Marine, Earth, and Atmospheric Systems
University of California Santa Cruz
1156 High Street
Santa Cruz, California 95064

**Abstract**—Somatic growth parameters are used in age-structured stock assessment models, such as those used to assess the federally managed northern anchovy (*Engraulis mordax*); therefore, incorrect estimation of growth can cause errors that affect estimates from stock assessments. To our knowledge, we completed the first comprehensive investigation to model somatic and otolith growth of the central subpopulation of northern anchovy (CSNA), which has a range from Northern California to Baja California, Mexico, by using fishery-dependent and fishery-independent data. Five growth models were fitted to length-at-age data, including 2 models that account for seasonal growth oscillations, to determine the model that best described growth. Seasonal growth oscillations were found for the CSNA, and the best fitting models were the ones that accounted for seasonality. The fastest growth occurred during summer, and growth decreased 90% in winter. Large variations in length at age and extensive overlap of lengths across ages were found for the CSNA, typical observations for fish with an opportunistic life history strategy that respond rapidly to changing environmental conditions in dynamic ecosystems. Traditional growth models overestimated mean asymptotic length and underestimated the growth coefficient in comparison to results from the seasonal growth models. Accurately describing growth of the CSNA by accounting for seasonality is important to limiting biases that may propagate in stock assessments and management decisions.

Manuscript submitted 20 April 2023.
Manuscript accepted 15 November 2023.
Fish. Bull. 121:172–187 (2023).
Online publication date: 6 December 2023.
doi: 10.7755/FB.121.4.3

The views and opinions expressed or implied in this article are those of the author (or authors) and do not necessarily reflect the position of the National Marine Fisheries Service, NOAA.

Somatic growth rate is an important determinant of population growth and recruitment in marine fish species (Kerns and Lombardi-Carlson, 2017). Clupeoids have an opportunistic life history strategy, which is characterized by rapid somatic growth, high mortality rates, short life spans, and protracted spawning seasons in response to environmental conditions (Blaxter and Hunter, 1982; Armstrong and Shelton, 1990; Winemiller and Rose, 1992). Clupeoids opportunistically utilize favorable environmental conditions that vary on different scales, such as the conditions of the California Current Ecosystem (CCE), which vary on daily, interannual, and decadal scales (McClatchie, 2014), leading to high variation in growth rates of individuals and large annual and seasonal fluctuations in growth (Spratt, 1975; Mallicoate and Parrish, 1981; Cubillos et al., 2001). The rapid response of fish to favorable environmental conditions leads to changes in growth rate and mortality that contribute to natural, large fluctuations in recruitment and population sizes of clupeoids (Blaxter and Hunter, 1982; Thayer et al., 2017; Sydeman et al., 2020).

Estimating somatic growth rate correctly is important, as it is a primary biological characteristic used in fisheries assessments, management, and research (Kerns and Lombardi-Carlson, 2017). Somatic growth characteristics are used as parameters in age-structured stock assessment models, such as those used to assess biomass of coastal pelagic species (CPS) in the North Pacific Ocean along the West Coast of the United States (Methot, 1989; Crone et al., 2019; Kuriyama et al., 2020, 2022). Incorrectly estimating growth characteristics, whether as a result of aging errors or use of improper growth models, can cause errors that affect estimates of other biological characteristics, such as age at maturity, length at age, and weight at age, and estimates of

fishery indices, such as catch at age and biomass, that depend on age data (Reeves, 2003). Incorrect estimation of growth characteristics can also lead to errors in estimates of recruitment and total allowable catch allocated to fisheries in assessment models (Reeves, 2003) and to errors that can significantly mask relationships between stocks and recruitment and between environmental factors and year-class strength (Fournier and Archibald, 1982; Richards et al., 1992).

Many fishes have seasonal oscillations in growth, and not incorporating this seasonality in data analysis when it is present can lead to incorrect estimation of somatic growth characteristics (Liu et al., 2021). Misspecifications of growth models can affect the computation of recruitment (age-0 fish) and estimation of biomass (age-1+ fish), information that is used to manage CPS stocks and set harvest guidelines (Reeves, 2003; Stawitz et al., 2019; Kuriyama et al., 2020). Unless seasonal effects can be explicitly accounted for in growth models, only information for samples collected from the same season should be compared (Shoup and Michaletz, 2017), an important consideration when samples are collected year-round. When seasonality was ignored for small species of commercial importance in coastal areas of the China Seas, the fat greenling (*Hexagrammos otakii*) and yellow croaker (*Larmichthys polyactis*), Liu et al. (2021) found that biological reference points were underestimated, an outcome that was attributed to incorrect estimation of growth parameters resulting from ignoring seasonal growth patterns. The underestimation of biological reference points indicates that a species is less productive than it actually is and can result in the loss of potential yield (Liu et al., 2021).

The most commonly used function to model fish growth is the von Bertalanffy growth function (VBGF) (von Bertalanffy, 1938; Ogle et al., 2017), which does not account for seasonality. Several models that modify the VBGF have been proposed to account for seasonal growth oscillations (Ogle et al., 2017). Seasonal growth models, like the 2 commonly used functions of Somers (1988) and Pauly et al. (1992), account for periods of faster and slower growth within a year. The Somers (1988) function allows modeled growth to be reduced, completely stopped, or decreased, whereas the function of Pauly et al. (1992) does not allow decreasing growth but can be used to model prolonged periods of no growth.

The northern anchovy (*Engraulis mordax*) is one of the most abundant forage fish species in the CCE and is consumed by many different species (e.g., marine mammals, seabirds, salmon, tunas, and sharks), making it an important part of the food web (Koehn et al., 2017; Thompson et al., 2022). Similar to other clupeoid species, the northern anchovy is characterized by high interannual variability in recruitment success and population abundance in response to environmental conditions (Methot, 1983; MacCall et al., 2016; Thayer et al., 2017; Sydeman et al., 2020). Additionally, the northern anchovy is a multiple batch spawner with a protracted spawning season; spawning may occur year-round, but peak spawning generally occurs from January through April (Hunter and Macewicz, 1980; Hunter and Leong, 1981; Dorval et al., 2018).

Three subpopulations, the northern, central, and southern subpopulations, are recognized for northern anchovy on the basis of morphometric and meristic characteristics (McHugh, 1951; Vrooman et al., 1981); however, Lecomte et al. (2004) did not detect genetic structure across its range. The central subpopulation of northern anchovy (CSNA) ranges between San Francisco, California, and the middle of the Baja California Peninsula in Mexico. The CSNA is managed in U.S. waters under the Coastal Pelagic Species Management Plan (PFMC, 2019) and was last assessed in 2021 (Kuriyama et al., 2022), 26 years after the previous assessment. The current assumption is that the overall population size is at or around its highest level since the development of quantitative monitoring in the CCE around 70 years ago (Thompson et al., 2019, 2022).

No recent work has included examination of somatic growth of the CSNA, despite its ecological role in the CCE and the importance of growth estimates in informing stock assessments. The most recent work examining growth of northern anchovy through the adult stage was done by Parrish et al. (1985), and a few limited studies have provided values of growth parameters (i.e., mean asymptotic length [$L_\infty$] and the growth coefficient [$K$]) calculated by using traditional growth models (Spratt, 1975; Cisneros et al., 1990). In no work have seasonal growth oscillations of northern anchovy been modeled by using traditional growth models (e.g., the VBGF) with data on fish collected year-round, but seasonal variations in growth of northern anchovy have been generally observed (Mallicoate and Parrish, 1981; Methot, 1983; Parrish et al., 1985; Butler, 1989; Takahashi et al., 2012). Seasonal growth oscillations have been reported for other engraulids (Palomares et al., 1987; Cubillos and Arancibia, 1993; Bellido et al., 2000; Bilgin et al., 2013; Cerna and Plaza, 2016). Northern anchovy reportedly live up to 8 years (Mallicoate and Parrish, 1981), but older individuals (i.e., age-4+ fish) are thought to be relatively scarce (Collins, 1969; Spratt, 1975; Mallicoate and Parrish, 1981; Parrish et al., 1985). Understanding the age structure and growth patterns of northern anchovy is important, as it is a model species for examining and projecting the effects of climate change on clupeoids and marine communities in the CCE and on fisheries management (Muhling et al., 2019, 2020; Tommasi et al., 2021).

The goal of this study was to update the age and growth patterns of the CSNA to inform future stock assessments. The objectives were to model growth and determine whether the CSNA has seasonal growth oscillations 1) by comparing estimates from 3 growth models, the Gompertz, logistic, and von Bertalanffy growth functions, to integer age data; 2) by calculating fractional ages and comparing estimates between the VBGF and 2 models allowing seasonal growth oscillations (Somers, 1988; Pauly et al., 1992); and 3) by examining seasonal variations in the relationships of weight to body length and of body length to otolith length.

## Materials and methods

### Data sources and collection methods

Samples from the CSNA were collected during both fishery-dependent and fishery-independent surveys from 2015 through 2021. Fishery-independent data were collected as part of acoustic-trawl surveys of CPS conducted aboard the NOAA Ships *Reuben Lasker* and *Bell M. Shimada* by the NOAA Southwest Fisheries Science Center (SWFSC) in summer and fall (June–September) for each year in 2015–2021, as well as in spring (March and April) in 2017 and 2021 (Dorval et al., 2018; Stierhoff et al., 2019; Zwolinski et al., 2019; Stierhoff et al., 2020, 2021a, 2021b). The primary objectives of the SWFSC trawl survey are 1) to survey the distributions and abundances of CPS and their abiotic environments in the CCE and 2) to measure size–frequency distributions and to gather life history information (Stierhoff et al., 2020; Renfree et al., 2022), in order to produce length and age composition data for use in acoustic biomass estimation and stock assessment models.

Sagittal otolith samples were collected by using a 2-stage sampling design that follows best practices (Miranda and Colvin, 2017). For the first stage, a maximum of 75 individuals of the CSNA were randomly collected from each nighttime trawl haul, and each individual fish was measured for standard length (SL) to the nearest millimeter and for total weight (TW) to the nearest 0.5 g. For the second stage, 25 individuals that had lengths that encompassed the size distribution of the first-stage samples were selected for otolith extraction and aging by the SWFSC. A complete description of the data collection methods of the SWFSC trawl survey can be found in Dorval et al. (2022) and Schwartzkopf et al. (2022).

Fishery-dependent samples were collected by the California Department of Fish and Wildlife (CDFW) during port sampling of commercial fishery landings. The CDFW sampling plan for CPS is based on a stratified-random design, where samples are collected during 12 random days within each month of the year for each of the port areas where the majority of landings occur: the areas of Monterey, Santa Barbara, and Los Angeles. The majority of fish were collected off Monterey, but in 2016 some additional samples were collected off Los Angeles. For each vessel from which landings were sampled, 25 fish were randomly selected throughout the offload period and brought back to a lab, where they were measured for SL to the nearest millimeter and for TW to the nearest 0.1 g. Otoliths were then extracted for aging to be completed by the CDFW. A complete description of the design and methods of data collection by the CDFW can be found in Dorval et al. (2022). The combined data from fishery-dependent and fishery-independent surveys used in the CSNA stock assessment models were collected year-round, allowing seasonality to be explored.

### Age determination

Whole (i.e., not sectioned) otoliths were immersed in distilled water in a glass dish with a black background for no longer than 3 min, counts were made of the number of annuli observed on the distal side of the otolith, and edge type was determined. Aging was conducted by using a dissecting microscope with reflected light at a magnification of 25×. An annulus is defined as the interface between an inner translucent growth increment and the successive outer opaque growth increment (Collins and Spratt, 1969; Yaremko, 1996; Schwartzkopf et al., 2022). To our knowledge, annual age determination has not been validated for the northern anchovy, but first annulus formation and annual age determination has been validated for the European anchovy (*E. encrasicolus*) (Aldanondo et al., 2016; Uriarte et al., 2016; Basilone et al., 2020); therefore, we assumed this validation held true for the northern anchovy.

Integer age was assigned on the basis of a June birthdate by using the capture date and interpretation of the most distal pair of increments (Collins and Spratt, 1969; Schwartzkopf et al., 2022). Because samples were collected year-round, fractional age was also determined by dividing the integer age by 12 and by using a June birthdate. Age data from both fishery-independent and fishery-dependent surveys and from all years were combined because we were interested in modeling growth of the CSNA as a whole (similar to the modeling done in the stock assessment) and because effects of these factors (i.e., year and type of survey) are beyond the scope of this work. Sample sizes by age for each month of sampling can be found in Supplementary Table 1 (online only).

### Relationships of standard length to weight and to otolith length

We fit a generalized linear model (GLM) incorporating *season* for all individuals measured for length and weight (sample size [*n*]=19,209) to examine the weight–length relationship of the CSNA, similar to the work done by Palance et al. (2019). The GLM was fitted by using the base function glm in R (vers. 4.2.1; R Core Team, 2022) and has the following structure:

$$l\left(\widehat{TW}_{i,j}\right) = \beta_0 + \beta_1 Season_j + \beta_2 \log_e\left(SL_{i,j}\right), \quad (1)$$

where $l$ = the log link function;

$\widehat{TW}_{i,j}$ = the total weight (in grams) of fish $i$ in season $j$;

*Season* = a categorical factor with fall, winter, spring, and summer; and

$SL_{i,j}$ = the standard length (in millimeters) of fish $i$ in season $j$.

Note that $\widehat{TW}_{i,j}$ has a gamma distribution, with the mean calculated as follows:

$$\widehat{TW}_{i,j} = e^{\left(\beta_0 + \beta_1 Season_j + \beta_2 \log_e\left(SL_{i,j}\right)\right)}. \quad (2)$$

The variance of the gamma distribution was calculated as follows:

$$\frac{\widehat{TW}_{i,j}^{\,2}}{\nu}, \quad (3)$$

where $\nu$ = a dispersion parameter estimated during fitting.

The season was determined on the basis of the month of capture, with months of capture from September through November assigned to the fall season, the months from December through February considered to be winter, the months from March through May assigned to spring, and the months from June through August considered to be summer. The model fit was determined with the adjusted amount of deviance accounted for by a GLM, $D^2$ (Guisan and Zimmermann, 2000), calculated by using the Dsquared function in the R package modEvA, vers. 3.8.4 (Barbosa et al., 2013). The effect of season among all season pairs was compared by running the GLM 4 times, each time with a different season as the intercept, and evaluating the $t$-statistic for every season effect (e.g., if fall was the intercept, the $t$-statistics for the individual effects of winter, spring, and summer were evaluated relative to the fall intercept).

We chose a random subset of otoliths ($n$=2036), from fish collected during both SWFSC trawl surveys and CDFW port sampling that had lengths that encompassed the size distribution within each season, to examine the relationship of SL to otolith length and to confirm that otolith growth reflects somatic growth. The right-side otolith was chosen when possible and was imaged by using a dissecting microscope with an AmScope camera (United Scope LLC, Irvine, CA) and analyzed with the R package shapeR (vers. 0.1-5; Libungan and Pálsson, 2015) to calculate otolith length (Feret length) at the time of capture. We fitted a linear model that has *season* as a variable and has the following structure:

$$\left(SL_{i,j}\right) = \beta_0 + \beta_1 Season_j + \beta_2\left(OL_{i,j}\right) + \beta_3\left(Season_j OL_{i,j}\right), \quad (4)$$

where $OL_{i,j}$ = the otolith length (in millimeters) of fish $i$ in season $j$.

A model with an interaction between *season* and $OL_{i,j}$ was chosen, given that previous work on CPS found reduced effects of seasonality on otolith length as the length of fish increased (Thomas, 1983). A model with no interaction term was also fitted, but the model with the interaction term had a lower Akaike information criterion (AIC) than the model with no interaction term (AIC: 13632 and 13800, respectively) and was deemed a better fit (Akaike, 1973; Burnham and Anderson, 2002; Burnham et al., 2011). The effect of season among all season pairs was compared by running the linear model 4 times, each time with a different season as the intercept, and evaluating the $t$-statistic for every season effect (e.g., if fall was the intercept, the $t$-statistics for the individual effects of winter, spring, and summer were evaluated relative to the fall intercept). Visual examination of the diagnostic plots of both of the models used to examine the relationships of weight to length and of length to otolith length revealed that the assumptions of normality and homogeneity of variance were met.

### Somatic growth modeling

We fitted 5 growth models to length-at-age data to examine which model best describes somatic growth of the CSNA. The Gompertz growth model (Gompertz, 1825) is as follows (Ricker, 1975; Ogle et al., 2017):

$$L_t = L_\infty e^{-e^{-g^*\left(t-t^*\right)}}, \quad (5)$$

where $L_t$ = the mean length at age $t$;
$L_\infty$ = the mean asymptotic length (i.e., the maximum mean length for the population);
$g^*$ = the instantaneous growth rate at the inflection point $t^*$; and
$t^*$ = the maximum instantaneous growth rate.

The logistic growth model (Campana and Jones, 1992; Ogle et al., 2017) is as follows:

$$L_t = L_\infty\left[1 - e^{-g_{-\infty}\left(t-t^*\right)}\right], \quad (6)$$

where $g_{-\infty}$ = the positive instantaneous growth rate as age approaches negative infinity.

The final 3 models are parameterizations or modifications of the VBGF (von Bertalanffy, 1938), which has the following common foundation:

$$L_t = L_\infty\left(1 - e^{-q}\right), \quad (7)$$

where $q$ = at least a function of $t$.

For the VBGF attributable to Beverton and Holt (1957), $q$ takes this form:

$$q = K\left(t - t_0\right), \quad (8)$$

where $K$ = the growth coefficient, a measure of the exponential rate at which $L_t$ approaches $L_\infty$; and
$t_0$ = the theoretical age at which $L_t$ is zero.

As CPS have seasonal variations in their somatic growth rates, 2 modifications to the VBGF were fitted to model seasonal oscillations in growth, similar to the adjustments to the VBGF done by Ogle (2017). The first modification of the VBGF is from Hoenig and Choudaray Hanumara (1982) and Somers (1988), with a clarification by García-Berthou et al. (2012). In this model, hereafter referred to as the *Somers model*, $q$ takes this form (Ogle, 2017):

$$q = K\left(t - t_0\right) + \frac{CK}{2\pi}\sin\left(2\pi\left(t - t_s\right)\right) - \frac{CK}{2\pi}\sin\left(2\pi\left(t_0 - t_s\right)\right), \quad (9)$$

where $t_s$ = the inflection point, or the amount of time between time zero and the start of the convex portion of the first sinusoidal growth oscillation; and
$C$ = the proportional decrease in growth at the depth of the growth oscillation, normally the "winter" season.

If $C$=0 (i.e., if there is no seasonal oscillation in mean length), the equation reduces to the VBGF. If $C$>0 and $C$<1, the increase in mean length is reduced but does not stop; if $C$=1, the increase in mean length comes to a complete stop; and if $C$>1, mean length decreases during "winter." The time of the year when growth is slowest, known as the *winter point* (WP), was calculated as follows:

$$WP = t_s + 0.5. \quad (10)$$

Pauly et al. (1992) argued that a $C$ greater than 1 is biologically improbable for fish vertebrates whose skeletons largely preclude shrinkage in length and, therefore, proposed a modification to the Somers model in which mean length was not allowed to decrease. In this model, hereafter referred to as the *Pauly model*, $q$ takes this form:

$$q = K'\left(t' - t_0\right) + \frac{K'\left(1 - NGT\right)}{2\pi}\sin\left(\frac{2\pi}{1 - NGT}\left(t' - t_s\right)\right) - \frac{K'\left(1 - NGT\right)}{2\pi}\sin\left(\frac{2\pi}{1 - NGT}\left(t_0 - t_s\right)\right), \quad (11)$$

where $NGT$ = the *no growth time*, the length of the no growth period as a fraction of a year.

The age $t'$ is found by "subtracting from the real age ($t$) the total no-growth time occurring up to age $t$" (Pauly et al., 1992; Ogle, 2017). Pauly et al. (1992) suggested using $K'$ to minimize confusion with $K$ in the VBGF as the units changed from year$^{-1}$ to (1–NGT)$^{-1}$.

Model parameters and 95% confidence intervals were estimated by using nonlinear least squares regression with the R package FSA (vers. 0.9.3; Ogle et al., 2022) and the nlsBoot function in the R package nlstools (vers. 2.0-0; Baty et al., 2015), respectively. Starting values were obtained by visually fitting the models to the observed data, and alternative starting values were used to confirm a global minimum was obtained. The best fitting model was chosen by using the AIC values (Akaike, 1973; Ogle, 2017), with the best fitting model having the lowest AIC and other models ranked according to the differences in their AIC values from that of the best model (Burnham and Anderson, 2002; Burnham et al., 2011).

## Results

### Length and age structure

A total of 19,209 individuals were measured for length and weight, and 12,520 otoliths from fish collected during both fishery-dependent and fishery-independent surveys were aged from 2015 to 2021 and used in subsequent analyses. Lengths from all measured fish ranged from 23 to 164 mm SL, lengths from aged fish ranged from 44 to 164 mm SL, and ages ranged from 0 to 6 years (Fig. 1, A and B). Age-0 and age-1 fish accounted for 62% of the samples, and a steady decline in the frequency of older aged fish was observed, with age-4+ fish accounting for 4% of the samples (Fig. 1B). All fish <69 mm SL were age 0.

The GLM used to examine the relationship of weight to length was significant ($P$<0.0001) and fit the data well ($D^2$=0.95). Winter did not differ from spring ($t$=0.36, $P$=0.71), but all other seasons were significantly different

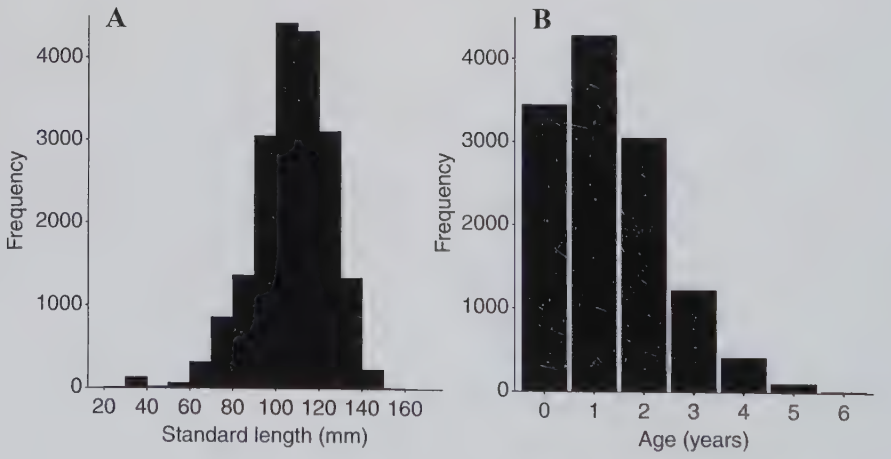


**Figure 1**

(**A**) Histogram of the standard lengths of all northern anchovy (*Engraulis mordax*) from the central subpopulation collected and measured for length (sample size [$n$]=19,209) and (**B**) histogram of the age distribution of sampled fish ($n$=12,520). This subpopulation ranges from Northern California to Baja California, Mexico. Data used in both histograms are from northern anchovy collected in 2015–2021 during sampling of ports by the California Department of Fish and Wildlife and acoustic-trawl surveys of coastal pelagic species conducted by the NOAA Southwest Fisheries Science Center.

from each other ($P$<0.0001), including fall from winter ($t$=4.11), spring ($t$=5.12), and summer ($t$=36.58) and winter from summer ($t$=22.57) and spring ($t$=–31.30) (Table 1). Looking at the model predictions, fish from summer had a larger weight at a given length (Fig. 2A). Although fish from winter and spring statistically differed from fish from fall, the model predictions look similar among these 3 seasons (Fig. 2A). Full results from the GLM can be found in Supplementary Table 2 (online only).

**Table 1**

Equations used to determine the relationship of total weight (TW) to standard length (SL) in the general linear model for each season for the central subpopulation of northern anchovy (*Engraulis mordax*). This subpopulation ranges from Northern California to Baja California, Mexico. Parameter estimates for each season are given within the equation. For example, the estimates from the fall model are as follows: –12.085 for the intercept and 3.122 for the slope. The model was fitted to a combination of fishery-independent and fishery-dependent data from 2015 through 2021, and the sample size ($n$) for each season is provided.

| Season | $n$ | Model equation |
|---|---|---|
| Fall | 5788 | $TW = e(-12.085)SL^{3.122}$ |
| Winter | 5743 | $TW = e(-12.071)SL^{3.122}$ |
| Spring | 5603 | $TW = e(-12.073)SL^{3.122}$ |
| Summer | 2075 | $TW = e(-12.001)SL^{3.122}$ |

A total of 2036 otoliths were imaged to calculate otolith length. The linear model of the relationship of SL to otolith length was significant ($P$<0.05) and fit the data well (coefficient of multiple determination [$R^2$]=0.90). Fall, winter, and spring did not differ from each other, including fall from winter ($t$=1.43, $P$=0.15) and spring ($t$=–0.31, $P$=0.75) and winter from spring ($t$=–1.58, $P$=0.11), but summer differed from all the other seasons (from fall: $t$=9.74; from winter: $t$=8.99; and from spring: $t$=7.77; $P$<0.0001) (Table 2). Looking at the model predictions, otolith length was greatest in winter, followed by fall, spring, and summer for small fish (less than ~120 mm SL) (Fig. 2B). As fish length increased, the effects of seasonality were reduced, and otolith length was similar between seasons for fish of the same size (Fig. 2B). Full results from the linear model can be found in Supplementary Table 3 (online only).

### Somatic growth modeling

Large variation in length at age was found among individuals from the CSNA, with higher variation in length at age for young fish (<2 years) and smaller variation for old fish (>5 years) (Fig. 3, A and B). The von Bertalanffy, Gompertz, and logistic growth functions yielded asymptotic growth patterns when fitted to both integer and fractional age data (Fig. 3, A and B). Curves for modeled length at age are nearly identical for all 3 models at all ages (Fig. 3, A and B), with similar parameter estimates within each age data set (Table 3). Notably, parameter

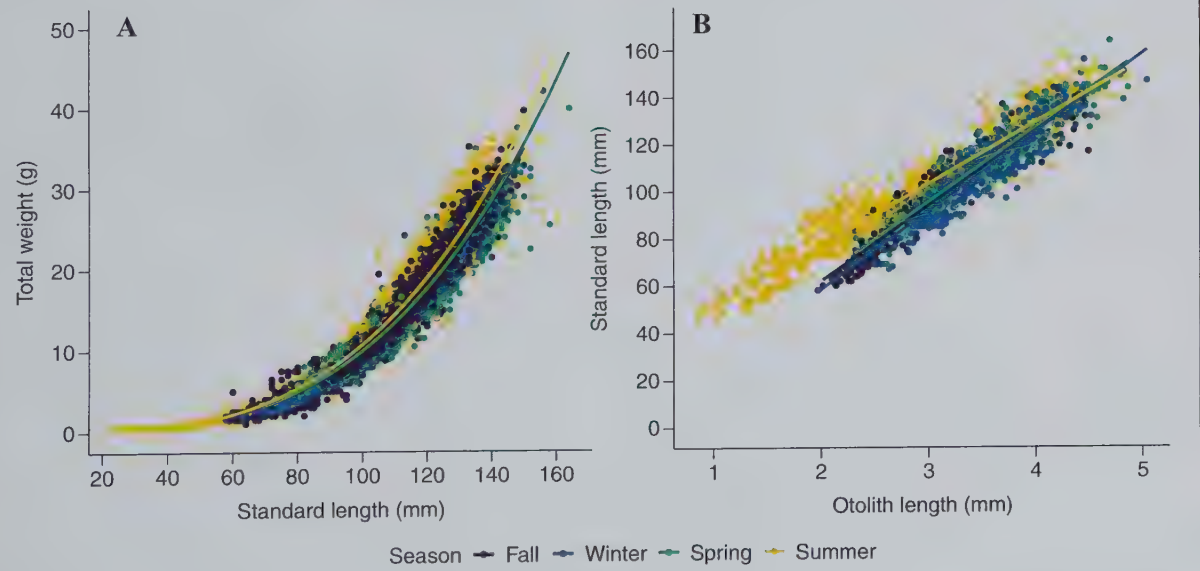


**Figure 2**

Relationships (**A**) between total weight and standard length and (**B**) between standard length and otolith length by season for the central subpopulation of northern anchovy (*Engraulis mordax*) that ranges from Northern California to Baja California, Mexico. The lines represent the predictions from the growth models used in this study, and the points represent the raw data for fish collected during fishery-independent and fishery-dependent surveys from 2015 through 2021.

**Table 2**

Equations used to determine the relationship of standard length (SL) to otolith length (OL) in the linear model for each season for the central subpopulation of northern anchovy (*Engraulis mordax*). This subpopulation ranges from Northern California to Baja California, Mexico. Parameter estimates for each season are given within the equation. For example, the estimates from the fall model are as follows: −2.316 for the intercept and 32.134 for the slope. The model was fitted to a combination of fishery-independent and fishery-dependent data from 2015 through 2021, and the sample size ($n$) for each season is provided.

| Season | $n$ | Model equation |
|---|---|---|
| Fall | 511 | $SL = -2.316 + 32.134(OL)$ |
| Winter | 317 | $SL = -8.584 + 33.460(OL)$ |
| Spring | 354 | $SL = 0.042 + 31.864(OL)$ |
| Summer | 854 | $SL = 24.491 + 26.243(OL)$ |

estimates differed between the integer age and fractional age data sets for the same model, with estimates of $L_\infty$ being greater and estimates of the growth coefficients (i.e., $K$, $g^*$, $g_{-\infty}$) being lower with a given model fitted to the integer age data set than with that model fitted to the fractional age data set (Table 3). For example, with the VBGF, $L_\infty$ was estimated at 130.6 mm SL and $K$ was estimated at 0.52 year$^{-1}$ when the integer age data set was used, whereas $L_\infty$ was estimated at 125.1 mm SL and $K$ was estimated at 0.72 year$^{-1}$ when the fractional age data set was used. The VBGF was the best fitting model for both the integer age and fractional age data sets, followed by the Gompertz and logistic models (Table 4).

When modeling seasonal oscillations of growth, the Somers model and Pauly model were indistinguishable (Fig. 4, Table 5) and fit the data better than the VBGF, although the Somers model had the lowest AIC value and was deemed the best fit. With the Somers model, $L_\infty$ was estimated at 126.2 mm SL and $K$ was estimated at 0.68 year$^{-1}$. Growth was fastest during the first year of growth. There was evidence of a 90% reduction in growth during the winter season ($C$=0.9), and the month of slowest estimated growth was December (WP=0.62). We fit a VBGF to integer age data from August and September to compare parameter outputs when seasonality was removed. Data from August and September were chosen because data for these months included information for individuals with the full range of ages in sufficient numbers (Suppl. Table 1) (online only). When seasonality was removed from this model fitted with integer age data, $L_\infty$ was estimated at 126.9 mm SL and $K$ was estimated at 0.78 year$^{-1}$, values similar to the parameter estimates from the Somers model.

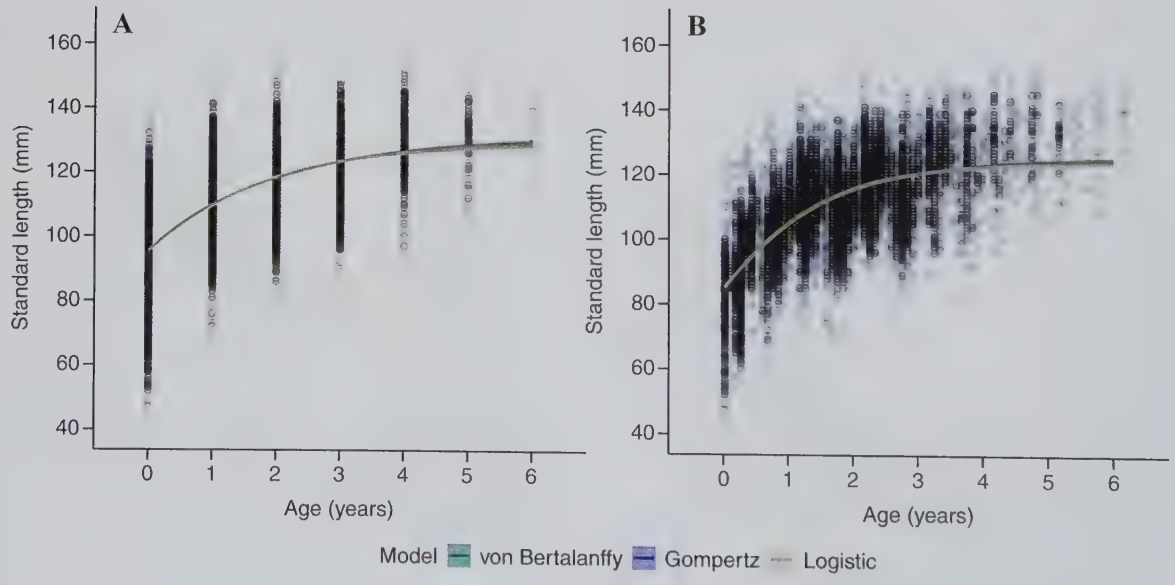


**Figure 3**

Growth curves from von Bertalanffy, Gompertz, and logistic growth functions fitted to (**A**) length-at-integer-age data and (**B**) length-at-fractional-age data for the central subpopulation of northern anchovy (*Engraulis mordax*) that ranges from Northern California to Baja California, Mexico. The solid lines indicate model predictions based on observed data, and the shaded areas indicate the 95% confidence intervals for these predictions. The black circles (with transparency) indicate the raw data points for individuals. The data used in the models are for fish collected from 2015 through 2021 during fishery-independent and fishery-dependent surveys. Parameter estimates from the model fits are provided in Table 3.

**Table 3**

Equations used in 3 growth models to estimate the mean length at age $t$ ($L_t$) for the central subpopulation of northern anchovy (*Engraulis mordax*) that ranges from Northern California to Baja California, Mexico. Parameter estimates from each model are given within the equation; for example, estimates from the first equation for the von Bertalanffy growth function are as follows: 130.6 mm in standard length for the mean asymptotic length, 0.52 year$^{-1}$ for the growth coefficient, and 2.51 years for the theoretical age at which $L_t$ is zero. The von Bertalanffy, Gompertz, and logistic growth functions were fitted to both integer and fractional age data for fish collected from 2015 through 2021 during fishery-independent and fishery-dependent surveys.

| Data set | Model | df | Model equation |
|---|---|---|---|
| Integer ages | von Bertalanffy | 12,517 | $L_t = 130.6\left[1 - e^{-0.52(t+2.51)}\right]$ |
| | Gompertz | 12,517 | $L_t = 129.5e^{(-(\frac{1}{0.60})e^{-0.60(t+1.95)}}$ |
| | Logistic | 12,517 | $L_t = 128.6\left[1 + e^{-0.68(t+1.52)}\right]^{-1}$ |
| Fractional ages | von Bertalanffy | 12,517 | $L_t = 125.1\left[1 - e^{-0.72(t+1.53)}\right]$ |
| | Gompertz | 12,517 | $L_t = 124.3e^{(-(\frac{1}{0.83})e^{-0.83(t+1.14)}}$ |
| | Logistic | 12,517 | $L_t = 123.7\left[1 + e^{-0.93(t+0.84)}\right]^{-1}$ |

**Table 4**

Statistical measures of fit for von Bertalanffy, Gompertz, and logistic growth functions fitted to data sets of lengths at integer and fractional ages for northern anchovy (*Engraulis mordax*) of the central subpopulation collected during 2015–2021. This subpopulation ranges from Northern California to Baja California, Mexico. For each model, number of parameters (K), the Akaike information criterion (AIC) and the difference in its AIC value from that of the best model (the one with the lowest AIC) (ΔAIC) are provided.

| Data set | Model | K | AIC | ΔAIC |
|---|---|---|---|---|
| Integer ages | von Bertalanffy | 4 | 97,208.86 | 0.00 |
| | Gompertz | 4 | 97,221.82 | 12.95 |
| | Logistic | 4 | 97,235.67 | 26.81 |
| Fractional ages | von Bertalanffy | 4 | 96,428.34 | 0.00 |
| | Gompertz | 4 | 96,477.62 | 49.28 |
| | Logistic | 4 | 96,526.79 | 98.45 |

## Discussion

The results of this study provide an update of the understanding of CSNA growth patterns, given that the last work examining growth of the CSNA through the adult stage was completed 38 years ago (i.e., Parrish et al., 1985). We found patterns in somatic growth of the CSNA that are typical of *r*-selected and opportunistic species, which have small body sizes, low maximum ages, and high growth rates (Adams, 1980; Winemiller and Rose, 1992; King and McFarlane, 2003). Additionally, fast growth during the first year of life, high individual variation in growth rates, and seasonal fluctuations in growth, as found in our study, are characteristic of CPS in upwelling environments (Cubillos et al., 2001; Takahashi et al., 2012). High variability in growth rates among individuals from the CSNA has been postulated to lead to increased population growth rates due to size-dependent mortality and, therefore, to lead to increased population size (Lo et al., 1995). The growth characteristics of the CSNA contribute to high interannual variability in recruitment success and population abundance observed for this population of northern anchovy (Lasker, 1981; MacCall et al., 2016; Thayer et al., 2017).

Large variations in length within each age class, extensive overlap of lengths across ages, rapid somatic growth during the first year of life, and high proportions of young fish (<4 years old) with scarcity of older individuals have been found in studies investigating the CSNA (Collins and Spratt, 1969; Spratt, 1975; Mais, 1981; Mallicoate and Parrish, 1981; Parrish et al., 1985) and other species of *Engraulis* (Bacha et al., 2010; Cerna and Plaza, 2016). Spratt (1975) modeled growth of individuals from the CSNA collected during both fishery-dependent and fishery-independent surveys and found a higher $L_\infty$ (165 mm SL) and lower $K$ (0.29 year$^{-1}$) than the estimates for those parameters from our study, and Cisneros et al. (1990) found an $L_\infty$ of 153 mm SL and a $K$ of 0.7 year$^{-1}$ for northern anchovy collected from the Gulf of California in Mexico (the southern subpopulation). The higher $L_\infty$ and

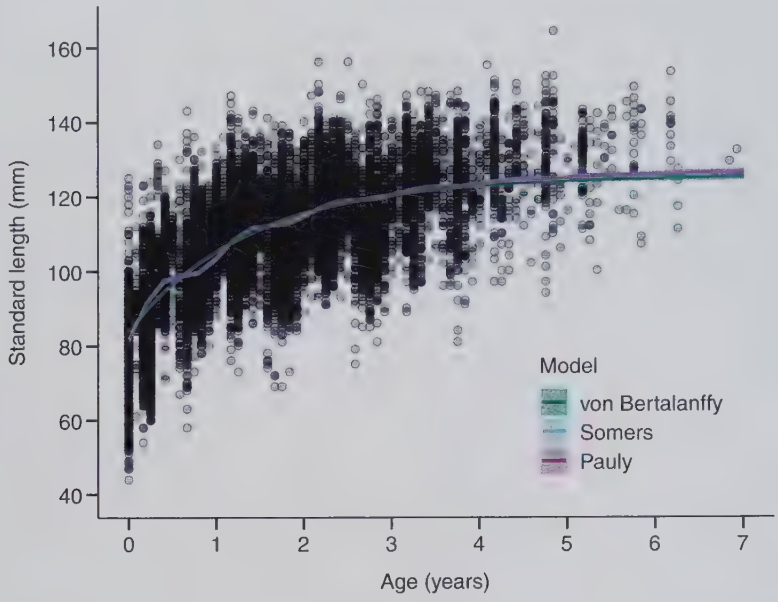


**Figure 4**

Growth curves from the von Bertalanffy growth function, Somers model, and Pauly model fitted to length-at-fractional-age data for the central subpopulation of northern anchovy (*Engraulis mordax*) that ranges from Northern California to Baja California, Mexico. The solid lines indicate model predictions based on observed data, and the shaded areas indicate the 95% confidence intervals for these predictions. The black circles (with transparency) indicate the raw data points for individuals. The data used in the models are for fish collected from 2015 through 2021 during fishery-independent and fishery-dependent surveys. Parameter estimates and their 95% confidence intervals from the model fits are provided in Table 5.

lower $K$ found by Spratt (1975) reflect their sample distribution, with lengths of sampled fish ranging from 88 to 160 mm SL and no age-0 fish. Without large and old fish, $L_\infty$ is underestimated and $K$ is overestimated (Bolser et al., 2018); therefore, it follows that the absence of small and young fish would result in overestimation of $L_\infty$ and underestimation of $K$, as is revealed when comparing estimates from Spratt (1975) and those from our study. Cisneros et al. (1990) collected fish with size and age ranges similar to the fish collected for our study (~50–140 mm SL, 0–5 years), likely contributing to similar $K$ values. However, they modeled growth using length–frequency analysis instead of ages calculated from otolith readings, possibly driving the differences in $L_\infty$.

Seasonal CSNA growth oscillations and large variations of length within each age class were not unexpected and reflect the life history characteristics of this species in response to environmental conditions of the CCE. Somatic growth of the CSNA was most rapid during the summer months in our study, with increased length at a given weight in summer compared to that in other seasons, a result that also has been found for northern anchovy collected in the CCE (Palance et al., 2019). This rapid summer growth is likely in response to warmer sea-surface temperatures and the increase in productivity from upwelled, nutrient-rich waters that stimulates growth of phytoplankton (Checkley and Barth, 2009; Jacox et al., 2018). Although productivity is increased during summer months, food aggregations are patchy and may be composed of prey of different levels of quality (Lasker and Zweifel, 1978; Litz et al., 2010), potentially resulting in large, opportunistic feeding events of variable nutritional quality for some individuals of the CSNA. Differences in the quality of prey encountered between individuals from the CSNA can contribute to high variability in their growth rates.

Additionally, the protracted spawning season of the CSNA may also contribute to large variations of length within each age class, especially at younger ages (Methot, 1983). For example, an age-0 fish born early in the year would be larger in length than an age-0 fish born later in the year when collected at the same time. The use of fractional ages in our work helped to address this phenomenon, but the birthdates of individual fish are still unknown. The lack of birthdates may bias any estimate of actual somatic growth; therefore, caution should be taken when making interpretations.

Somatic growth of the CSNA was slowest in winter, a result that is linked to cool sea-surface temperatures and reproductive strategies (Cubillos and Arancibia, 1993; Cubillos et al., 2002; Bilgin et al., 2013). The peak CSNA spawning season is from January through April (Hunter and Leong, 1981; Reiss et al., 2008); therefore, the slowest growth in December aligns with a shift from somatic growth to gametic growth in preparation for spawning. The duration of spawning season increases with female length, weight, and age, and although a large majority of individuals are mature by age 0, older females contribute disproportionately more to total annual egg production than first-time spawners (Hunter and Macewicz, 1985; Parrish et al., 1986; Schwartzkopf et al., 2022). The reduction in seasonality in somatic growth of older individuals is likely due to the increased investment in reproduction over more of the year and reduced somatic growth at older ages (>3 years) (Armstrong and Shelton, 1990; Kozlowski, 1996). If fish mature at different ages, individual variability in reproductive investment may also contribute to high variability in growth rates among individuals (Brosset et al., 2016; Claireaux et al., 2021).

Large variations and extensive overlaps in length at age present challenges in estimating other life history characteristics and consequently in conducting stock

**Table 5**

Estimates and 95% confidence intervals for parameters of the von Bertalanffy growth function (VBGF) fitted to integer age data, the VBGF fitted to fractional age data, the Somers model, and the Pauly model used to examine the growth of the central subpopulation of northern anchovy (*Engraulis mordax*) that ranges from Northern California to Baja California, Mexico. The model parameters are mean asymptotic length ($L_\infty$); growth coefficients ($K$ and $K'$); the theoretical age at which length is zero ($t_0$), the inflection point, or the amount of time between time zero and the start of the convex portion of the first sinusoidal growth oscillation ($t_s$); the proportional decrease in growth at the depth of the growth oscillation ($C$); and *no growth time* (NGT), or the length of the period of no growth as a fraction of a year. For each model, the Akaike information criterion (AIC) and the difference in its AIC value from that of the best model (the one with the lowest AIC) (ΔAIC) are provided. No AIC or ΔAIC values are given for the VBGF fitted to integer age data as that data set is different from the data set of fractional ages used with the other models. All models were fitted to length-at-age data for fish collected during fishery-independent and fishery-dependent surveys from 2015 through 2021. SL=standard length.

| | Parameter estimates (95% confidence intervals) | | | | | | | | |
|---|---|---|---|---|---|---|---|---|---|
| Model | $L_\infty$ (mm SL) | $K$ (year$^{-1}$) | $K'$ ((1–NGT)$^{-1}$) | $t_0$ (years) | $t_s$ (year) | $C$ | NGT (year) | AIC | ΔAIC |
| VBGF (integer) | 130.6 (129.1–132.3) | 0.52 (0.47–0.56) | – | –2.51 (–2.68––2.35) | – | – | – | – | – |
| VBGF (fractional) | 125.1 (124.2–125.9) | 0.73 (0.69–0.77) | – | –1.53 (–1.63––1.45) | – | – | – | 96,428.3 | 172.10 |
| Somers model | 126.2 (125.4–127.1) | 0.68 (0.64–0.71) | – | –1.74 (–1.79––1.67) | 0.12 (0.10–0.15) | 0.90 (0.77–1.00) | – | 96,256.2 | 0.00 |
| Pauly model | 126.4 (125.5–127.4) | – | 0.67 (0.63–0.73) | –1.76 (–1.81––1.61) | 0.13 (0.11–0.15) | – | 0.00 (0.00–0.08) | 96,257.9 | 1.69 |

assessments. When time or costs do not allow all samples that were measured for length to be aged, age–length keys (ALKs) are used to draw inferences about the age composition of a stock and are used in stock assessments to estimate growth or mortality rates (Coggins et al., 2013) and to estimate abundance and catch at age (Kimura, 1977). When ages and growth characteristics are estimated with extrapolation-based methods (e.g., ALKs), more errors are generated for populations with extensive overlap of length distributions across ages and large variability in length at age (Miranda and Colvin, 2017). These errors could propagate throughout an assessment when an ALK is used to calculate weight at age, as has been done in the CSNA stock assessment (Kuriyama et al., 2022), which is ultimately used to calculate recruitment and biomass quantities relevant for management of this population.

Although the VBGF is the most typical model used to describe growth of CPS on the U.S. Pacific coast (Armstrong and Shelton, 1990; Crone et al., 2019; Kuriyama et al., 2020, 2022), no other work has examined seasonal modifications to the VBGF for northern anchovy. We found that the best fitting growth model for the CSNA was the Somers model, which allows growth to oscillate seasonally. Seasonal growth oscillations have been reported for small CPS around the world: the European anchovy (*E. encrasicolus*) (Bellido et al., 2000; Bilgin et al., 2013), Peruvian anchoveta (*E. ringens*) (Palomares et al., 1987; Cubillos and Arancibia, 1993; Cerna and Plaza, 2016), European pilchard (*Sardina pilchardus*) (Silva et al., 2008), and Araucanian herring (*Strangomera bentincki*) (Cubillos et al., 2002; Feltrim and Ernst, 2010). However, in many of the studies that generated these reports, length-based methods were used to estimate growth parameters with seasonal growth models, possibly yielding less reliable estimations than those from the use of age-based methods (Liu et al., 2021).

We found that the VBGF overestimated $L_\infty$ and underestimated $K$ in comparison to estimation with the Somers model, and Liu et al. (2021) had the same observation when seasonal growth oscillations of small species were ignored. The misestimation of growth parameters when seasonality is ignored can propagate biases in stock assessments because underestimating $K$ results in underestimation of natural mortality and possibly in characterization of a stock as less productive than it actually is (Scherrer et al., 2021). Additionally, when seasonality was included with the estimation of fractional ages, overlaps in length at age were reduced, and that reduction may result in more accurate ALKs and, therefore, reduce bias in stock assessments.

Validating that otolith growth has a relationship with somatic growth is imperative, as it permits the use of data from otolith studies (e.g., increment widths) to test for relationships between fish growth and climate indices or regional environmental conditions, and information about such relationships is important for projections of climate- and ecosystem-level change on marine communities (Muhling et al., 2018; Erisman et al., 2021; Tommasi et al., 2021). The linear relationship between otolith length and fish length indicates that otolith growth does reflect somatic growth to a degree for the CSNA; however, it is not uncommon for otolith and somatic growth

to be decoupled because somatic growth is tied to the environment and otolith growth is tied to metabolic rate (Buckmeier et al., 2017).

The differences in otolith growth among seasons observed in our study may also provide examples of the uncoupling of otolith and somatic growth reported for some other fish species that have seasonally different growth rates (e.g., Francis et al., 1993). In the summer season, when the fastest growth was found, mean otolith length for fish of a given length was smaller than that for fish in other seasons (and growth rates were lower), with seasonal differences diminished at larger fish lengths (greater than ~120 mm SL). The larger otolith lengths in winter may also indicate that otoliths continue to grow in seasons during which somatic growth is reduced, a common phenomenon (Secor and Dean, 1992; Buckmeier et al., 2017). The negative relationship between otolith size and somatic growth rate is predicted for individuals growing according to the VBGF (Xiao, 1996), but the presence of a strong growth effect can create substantial errors for studies in which otoliths are used to back-calculate fish length (Campana, 1990). Although we did not directly test the effect of growth rates on the relationship between otolith length and fish length, the results of our study provide a starting point for examination of this relationship in the future.

One potential source of uncertainty in this study is the sample distribution. Only 162 fish (0.008%) in our study were <50 mm SL, possibly a reflection of the selectivity of the commercial fishery, size selectivity of trawl nets, locality of trawl tows, or a combination of these factors. The commercial fishery is known to avoid small fish (generally <90 mm SL) because small individuals may clog nets (Huppert et al., 1980). More importantly, the fishery is extremely limited by market demand because large anchovies have a higher fat content and are, therefore, more desirable for their main uses as feed for the finfish mariculture industry, pet food, oil for pharmaceuticals, live bait, and fresh or canned food for human consumption (CDFW, 2022; Kuriyama et al., 2022). Therefore, fishery-dependent data will consistently have this source of uncertainty, and fishery-independent data can help fill this gap.

The net used in SWFSC acoustic-trawl surveys has an 8-mm mesh liner to retain juvenile and adult fish as small as 50 mm SL and potentially as large as 800 mm SL (Dotson and Griffith, 1996; Dotson et al., 2010; Dorval et al., 2022), but small fish are known to be poorly represented in catches made with nets with similar sizes of mesh liner in contrast to their representation in purse seine samples (Dotson and Griffith, 1996). Small juveniles of the CSNA tend to remain closer to shore (Parrish et al., 1985), but NOAA research vessels are unable to operate in waters with depths less than 20–30 m. Therefore, any CPS aggregations in shallow, nearshore areas are missed; it should be noted that the SWFSC is addressing this data gap through the inclusion of sampling of nearshore areas by commercial fishing vessels with the sampling conducted during its fishery-independent surveys (Dorval et al., 2022; Renfree et al., 2022). Except for 1 individual, all fish <50 mm SL were caught in 2015, the year in which abundances of young of the year in the CSNA were found to have increased drastically (Zwolinski et al., 2017; Thompson et al., 2019). The presence of small individuals in 2015 indicates that small fish (<50 mm SL) will be collected when they are present in high numbers with the current sampling design and trawl net.

The disproportionate distribution of samples from both the fishery-independent and fishery-dependent surveys, with a decline in older age classes (>4 years), may also be due to the sampling designs used. The commercial fishery fleet fishes anchovy close to shore, where younger fish are common (Parrish et al., 1985), and close to ports because fish do not survive well in the holds over the time it takes to cover long distances from shore (Kuriyama et al., 2022). The SWFSC trawl survey is designed to sample the entire populations of CPS to assess their biomass (Stierhoff et al., 2020), a different objective than that of a survey focused purely on age and growth in which ideally all age classes are sampled uniformly regardless of relative abundance (Bolser et al., 2018).

It is important to ensure that growth data accurately represent the variability of the lengths at each age, as sampling that is not representative of the underlying population may produce biased estimates of growth characteristics and mortality (Sainsbury, 1980; Goodyear, 2019). Further sampling of older age classes could cause the current estimates of growth characteristics to change, but attempting to add samples in size bins for which catch is more rare in size-stratified sampling can substantially increase bias in mean size estimates (Goodyear, 2019). The current 2-stage sampling design of the SWFSC trawl survey meets both of these important needs through minimization of bias due to sampling distribution by first selecting samples at random so that they are representative of what is caught and then by making sure a sufficient number of otoliths from all length (and age) classes of a species or population are aged to accurately approximate the true variation in length at age (Schwartzkopf et al., 2022).

The high percentage of fish from age 0 to age 2 in sampling and the low percentage of fish at age 4+ reflect the current belief that the maximum age of northern anchovy has declined over time with catches being heavily dominated by age-0 and age-1 fish and having diminished levels of older age groups (Mais, 1981; MacCall, 2009). This result is in line with a high mortality rate typical of clupeoids (Armstrong and Shelton, 1990) and the CSNA (Kuriyama et al., 2022), assuming that the survey samples are representative of the adult population. Given the low harvest rate by the commercial fishery (PFMC, 2022), it is reasonable to conclude that the high mortality rates reflect natural mortality (e.g., mortality that results from predation or starvation). Additionally, true length at age may be underestimated because slower-growing marine fish can have higher predation mortality rates (Fennie et al., 2020). The northern subpopulation of northern anchovy is thought to have larger, older, and faster-growing fish than those in the CSNA (Parrish et al., 1985; Stierhoff et al., 2020; senior author, unpubl. data). Future work could

examine growth characteristics for the entire species with the addition of older individuals (>4 years old) as well as could compare characteristic estimates between subpopulations and stratify by latitude.

## Conclusions

This work is the first comprehensive investigation into modeling non-seasonal and seasonal growth oscillations in northern anchovy by using an age-based method. The results indicate the importance of incorporating seasonality when modeling somatic growth of CPS with data from samples collected year-round. If seasonality is ignored, $L_\infty$ may be overestimated and growth coefficients (i.e., $K$) may be underestimated. The similarity in parameter estimates from the VBGF fitted to integer age data when only 2 months of data were included and from the Somers model fitted to fractional age data when data from year-round sampling were included indicates that 1) the seasonal model appears to account well for seasonal growth oscillations of the CSNA and 2) a VBGF fitted with integer ages may be appropriate for use with data collected over a short time period. Accurately describing growth is important to decrease biases that may propagate in stock assessments and subsequently in management decisions.

## Resumen

Los parámetros de crecimiento somático se utilizan en modelos de evaluación de poblaciones estructurados por edades, como los que se emplean para evaluar y manejar federalmente la anchoa del norte (*Engraulis mordax*); por lo tanto, un estimado incorrecto del crecimiento puede causar errores que afecten a los estimados de las evaluaciones de poblaciones. Hasta donde sabemos, hemos completado la primera investigación exhaustiva para modelar el crecimiento somático y de los otolitos de la subpoblación central de la anchoa del norte (CSNA), que tiene su distribución desde el norte de California hasta Baja California, México, utilizando datos dependientes e independientes de la pesca. Para determinar el modelo que mejor describía el crecimiento, se ajustaron cinco modelos de crecimiento a los datos de talla por edad, incluidos 2 modelos que tienen en cuenta las oscilaciones estacionales del crecimiento. Se observaron oscilaciones estacionales del crecimiento en el CSNA, y los modelos que mejor se ajustaban fueron los que tenían en cuenta la estación. El crecimiento más rápido se produjo durante el verano, y disminuyó 90% en invierno. Se observaron grandes variaciones en la longitud a la edad y un amplio solapamiento de longitudes entre edades en el CSNA, observaciones típicas de peces con un modo de vida oportunista que responden rápidamente a las condiciones ambientales cambiantes en ecosistemas dinámicos. Los modelos de crecimiento tradicionales sobrestimaron la longitud asintótica media y subestimaron el coeficiente de crecimiento en comparación con los resultados de los modelos de crecimiento estacional. Describir con precisión el crecimiento de la CSNA teniendo en cuenta la estacionalidad es importante para limitar los sesgos que pueden propagarse en las evaluaciones de las poblaciones y en las decisiones de manejo.

## Acknowledgments

We thank participants of the SWFSC trawl surveys, including the officers and crew of the NOAA Ships *Reuben Lasker* and *Bell M. Shimada*, the wetfish fishermen and respective markets in California for accommodating sampling of their catches, C. Protasio, K. Grady, M. Horeczko, B. Brady, and scientific aids of the CDFW for support in sample collection, and C. Allen Akselrud, J. Ugoretz, A. Yau, and 2 anonymous reviewers for manuscript evaluations.

## Literature cited

Adams, P. B.
1980. Life history patterns in marine fishes and their consequences for fisheries management. Fish. Bull. 78:1–12.

Akaike, H.
1973. Information theory as an extension of the maximum likelihood principle. *In* Second International Symposium on Information Theory; Tsahkadsor, 2–8 September 1971 (B. N. Petrov and F. Csáki, eds.), p. 267–281. Akadémiai Kiadó, Budapest, Hungary.

Aldanondo, N., U. Cotano, P. Alvarez, and A. Uriarte.
2016. Validation of the first annual increment deposition in the otoliths of European anchovy in the Bay of Biscay based on otolith microstructure analysis. Mar. Freshw. Res. 67:943–950.

Armstrong, M. J., and P. A. Shelton.
1990. Clupeoid life-history styles in variable environments. Environ. Biol. Fishes 28:77–85.

Bacha, M., A. Moali, N.-E. Benmansour, J.-M. Brylinski, K. Mahé, and R. Amara.
2010. Relationships between age, growth, diet and environmental parameters for anchovy (*Engraulis encrasicolus* L.) in the Bay of Bénisaf (SW Mediterranean, west Algerian coast). Cybium 34:47–57.

Barbosa, A. M., R. Real, A.-R. Muñoz, and J. A. Brown.
2013. New measures for assessing model equilibrium and prediction mismatch in species distribution models. Divers. Distrib. 19:1333–1338.

Basilone, G., M. Barra, R. Ferreri, S. Mangano, M. Pulizzi, G. Giacalone, I. Fontanta, S. Aronica, A. Gargano, P. Rumolo, et al.
2020. First annulus formation in the European anchovy; a two-stage approach for robust validation. Sci. Rep. 10:1079.

Baty, F., C. Ritz, S. Charles, M. Brutsche, J.-P. Flandrois, and M.-L. Delignette-Muller.
2015. A toolbox for nonlinear regression in R: the package nlstools. J. Stat. Softw. 66(5):1–21.

Bellido, J. M., G. J. Pierce, J. L. Romero, and M. Millán.
2000. Use of frequency analysis methods to estimate growth of anchovy (*Engraulis encrasicolus* L. 1758) in the Gulf of Cádiz (SW Spain). Fish. Res. 48:107–115.

Beverton, R. J. H., and S. J. Holt.
1957. On the dynamics of exploited fish populations. Minist. Agric. Fish. Food, Fish Invest. ser. 2, vol. 19, 533 p. HMSO, London.

Bilgin, S., B. Taşçi, and H. Bal.
2013. Sexual seasonal growth of the European anchovy (*Engraulis encrasicolus*) caught by mid-water trawl and purse seine in the southern Black Sea. J. Mar. Biol. Assoc. UK. 93:333–339.

Blaxter, J. H. S., and J. R. Hunter.
1982. The biology of the clupeoid fishes. Adv. Mar. Biol. 20:3–223.

Bolser, D. G., A. Grüss, M. A. Lopez, E. M. Reed, I. Mascareñas-Osorio, and B. E. Erisman.
2018. The influence of sample distribution on growth model output for a highly-exploited [sic] marine fish, the Gulf Corvina (*Cynoscion othonopterus*). PeerJ 6:e5582

Brosset, P., J. Lloret, M. Muñoz, C. Fauvel, E. Van Beveren, V. Marques, J.-M. Fromentin, F. Ménard, and C. Saraux.
2016. Body reserves mediate trade-offs between life-history traits: new insights from small pelagic fish reproduction. R. Soc. Open Sci. 3:160202.

Buckmeier, D. L., P. C. Sakaris, and D. J. Schill.
2017. Validation of annual and daily increments in calcified structures and verification of age estimates. *In* Age and growth of fishes: principles and techniques (M. C. Quist and D. A. Isermann, eds.), p. 33–79. Am. Fish. Soc., Bethesda, MD.

Burnham, K. P., and D. R. Anderson.
2002. Model selection and multi-modal inference: a practical information-theoretical approach, 488 p. Springer, New York.

Burnham, K. P., D. R. Anderson, and K. P. Huyvaert.
2011. AIC model selection and multimodal inference in behavior ecology: some background, observations, and comparisons. Behav. Ecol. Sociobiol. 65:23–35.

Butler, J. L.
1989. Growth during the larval and juvenile stages of the northern anchovy, *Engraulis mordax*, in the California Current during 1980–84. Fish. Bull. 87:645–652.

Campana, S. E.
1990. How reliable are growth back-calculations based on otoliths? Can. J. Fish. Aquat. Sci. 47:2219–2227.

Campana, S. E., and C. M. Jones.
1992. Analysis of otolith microstructure data. *In* Otolith microstructure examination and analysis (D. K. Stevenson, and S. E. Campana, eds.), p. 73–100. Can. Spec. Publ. Fish. Aquat. Sci. 117.

CDFW (California Department of Fish and Wildlife).
2022. Northern anchovy. Last modified 6 April 2022. website

Cerna, F., and G. Plaza.
2016. Daily growth patterns of juveniles and adults of the Peruvian anchovy (*Engraulis ringens*) in northern Chile. Mar. Freshw. Res. 67:899–912.

Checkley, D. M., Jr., and J. A. Barth.
2009. Patterns and processes in the California Current System. Prog. Oceanogr. 83:49–64.

Cisneros, M. A., J. Estrada, and G. Montemayer.
1990. Growth, mortality and recruitment of exploited small pelagic fishes in the Gulf of California, Mexico. Fishbyte 8:15–17.

Claireaux, M., T. C. dos Santos Schmidt, E. M. Olsen, A. Slotte, Ø. Varpe, M. Heino, and K. Enberg.
2021. Eight decades of adaptive changes in herring reproductive investment: the joint effect of environment and exploitation. ICES J. Mar. Sci. 78:631–639.

Coggins, L. G., Jr., D. C. Gwinn, and M. S. Allen.
2013. Evaluation of age–length key sample sizes required to estimate fish total mortality and growth. Trans. Am. Fish. Soc. 142:832–840.

Collins, R. A.
1969. Size and age composition of northern anchovies (*Engraulis mordax*) in the California anchovy reduction fishery for the 1965–66, 1966–67, and 1967–68 seasons. *In* The northern anchovy (*Engraulis mordax*) and its fishery 1965–1968, p. 56–74. Calif. Dep. Fish Game, Fish Bull. 147.

Collins, R. A., and J. D. Spratt.
1969. Age determination of northern anchovies, *Engraulis mordax*, from otoliths. *In* The northern anchovy (*Engraulis mordax*) and its fishery 1965–1968, p. 39–55. Calif. Dep. Fish Game, Fish Bull. 147.

Crone, P. R., K. T. Hill, J. P. Zwolinski, and M. J. Kinney.
2019. Pacific mackerel (*Scomber japonicus*) stock assessment for U.S. management in the 2019–20 and 2020–21 fishing years, 112 p. Pac. Fish. Manage. Counc., Portland, OR. [Available from website.]

Cubillos, L., and H. Arancibia.
1993. On the seasonal growth of common sardine (*Strangomera bentincki*) and anchovy (*Engraulis ringens*) off Talcahuanon, Chile. Rev. Biol. Mar. (Valparaíso) 28:43–49.

Cubillos, L. A., D. F. Arcos, D. A. Bucarey, and M. T. Canales.
2001. Seasonal growth of small pelagic fish off Talcahuano, Chile (37°S, 73°W): a consequence of their reproductive strategy to seasonal upwelling? Aquat. Living Resour. 14:115–124.

Cubillos, L. A., D. A. Bucarey, and M. Canales.
2002. Monthly abundance estimation for common sardine *Strangomera bentincki* and anchovy *Engraulis ringens* in the central-southern area off Chile (34–40°S). Fish. Res. 57:117–130.

Dorval, E., B. J. Macewicz, D. A. Griffith, and Y. Gu.
2018. Spawning biomass of the central stock of northern anchovy (*Engraulis mordax*) estimated from the daily egg production method off California in 2017. NOAA Tech. Memo. NMFS-SWFSC-607, 31 p.

Dorval, E., D. Porzio, B. D. Schwartzkopf, K. C. James, L. Vasquez, and B. Erisman.
2022. Sampling methodology for estimating life history parameters of coastal pelagic species along the U.S. Pacific coast. NOAA Tech. Memo. NMFS-SWFSC-660, 40 p.

Dotson, R. C., and D. A. Griffith.
1996. A high-speed midwater rope trawl for collecting coastal pelagic fishes. CalCOFI Rep. 37:134–139. [Available from website.]

Dotson, R. C., D. A. Griffith, D. L. King, and R. L. Emmett.
2010. Evaluation of a marine mammal excluder device (MMED) for a Nordic 264 midwater rope trawl. NOAA Tech. Memo. NMFS-SWFSC-455, 14 p.

Erisman, B. E., E. M. Reed, M. J. Román, I. Mascareñas-Osorio, P. van der Sleen, C. López-Sagástegui, O. Aburto-Oropeza, K. Rowell, and B. A. Black.
2021. Relationships among somatic growth, climate, and fisheries production in an overexploited marine fish from the Gulf of California, Mexico. Fish. Oceanogr. 30:556–568.

Feltrim, M., and B. Ernst.
2010. Inter-cohort growth variability and its implication for fishery management of the common sardine (*Strangomera bentincki*) stock off the coast of south-central Chile. Fish. Res. 106:368–377.

Fennie, H. W., S. Sponaugle, E. A. Daly, and R. D. Brodeur.
2020. Prey tell: what quillback rockfish early life history traits reveal about their survival in encounters with juvenile coho salmon. Mar. Ecol. Prog. Ser. 650:7–18.

Fournier, D., and C. P. Archibald.
1982. A general theory for analyzing catch at age data. Can. J. Fish. Aquat. Sci. 39:1195–1207.

Francis, M. P., M. W. Williams, A. C. Pryce, S. Pollard, and S. G. Scott.
1993. Uncoupling of otolith and somatic growth in *Pagrus auratus* (Sparidae). Fish. Bull. 91:159–164.

García-Berthou, E., G. Carmona-Catot, R. Merciai, and D. H. Ogle.
2012. A technical note on seasonal growth models. Rev. Fish Biol. Fish. 22:635–640.

Gompertz, B.
1825. On the nature of the function expressive of the law of human mortality, and on a new mode of determining the value of life contingencies. In a letter to Francis Baily, Esq. F. R. S. &c. Philos. Trans. R. Soc. Lond. 115:513–583.

Goodyear, C. P.
2019. Modeling growth: consequences from selecting samples by size. Trans. Am. Fish. Soc. 148:528–551.

Guisan, A., and N. E. Zimmermann.
2000. Predictive habitat distribution models in ecology. Ecol. Model. 135:147–186.

Hoenig, N., and R. Choudaray Hanumara.
1982. A statistical study of a seasonal growth model for fishes. Univ. Rhode Island, Dep. Comput. Sci. Stat., Tech. Rep., 91 p.

Hunter, J. R., and R. Leong.
1981. The spawning energetics of female northern anchovy, *Engraulis mordax*. Fish. Bull. 79:215–230.

Hunter, J. R., and B. J. Macewicz.
1980. Sexual maturity, batch fecundity, spawning frequency, and temporal pattern of spawning for the northern anchovy, *Engraulis mordax*, during the 1979 spawning season. CalCOFI Rep. 21:139–149. [Available from website.]
1985. Rates of atresia in the ovary of captive and wild northern anchovy, *Engraulis mordax*. Fish. Bull. 83:119–136.

Huppert, D. D., A. D. MacCall, G. D. Stauffer, K. R. Parker, J. A. McMillan, and H. W. Frey.
1980. California's northern anchovy fishery: biological and economic basis for fishery management. NOAA Tech. Memo. NMFS-SWFSC-1, 121 p.

Jacox, M. G., C. A. Edwards, E. L. Hazen, and S. J. Bograd.
2018. Coastal upwelling revisted: Ekman, Bakun, and improved upwelling indices for the U.S. West Coast. J. Geophys. Res. Oceans 123:7332–7350.

Kerns, J. A., and L. A. Lombardi-Carlson.
2017. History and importance of age and growth information. *In* Age and growth of fishes: principles and techniques (M. C. Quist and D. A. Isermann, eds.), p. 1–8. Am. Fish. Soc., Bethesda, MD.

Kimura, D. K.
1977. Statistical assessment of the age–length key. J. Fish. Res. Board Can. 34:317–324.

King, J. R., and G. A. McFarlane.
2003. Marine fish life history strategies: applications to fishery management. Fish. Manag. Ecol. 10:249–264.

Koehn, L. E., T. E. Essington, K. N. Marshall, W. J. Sydeman, A. I. Szoboszlai, and J. A. Thayer.
2017. Trade-offs between forage fish fisheries and their predators in the California Current. ICES J. Mar. Sci. 74:2448–2458.

Kozlowski, J.
1996. Optimal allocation of resources explains interspecific life-history patterns in animals with indeterminate growth. Proc. R. Soc., B 263:559–566.

Kuriyama, P. T., J. P. Zwolinski, K. T. Hill, and P. R. Crone.
2020. Assessment of the Pacific sardine resource in 2020 for U.S. management in 2020–2021. NOAA Tech. Memo. NMFS-SWFSC-628, 117 p.

Kuriyama, P. T., J. P. Zwolinski, S. L. H. Teo, and K. T. Hill.
2022. Assessment of the northern anchovy (*Engrualis mordax*) central subpopulation in 2021 for U.S. management. NOAA Tech. Memo. NMFS-SWFSC-665, 91 p.

Lasker, R.
1981. Factors contributing to variable recruitment of the northern anchovy *Engraulis mordax* in the California Current USA contrasting years 1975–1978. Rapp. P.-v. Réun. Cons. Int. Explor. Mer 178:375–388.

Lasker, R., and J. R. Zweifel.
1978. Growth and survival of first-feeding northern anchovy larvae (*Engraulis mordax*) in patches containing different proportions of large and small prey. *In* Spatial pattern in plankton communities, NATO Conf. Ser., vol. 3 (J. H. Steele, ed.), p. 329–354. Springer Science+Business Media, New York.

Lecomte, F., W. S. Grant, J. J. Dodson, R. Rodríguez-Sánchez, and B. W. Bowen.
2004. Living with uncertainty: genetic imprints of climate shifts in East Pacific anchovy (*Engraulis mordax*) and sardine (*Sardinops sagax*). Mol. Ecol. 13:2169–2182.

Libungan, L. A., and S. Pálsson.
2015. ShapeR: an R package to study otolith shape variation among fish populations. PLoS ONE 10(3):e0121102.

Litz, M. N. C., R. D. Brodeur, R. L. Emmett, S. S. Heppell, R. S. Rasmussen, L. O'Higgins, and M. S. Morris.
2010. Effects of variable oceanographic conditions on forage fish lipid content and fatty acid composition in the northern California Current. Mar. Ecol. Prog. Ser. 405:71–85.

Liu, Y., C. Zhang, B. Xu, Y. Xue, Y. Ren, and Y. Chen.
2021. Accounting for seasonal growth in per-recruit analyses: a case study of four commercial fish in coastal China Seas. Front. Mar. Sci. 8:567240.

Lo, N. C. H., P. E. Smith, and J. L. Butler.
1995. Population growth of northern anchovy and Pacific sardine using stage-specific matrix models. Mar. Ecol. Prog. Ser. 127:15–26.

MacCall, A. D.
2009. Mechanisms of low-frequency fluctuations in sardine and anchovy populations. *In* Climate change and small pelagic fish (D. Checkley, J. Alheit, Y. Oozeki, and C. Roy, eds.), p. 285–299. Cambridge Univ. Press, Cambridge, UK.

MacCall, A. D., W. J. Sydeman, P. C. Davison, and J. A. Thayer.
2016. Recent collapse of northern anchovy biomass off California. Fish. Res. 175:87–94.

Mais, K. F.
1981. Age-composition changes in the anchovy, *Engraulis mordax*, central population. CalCOFI Rep. 22:82–87. [Available from website.]

Mallicoate, D. L., and R. H. Parrish.
1981. Seasonal growth patterns of California stocks of northern anchovy, *Engraulis mordax*, Pacific mackerel, *Scomber japonicus*, and jack mackerel, *Trachurus symmetricus*. CalCOFI Rep. 22:69–81. [Available from website.]

McClatchie, S.
2014. Regional fisheries oceanography of the California Current system: the CalCOFI program, 235 p. Springer Science+Business Media, Dordrecht, Netherlands.

McHugh, J. L.
1951. Meristic variations and populations of northern anchovy (*Engraulis mordax mordax*). Bull. Scripps Inst. Oceanogr. Univ. Calif. 6:123–160.

Methot, R. D., Jr.
1983. Seasonal variation in survival of larval northern anchovy, *Engraulis mordax*, estimated from the age distribution of juveniles. Fish. Bull. 81:741–750.

1989. Synthetic estimates of historical abundance and mortality for northern anchovy. Am. Fish. Soc. Symp. 6:66–82.

Miranda, L. E., and M. E. Colvin.
2017. Sampling for age and growth estimation. *In* Age and growth of fishes: principles and techniques (M. C. Quist and D. A. Isermann, eds.), p. 107–125. Am. Fish. Soc., Bethesda, MD.

Muhling, B., M. Lindegren, L. W. Clausen, A. Hobday, and P. Lehodey.
2018. Impacts of climate change on pelagic fish and fisheries. *In* Climate change impacts on fisheries and aquaculture: a global analysis (B. F. Phillips and M. Pérez-Ramírez, eds.), p. 771–814. John Wiley & Sons, New York.

Muhling, B., S. Brodie, O. Snodgrass, D. Tommasi, H. Dewar, D. Tommas, J. Childers, M. Jacox, C. A. Edwards, Y. Xu, et al.
2019. Dynamic habitat use of albacore and their primary prey species in the California Current System. CalCOFI Rep. 60:79–93. [Available from website.]

Muhling, B. A., S. Brodie, J. A. Smith, D. Tommasi, C. F. Gaitan, E. L. Hazen, M. G. Jacox, T. D. Auth, and R. D. Brodeur.
2020. Predictability of species distributions deteriorates under novel environmental conditions in the California Current System. Front. Mar. Sci. 7:589.

Ogle, D. H.
2017. An algorithm for the von Bertalanffy seasonal cessation in growth function of Pauly et al. (1992). Fish. Res. 185:1–5.

Ogle, D. H., T. O. Brenden, and J. K. McCormick.
2017. Growth estimation: growth models and statistical inference. *In* Age and growth of fishes: principles and techniques (M. C. Quist and D. A. Isermann, eds.), p. 265–359. Am. Fish. Soc., Bethesda, MD.

Ogle, D. H., J. C. Doll, P. Wheele r, and A. Dinno.
2022. FSA: simple fisheries stock assessment methods. R package, vers. 0.9.3. [Available from website.]

Palance, D. G., B. J. Macewicz, K. Stierhoff, D. A. Demer, and J. P. Zwolinski.
2019. Length conversions and mass–length relationships of five forage-fish species in the California Current ecosystem. J. Fish Biol. 95:1116–1124.

Palomares, M. L., P. Muck, J. Mendo, E. Chuman, O. Gomez, and D. Pauly.
1987. Growth of the Peruvian anchoveta (*Engraulis ringens*), 1953 to 1982. *In* The Peruvian anchoveta and its upwelling ecosystem: three decades of change (D. Pauly and I. Tsukayama, eds.), p. 117–141. ICLARM Stud. Rev.15. Inst. Mar Peru (IMARPE), Callao, Peru; Dtsch. Ges. Tech. Zusammenarbeit (GTZ), Eschborn, Germany; Int. Cent. Living Aquat. Resour. Manage. (ICLARM), Manila, Philippines.

Parrish, R. H., D. L. Mallicoate, and K. F. Mais.
1985. Regional variations in the growth and age composition of northern anchovy, *Engraulis mordax*. Fish. Bull. 83:483–496.

Parrish, R. H., D. L. Mallicoate, and R. A. Klingbeil.
1986. Age dependent fecundity, number of spawnings per year, sex ratio, and maturation stages in northern anchovy, *Engraulis mordax*. Fish. Bull. 84:503–517.

Pauly, D., M. Soriano-Bartz, J. Moreau, and A. Jarre-Teichmann.
1992. A new model accounting for seasonal cessation of growth in fishes. Aust. J. Mar. Freshw. Res. 43:1151–1156.

PFMC (Pacific Fishery Management Council).
2019. Coastal pelagic species fishery management plan as amended through Amendment 17, 49 p. Pac. Fish. Manage. Counc., Portland, OR. [Available from website.]
2022. Status of the Pacific coast coastal pelagic species fishery and recommended acceptable biological catches. Stock assessment and fishery evaluation 2021, including information through June 2021, 95 p. Pac. Fish. Manage. Counc., Portland, OR. [Available from website.]

R Core Team.
2022. R: a language and environment for statistical computing. R Foundation for Statistical Computing, Vienna, Austria. [Availbale from website, accessed July 2022.]

Reeves, S. A.
2003. A simulation study of the implications of age-reading errors for stock assessment and management advice. ICES J. Mar. Sci. 60:314–328.

Reiss, C. S., D. M. Checkley Jr., and S. J. Bograd.
2008. Remotely sensed spawning habitat of Pacific sardine (*Sardinops sagax*) and Northern [sic] anchovy (*Engraulis mordax*) within the California Current. Fish. Oceanogr. 17:126–136.

Renfree, J. S., N. M. Bowlin, B. E. Erisman, R. I. Rojas-González, G. E. Johnson, S. A. Mau, D. W. Murfin, B. D. Schwartzkopf, T. S. Sessions, K. L. Stierhoff, et al.
2022. Report on the summer 2021 California Current Ecosystem Survey (CCES) (2107RL), 6 July to 15 October 2021, conducted aboard NOAA ship [sic] *Reuben Lasker*, Mexican research vessel *Dr. Jorge Crranza Fraser*, fishing vessels *Lisa Marie* and *Long Beach Carnage*, and uncrewed surface vehicles. NOAA Tech. Memo. NMFS-SWFSC-669, 34 p.

Richards, L. J., J. T. Schnute, A. R. Kronlund, and R. J. Beamish.
1992. Statistical models for the analysis of ageing error. Can. J. Fish. Aquat. Sci. 49:1801–1815.

Ricker, W. E.
1975. Computation and interpretation of biological statistics of fish populations. Bull. Fish. Res. Board Can. 191:1–382.

Sainsbury, K. J.
1980. Effect of individual variability on the von Bertalanffy growth equation. Can. J. Fish. Aquat. Sci. 37:241–247.

Scherrer, S. R., D. R. Kobayashi, K. C. Weng, H. Y. Okamoto, F. G. Oishi, and E. C. Franklin.
2021. Estimation of growth parameters integrating tag-recapture, length-frequency, and direct aging data using likelihood and Bayesian methods for the tropical deepwater snapper *Pristipomoide filamentosus* in Hawaii. Fish. Res. 233:105753.

Schwartzkopf, B. D., E. Dorval, K. C. James, J. M. Walker, O. E. Snodgrass, D. L. Porzio, and B. E. Erisman.
2022. A summary report on life history information on the central subpopulation of Northern Anchovy (*Engraulis mordax*) for the 2021 stock assessment. NOAA Tech. Memo. NMFS-SWFSC-659, 67 p.

Secor, D. H., and J. M. Dean.
1992. Comparison of otolith-based back-calculation methods to determine individual growth histories of larval striped bass, *Morone saxatilis*. Can. J. Fish. Aquat. Sci. 49:1439–1454.

Shoup, D. E., and P. H. Michaletz.
2017. Growth estimation: summarization. *In* Age and growth of fishes: principles and techniques (M. C. Quist and D. A. Isermann, eds.), p. 233–264. Am. Fish. Soc., Bethesda, MD.

Silva, A., P. Carrera, J. Masse, A. Uriarte, M. B. Santos, P. B. Oliveira, E. Soares, C. Porteiro, and Y. Stratoudakis.
2008. Geographic variability of sardine growth across the northeastern Atlantic and the Mediterranean Sea. Fish. Res. 90:56–69.

Somers, I. F.
1988. On a seasonally oscillating growth function. Fishbyte 6:8–11.

Spratt, J. D.
1975. Growth rate of the northern anchovy, *Engraulis mordax*, in southern California waters, calculated from otoliths. Calif. Fish Game 61:116–126.
Stawitz, C. C., M. A. Haltuch, and K. F. Johnson.
2019. How does growth misspecification affect management advice derived from an integrated fisheries stock assessment model? Fish. Res. 213:12–21.
Stierhoff, K. L., J. P. Zwolinski, and D. A. Demer.
2019. Distribution, biomass, and demography of coastal pelagic fishes in the California Current Ecosystem during summer 2018 based on acoustic-trawl sampling. NOAA Tech. Memo. NMFS-SWFSC-613, 63 p.
2020. Distribution, biomass, and demography of coastal pelagic fishes in the California Current Ecosystem during summer 2019 based on acoustic-trawl sampling. NOAA Tech. Memo. NMFS-SWFSC-626, 80 p.
2021a. Distribution, biomass, and demography of coastal pelagic fishes in the California Current Ecosystem during summer 2016 based on acoustic-trawl sampling. NOAA Tech. Memo. NMFS-SWFSC-649, 79 p.
2021b. Distribution, biomass, and demography of coastal pelagic fishes in the California Current Ecosystem during summer 2015 based on acoustic-trawl sampling. NOAA Tech. Memo. NMFS-SWFSC-648, 57 p.
Sydeman, W. J., S. Dedman, M. García-Reyes, S. A. Thompson, J. A. Thayer, A. Bakun, and A. D. MacCall.
2020. Sixty-five years of northern anchovy population studies in the southern California Current: a review and suggestion for sensible management. ICES J. Mar. Sci. 77:486–499.
Takahashi, M., D. M. Checkley Jr., M. N. C. Litz, R. D. Brodeur, and W. T. Peterson.
2012. Responses in growth rate of larval northern anchovy (*Engraulis mordax*) to anomalous upwelling in the northern California Current. Fish. Oceanogr. 21:393–404.
Thayer, J. A., A. D. MacCall,, W. J. Sydeman, and P. C. Davison.
2017. California anchovy population remains low, 2012–2016. CalCOFI Rep. 58:69–76. [Available from website.]
Thomas, R. M.
1983. Seasonal variation in the relationship between otolith radius and fish length in the pilchard off South West Africa. S. Afr. J. Mar. Sci. 1:133–138.
Thompson, A. R., I. D. Schroeder, S. J. Bograd, E. L. Hazen, M. G. Jacox, A. Leising, B. K. Wells, J. L. Largier, J. L. Fisher, K. C. Jacobson, et al.
2019. State of the California Current 2018–19: a novel anchovy regime and a new marine heat wave? CalCOFI Rep. 60:1–65. [Available from website.]
Thompson, A. R., E. P. Bjorkstedt, S. J. Bograd, J. L. Fisher, E. L. Hazen, A. Leising, J. A. Santora, E. V. Satterthwaite, W. J. Sydeman, M. Alksne, et al.
2022. State of the California Current Ecosystem in 2021: winter is coming? Front. Mar. Sci. 9:958727.
Tommasi, D., Y. deReynier, H. Townsend, C. J. Harvey, W. H. Satterthwaite, K. N. Marshall, I. C. Kaplan, S. Brodie, J. C. Field, E. L. Hazen, et al.
2021. A case study in connecting fisheries management challenges with models and analysis to support ecosystem-based management in the California Current Ecosystem. Front. Mar. Sci. 8:624161.
Uriarte, A., I. Rico, B. Villamor, E. Duhamel, C. Dueñas, N. Aldanondo, and U. Cotano.
2016. Validation of age determination using otoliths of the European anchovy (*Engraulis encrasicolus* L.) in the Bay of Biscay. Mar. Freshw. Res. 67:951–966.
von Bertalanffy, L.
1938. A quantitative theory of organic growth (inquiries on growth laws. II). Hum. Biol. 10:181–213.
Vrooman, A. M., P. A. Paloma, and J. R. Zweifel.
1981. Electrophoretic, morphometric, and meristic studies of subpopulations of northern anchovy, *Engraulis mordax*. Calif. Fish Game 67:39–51.
Winemiller, K. O., and K. A. Rose.
1992. Patterns of life-history diversification in North American fishes: implications for population regulation. Can. J. Fish. Aquat. Sci. 49:2196–2218.
Xiao, Y.
1996. How does somatic growth rate affect otolith size in fishes? Can. J. Fish. Aquat. Sci. 53:1675–1682.
Yaremko, M. L.
1996. Age determination in Pacific sardine, *Sardinops sagax*. NOAA Tech. Memo. NMFS-SWFSC-223, 34 p.
Zwolinski, J. P., D. A. Demer, B. J. Macewicz, S. Mau, D. Murfin, D. Palance, J. S. Renfree, T. S. Sessions, and K. Stierhoff.
2017. Distribution, biomass and demography of the central-stock of northern anchovy during summer 2016, estimated from acoustic-trawl sampling. NOAA Tech. Memo. NMFS-SWFSC-572, 18 p.
Zwolinski, J. P., K. L. Stierhoff, and D. A. Demer.
2019. Distribution, biomass, and demography of coastal pelagic fishes in the California Current Ecosystem during summer 2017 based on acoustic-trawl sampling. NOAA Tech. Memo. NMFS-SWFSC-610, 56 p.

National Marine
Fisheries Service
NOAA

*Fishery Bulletin*
established in 1881

Spencer F. Baird
First U.S. Commissioner
of Fisheries and founder
of *Fishery Bulletin*

# Examining the periodicity of annular deposition of otolith microconstituents as a means of age validation

**Benjamin Frey (contact author)**[1]
**Vyacheslav Lyubchich**[1]
**Michelle Zapp Sluis**[2]
**Nathaniel Miller**[3]
**David Secor**[1]

Email address for contact author: benalexfrey@gmail.com

[1] Chesapeake Biological Laboratory
University of Maryland
Center for Environmental Science
146 Williams Street
Solomons, Maryland 20688

[2] Department of Marine Biology
Texas A&M University at Galveston
1001 Texas Clipper Road
Galveston, Texas 77553

[3] Jackson School of Geosciences
The University of Texas at Austin
2305 Speedway, Stop C1100
Austin, Texas 78712-1692

**Abstract**—In this study, we examined whether otolith microconstituents are deposited seasonally in a manner similar to optical annulus formation and thereby can be used to validate age interpretations. In temperate species, seasonal temperature changes drive the formation of optical annuli, and we hypothesized that they similarly caused oscillations in microconstituent deposition. Using laser ablation inductively coupled plasma mass spectrometry analysis, we tested for periodicity in the deposition of barium (Ba), calcium, copper, magnesium (Mg), manganese (Mn), phosphorus (P), strontium, and zinc in otoliths and compared that periodicity to the periodicity of the annulus zonation (optical opaque and translucent zones). For this investigation of chemical annulus periodicity, we used black sea bass (*Centropristis striata*), a species with yearly optical annulus formation that has been validated. Periodicities in elemental profiles in otoliths from black sea bass were detected by using Lomb–Scargle periodogram analyses. Optical annulus formation aligned with Mg profiles, but periodicity in annular deposition of other elements—Ba, Mn, and P—was observed only after the first optical annulus, an outcome that is indicative of ontogenetic changes in habitat (from coastal to near-shelf waters) known to occur during the juvenile life stage of this species. Certain elements, such as Mg, identified through this otolith analysis and the periodogram analyses could be applied to species for which no validated aging procedure exists.

Manuscript submitted 17 March 2023.
Manuscript accepted 29 November 2023.
Fish. Bull. 121:188–198 (2023).
Online publication date: 14 December 2023.
doi: 10.7755/FB.121.4.4

The views and opinions expressed or implied in this article are those of the author (or authors) and do not necessarily reflect the position of the National Marine Fisheries Service, NOAA.

The lack of validated methods for age determination directly affects many fisheries assessments and management efforts. The use of unvalidated aging techniques can affect estimation of catch at age, selectivity at age, numbers at age, maturity at age, and weight at age, and errors in estimates of these factors can contribute to major bias and errors in age-based assessments (Bradford, 1991; Wilhelm et al., 2008; Elvarsson et al., 2018). An error in aging can result in overexploitation and the eventual collapse of a stock and its associated fishery (Mills and Beamish, 1980; Chale-Matsau et al., 2001; Yule et al., 2008). Despite the importance of accurate age determinations, validation studies on annulus formation are rare for many important commercial stocks, including the majority of species harvested in waters along the Atlantic coast from Maine to South Carolina (Suppl. Table) (online only). Validation studies have been done for only slightly more than half (10 of 19; Suppl. Table) (online only) of the species routinely aged by the NOAA Northeast Fisheries Science Center.

Interpretation of optical zones (annuli) in fish hard parts is considered a direct method of aging and is the conventional approach for age determination, which is needed in age-based assessments (Casselman, 1983; Vitale et al., 2019). Hard parts are calcified structures, which include otoliths, vertebrae, opercula, fin rays, and scales. They often have patterns of seasonal zonation, which can be optically distinguished through microscopy as alternating dark and light (translucent and opaque) zones that vary in their organic concentrations (Jolivet et al., 2008) (Fig. 1). Opaque zones typically have higher protein content, are relatively narrow in comparison to translucent zones, and are interpreted as representing periods of lower seasonal growth rates such as temperate winters (Thomas, 1983; Machias et al., 1998; Zlokovitz et al., 2003). The 2 zones together constitute an annulus, but it remains the task of the investigator to determine whether each annulus forms annually and therefore whether it is valid to use the structure for determining ages of fish (Campana, 2001).

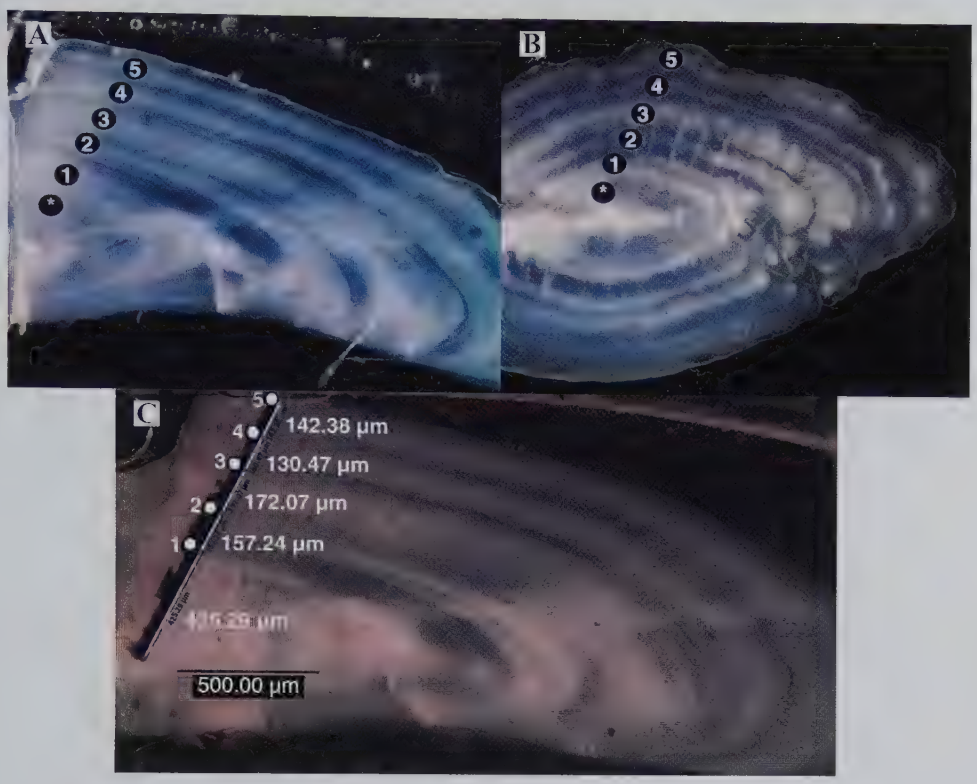


**Figure 1**

Age annotations for each optical annulus identified on a (**A**) sectioned and (**B**) whole otolith from a black sea bass (*Centropristis striata*) caught on 15 July 2018 off Ocean City, Maryland. (**C**) Otolith sections, like the one shown in the bottom panel, were annotated following analysis through laser ablation inductively coupled plasma mass spectrometry. Distances were measured from the ablated point within the core region of an otolith to the distal edge of each opaque zone found in optical annulus assignments. Images were captured with reflected light on a black background. In the top panels, the asterisk indicates the central opaque core, which was not counted according to the otolith aging approach used by the NOAA Northeast Fisheries Science Center.

Efforts to validate age determination can be hampered by the requirement to test age interpretations on fish of known ages. The approaches used to validate the annual formation of presumed annuli in hard parts can be direct or indirect (Vitale et al., 2019). In direct validation methods, individuals are tracked over time as annular zones form over seasons and years, by using temporal reference points (markers) on hard parts (Vitale et al., 2019). In indirect validation methods, annular structures are examined in relation to changes in season, year-class strength, or size modes and include length–frequency analysis, marginal increment analysis, and microchemistry (Vitale et al., 2019).

In a promising approach for age validation, periodicity in annular deposition of microconstituents in hard parts is examined by using microchemistry. Otolith microconstituent uptake can vary seasonally and can be regarded as a "chemical calendar-clock" with time-keeping properties similar to the optical annuli on hard parts (Limburg et al., 2018). The results of the study by Hüssy et al. (2021a) reveal that the elemental composition of otoliths can vary seasonally and that these variations can be used to validate the accuracy of otolith chemical chronologies in determining the age of fish. Siskey et al. (2016) and Brophy[1], employing periodogram analysis, have shown that the periodicity of some elements in hard parts is annual and synchronizes with the optical patterns that form annuli.

The underlying premise of microconstituent validation is that optical banding patterns (annuli) in hard parts coincide with changes in chemical composition, both of which represent seasonal changes in otolith organic content and environmental temperature. Fish that reside or migrate through coastal and shelf environments are exposed to mixtures of terrestrial, anthropogenic, and marine sources of aqueous metals and isotopes. Found in higher abundance in hard parts than calcium (Ca), the elements strontium (Sr), magnesium (Mg), manganese (Mn), and

[1] Brophy, D. (coord.). 2019. Validating age-determination [sic] of anglerfish and hake, 97 p. EASME/EMFF/2016/1.3.2.7/SI2.762036. Final report. Publ. Off. Eur. Union, Luxembourg, Luxembourg. [Available from website.]

barium (Ba) substitute for Ca within the crystalline lattice of aragonitic otoliths in proportion to environmental exposure but at rates modified by temperature and growth (Hüssy et al., 2021b). Trace constituents, such as phosphorus (P), cobalt (Co), copper (Cu), and zinc (Zn), are bound in the protein matrix of otoliths and it has been hypothesized that they are physiologically controlled (Hüssy et al., 2021b), albeit some evidence indicates a role for environmental exposure (Arslan and Secor, 2005). Therefore, across the elements that we considered candidates for use in age determination, the kinetics of tracer incorporation are driven variously by exposure, temperature, and physiology, the relative contribution of which remains an unsettled question (e.g., Hussy et al., 2020).

In temperate shelf environments, concentrations of candidate elements do not vary as substantially as they would in freshwater, estuarine, and nearshore environments. In this study, we assumed that exposure to seasonally changing temperatures drives variation in microconstituent concentrations. We tested this assumption by comparing known seasonal patterns of optical annulus zonation with those of microconstituent zonation in otoliths.

To evaluate chemical annulus periodicity, it's important to test a model species for which age determination has been validated previously. The black sea bass (*Centropristis striata*) is a ubiquitous reef fish species found in the Gulf of Mexico and along the Atlantic coast of the United States, from Florida to the Gulf of Maine. This species is a target for important commercial and recreational fisheries along the Atlantic coast that are assessed by using statistical catch-at-age models (Musick and Mercer, 1977; NEFSC, 2020; ASMFC[2]). Adult black sea bass are most abundant in temperate shelf environments, although their young (<2 years in age) often occur in estuarine and coastal habitats. The aging method for black sea bass has been validated through marginal increment analysis (Dery and Mayo, 1988; Penttila and Dery, 1988; Robillard et al.[3]; Koob et al., 2021).

We hypothesized that cycles of microconstituent deposition (i.e., chemical zonation) would relate to age with a dominant periodicity of 1 cycle per optical annulus. By linking the optical interpretation to the chemical measures, the periodicity of each cycle can be tested through time-series analysis. We first identified candidate microconstituents through elemental profiles and 2-dimensional (2D) maps. We then conducted Lomb–Scargle periodogram analyses on candidate microconstituent profiles to test the hypothesis that the dominant periodicity is 1.0 cycle per optical annulus. Under the premise that black sea bass undertake a habitat shift from inshore to offshore waters during their second year of life, 2 alternate periodogram analyses were conducted with data sets containing concentrations of microconstituents along a line from the core to the edge of otoliths for 1) the entire series of annuli on each otolith or 2) the series of annuli after the first one.

## Materials and methods

### Analysis of otoliths

Sagittal otoliths were collected from black sea bass (sample size [*n*]=125) ranging in total length from 19.5 to 36.3 cm and captured through hook and line at wreck and artificial reef sites (depths: 20–30 m) off Ocean City, Maryland, during the summer and fall of 2016 and 2018. Annuli in whole and sectioned otoliths were defined as continuous opaque zones with no breaks (Fig. 1). Aging conventions were adopted from Robillard et al.[3] and Koob et al. (2021), who discounted initial opaque material deposited around the core of an otolith as material formed during age 0 and identified a second opaque region as the completion of the first annulus (Fig. 1) (Penttila and Dery, 1988; Robillard et al.[3]).

By convention, a birth date of 1 January was assumed (given that spawning occurs in the spring for this species) (Vanderkooy et al.[4]). The seasonality of optical and chemical annuli could vary; therefore, fish collected before 30 June were assumed to have completed less than half of their most recent year of life, and counts of opaque zones were assumed to represent the estimated age. For those captured after 30 June, the edge was counted as an integer because these fish had completed >0.5 years of life and so that we could consider the indication of growth patterns beyond the last opaque zone (Dery and Mayo, 1988; Vanderkooy et al.[4]). Whole otoliths from black sea bass were photographed under reflected light at 1.5× magnification by using a microscope camera and Infinity Analyze and Capture[5] software (vers. 6.5.6; Teledyne Lumenera, Ottawa, Canada). Following age assignment with whole otoliths, otoliths were then embedded in Struers epoxy resin (Struers A/S, Ballerup, Denmark) for sectioning. A 2.0-mm-thick section containing the core region (the innermost portion of the otolith, pertaining to the first year of life) was cut along a transverse plane with an IsoMet Low Speed Saw (Beuhler Ltd., Lake Bluff, IL). The otolith section was then attached to a glass slide by using Crystalbond 509 mounting adhesive (Aremco Products Inc., Valley Cottage, NY) in preparation for microchemical analysis and further interpretations of annuli.

[2] ASMFC (Atlantic States Marine Fisheries Commission). 2021. Review of the interstate fishery management plan for black sea bass (*Centropristis striata*): 2020 fishing year, 15 p. ASMFC, Arlington, VA. [Available from website.]

[3] Robillard, E., J. W. Gregg, J. Dayton, and J. Gartland. 2016. Validation of black sea bass, *Centropristis striata*, ages using oxytetracycline marking and scale margin increments, 17 p. Stock Assess. Rev. Comm., SARC 62 working paper. [Available from Northeast Fish. Sci. Cent., Natl. Mar. Fish. Serv., NOAA, 166 Water St., Woods Hole, MA.]

[4] Vanderkooy, S., J. Carroll, S. Elzey, J. Gilmore, and J. Kipp. 2020. A practical handbook for determining the ages of Gulf of Mexico and Atlantic coast fishes, 3rd ed., 268 p. Gulf States Mar. Fish. Comm., Ocean Springs, MS. [Available from website.]

[5] Mention of trade names or commercial companies is for identification purposes only and does not imply endorsement by the National Marine Fisheries Service, NOAA.

Microchemical analysis of elemental variations from the core region to the otolith's periphery was done by using laser ablation inductively coupled plasma mass spectrometry (LA-ICP-MS) at the Department of Geological Sciences of the University of Texas at Austin. Analysis was limited to 34 of the 125 otoliths collected because of the cost of the analysis; otoliths were randomly selected from among otoliths taken from fish assigned ages >1 year. The instrumentation used was an NWR193 excimer laser ablation system (193-nm wavelength, 4-ns pulse width; Elemental Scientific Inc., Omaha, NE) coupled to an Agilent 7500ce ICP-MS (Agilent, Santa Clara, CA). This LA-ICP-MS system was equipped with a large-format, 2-volume sample cell with fast washout (<1 s) that accommodated all samples and standards (USGS MACS-3, NIST 612, and ECRM-752-NP) in 3 laser cell loadings.

The LA-ICP-MS system was optimized daily for sensitivity across the atomic mass unit range and low oxide production (ratio of thorium monoxide to thorium: 0.58 [standard deviation (SD) 0.06]) by tuning with a standard glass (NIST 612), and sensitivity was checked with trial transects on representative specimens. Following pre-ablation (75-µm spot, 50-µm/s scan rate, 3.3-J/cm$^2$ energy density [fluence]) to remove shallow surface contaminants, core-to-edge profiles were collected from each otolith along the sulcal ridge for consistency, by using a spot with a 50-µm diameter, a 5-µm/s scan rate, a fluence of 2.92 J/cm$^2$ (SD 0.15), a 15-Hz repetition rate, and carrier gas flows of 0.8 L/min for argon and 0.80–0.85 L/min for helium. The quadrupole time-resolved method was used to measure 12 masses with integration times of 10 ms ($^{24}$Mg, $^{43–44}$Ca, and $^{88}$Sr), 20 ms ($^{25}$Mg, $^{31}$P, and $^{55}$Mn), and 25 ms ($^{59}$Co, $^{63}$Cu,$^{66}$Zn, and $^{137–138}$Ba). The quadrupole duty cycle of 0.3732 s corresponds to 94% of total measurement time, with a resultant linear sampling rate of 1.867 µm/s, equivalent to 13.4 measurements captured within the footprint of either aperture. Measured intensities were converted to elemental concentrations (parts per million) by using iolite 4 software (Paton et al., 2011), with $^{43}$Ca as the internal standard and a Ca index weight percentage of 38.3% for unknowns.

For the otoliths, USGS MACS-3 (synthetic aragonite) was used as the primary calibration standard, and NIST 612 (glass) and ECRM-752-NP (nanoparticulate pressed limestone powder pellet made from BCS-CRM 393 limestone from Bureau of Analysed Samples Ltd., Middlesbrough, UK) were used as external reference standards. The grand average of secondary standard recovery fractions for all elements was typically within 5% of preferred values in the GeoReM database (Jochum et al., 2005).

To create 2D maps of otolith microconstituents, areas were scanned by using contiguous line traverses with a 17-µm$^2$ aperture, spaced 17 µm apart. The scan rate (105 µm/s) was set to provide 1 quadrupole measurement cycle per aperture footprint. Using the quadrupole method for mapping, we surveyed elements with integration times of 10 ms ($^{43–44}$Ca and $^{88}$Sr), 20 ms ($^{55}$Mn and $^{138}$Ba), and 25 ms ($^{24}$Mg, $^{65}$Cu, and $^{66}$Zn) and with a significantly shorter duty cycle of 0.1612 s corresponding to 90% of total measurement time. Calibration and secondary standards were as described previously. External reference standard recoveries were typically within 10% of certified reference values. Image conversions, from contiguous-line traverses along the otolith to 2D maps of element deposition, were performed by using iolite 4 software (Paton et al., 2011).

### Analysis of time series

To determine if optical annuli coincide with the microconstituent profiles, LA-ICP-MS data were aligned with micrographs of transverse otolith sections through image analysis. Optical annuli were assigned and measured for each cycle of a paired translucent zone and opaque zone. Distances along the trench formed through ablation on the surface of an otolith were measured from the ablated point within the core region to the distal edge of each opaque zone according to optical annulus assignments (Fig. 1C), with a minimum of 39 measurements per year of growth. Each opaque zone was considered the terminus of each annulus (1 year of growth), and zones measured through LA-ICP-MS within a cycle (pair of translucent and opaque zones) were converted to fractional ages within each annulus cycle, assuming that otolith growth was linear.

Typical concentrations of elements over transects on otoliths from representative specimens were 10–10,000 times higher than the limits of detection for most elements (Table 1). A rule-of-thumb ratio of signal to noise of 2 to 3 was employed as a threshold for inclusion (mean transect concentration divided by minimum detection limit) (Armbruster and Pry, 2008; Rajaković et al., 2012). Consecutive moving average filters were used to smooth derived elemental time series (profiles) by using a 9-point boxcar width (13- and 26-µm equivalent distances), and the profiles were converted to *Z*-scores, resulting in smooth, locally weighted signals that were free from high-frequency outliers. Signals were converted to distance (in microns) from the core on the basis of scan rate and duty cycle. Because signals for elements measured with

**Table 1**

Average concentrations (in parts per million) of elements in otoliths of black sea bass (*Centropristis striata*) ($n$=34) caught off Ocean City, Maryland, during the summer and fall of 2016 and 2018. Also provided for each element are the standard deviation (SD) of the average concentration and the ratio of signal to noise (S:N), which is the mean transect concentration divided by the estimated mean detection limit among the analyzed otoliths. The elements are magnesium (Mg), phosphorus (P), manganese (Mn), cobalt (Co), copper (Cu), zinc (Zn), strontium (Sr), and barium (Ba). An asterisk (*) indicates that the average concentration of the element was less than twice as high as detection limits.

| Value | Mg | P | Mn | Co | Cu | Zn | Sr | Ba |
|---|---|---|---|---|---|---|---|---|
| Average | 13.6 | 78.6 | 2.3 | 0.2 | 0.3 | 0.4 | 2148.9 | 10.1 |
| SD | 3.0 | 32.5 | 0.8 | 0.0 | 1.2 | 0.4 | 168.4 | 3.5 |
| S:N | 23.7 | 2.7 | 4.6 | 3.2 | 0.3* | 0.3* | 45,000.0 | 370.0 |

multiple isotopes were identical, we used the isotopes with the highest abundance (e.g., $^{24}Mg$ and $^{138}Ba$) for plotting and statistical analysis. The detrended time series for each individual fish and element were subjected to Lomb–Scargle periodogram analysis, a flexible approach that accounts for unequally spaced measurements across the annuli of multiple otoliths (Lomb, 1976; Scargle, 1982; Ruf, 1999). Normalized power was used to evaluate significant frequencies. Alternate periodogram analyses were performed with data for the entire series of annuli on each otolith and with data for the series of annuli after the first one on each otolith.

## Results

### Analysis with mass spectrometry

The elements Mg, Mn, Co, Cu, Zn, Sr, and Ba were all measured at detectable levels though LA-ICP-MS (Table 1). Copper and Zn were below the signal, a noise threshold of 2.0–3.0 (both at a signal-to-noise ratio of 0.3), and were not considered further in analyses. Concentration amplitudes were within the range expected for otoliths from marine teleost fish: <1 ppm for transition metals Mn, Co, Cu, and Zn; <8 ppm for Mg, P, and Ba; and <2000 ppm for Sr (Campana, 1999; Hüssy et al., 2021b).

Among measured elements, Mg had the sharpest contrast across presumed chemical annuli as revealed in 2D maps of element deposition for the 2 analyzed otoliths (Fig. 2). The chemical zonation for 4 of the 6 elements analyzed, Ba, Mg, Mn, and Sr, aligned with conventional light microscopy. For Ba, chemical zonation was most apparent for annuli after the second one, with weak contrast prior to the third annulus. Strong zonation of Mg was observed for the entire series of annuli. For Mn, concentrations were elevated in the core region for both scanned otoliths, and chemical zonation was faint but distinct across the series of annuli. Zonation of Sr was inconsistent between the 2 otoliths (Fig. 2, "Sr" panel in both sets of panels), with a faint series of annuli in one otolith and a narrow chemical zonation for annuli after the second one in the other otolith.

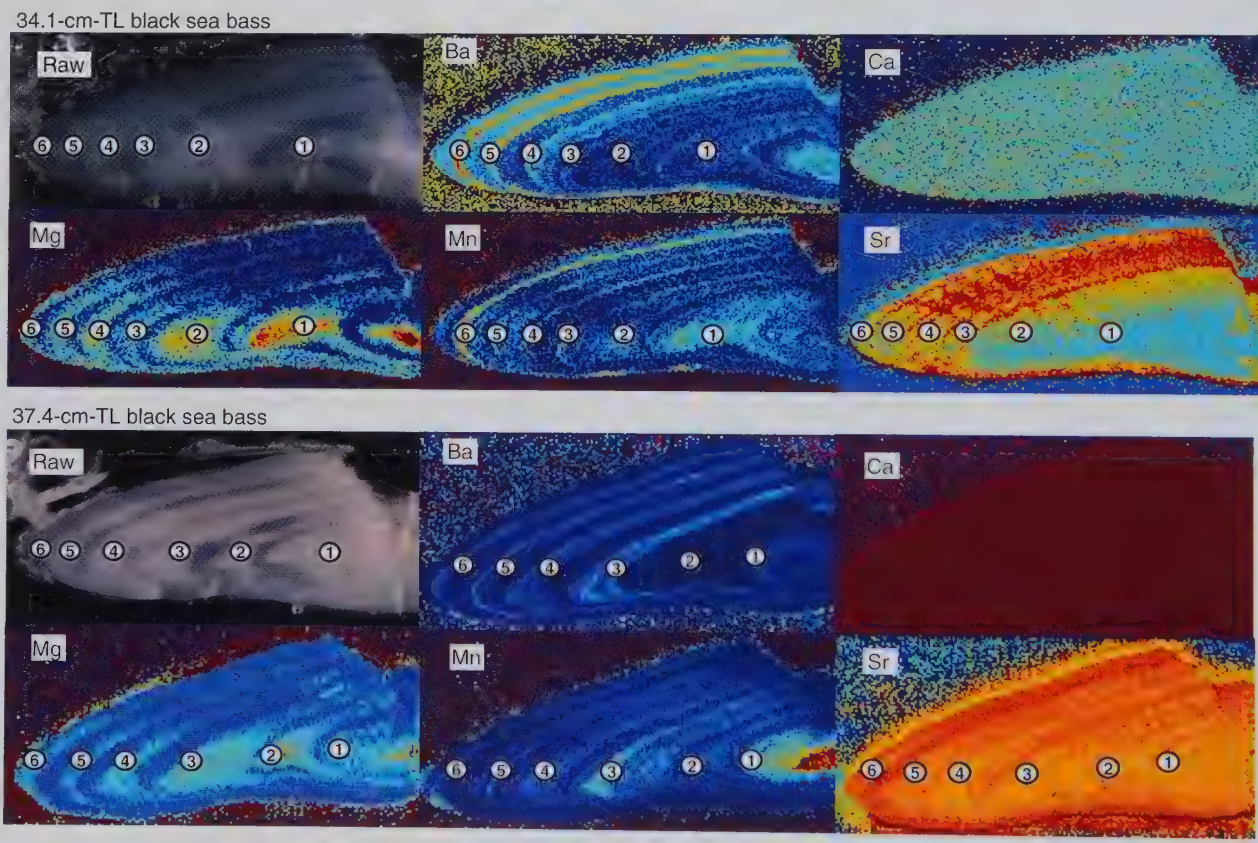


**Figure 2**

Two-dimensional maps of element deposition, with a light micrograph (Raw) image, for each of the sectioned otoliths from 2 black sea bass (*Centropristis striata*) caught on 15 July 2018 off Ocean City, Maryland. The elements are barium (Ba), calcium (Ca), magnesium (Mg), manganese (Mn), and strontium (Sr). Colors in the maps indicate the concentration of elements from blue (low) to red (high). Note that contrast is optimized and depicted through pseudocolor for each map, and it is not common across elements. White circles indicate optical annuli, and the associated numerals indicate assigned ages; the central opaque core is not included because it was not counted in otolith aging.

Zonation of Ca was homogeneous in both 2D maps as expected.

Despite notable zonation in the 2D maps, oscillating patterns in standardized elemental profiles were not aligned across individuals nor clearly associated with age (Fig. 3). Note that the majority of profiles correspond to estimated ages ≤4 years, with 2 profiles continuing to age 6. Profiles for the transition metal Co were especially noisy, corresponding to the lack of patterning in the 2D scan. For Ba, Mg, and Mn, peaks and nadirs of oscillations give some indication of association with optical annuli, but visual classifications were deemed too subjective.

### Analysis with periodograms

The results of the principal periodogram analysis of the entire elemental time series, inclusive of the first annulus, indicate a significant periodicity in microchemical transects, albeit at frequencies that mostly differed from the expected 1 year (Fig. 4, top set of panels). Only annular deposition of Mg had significant periodicity of 1 cycle per annulus. Significant periodicity in deposition is evident for the elements Ba and Mn but at a rate of ~1.5 cycles per annulus, each at a lower normalized power than that for deposition of Mg (Fig. 4, top set of panels). Strontium had no defined peak in oscillations and, therefore, no determinable primary chemical cycle. In the periodograms for oscillations of P and Co, the frequencies are 1.5 cycles and 1 cycle per annulus, respectively, albeit at low normalized power (i.e., reduced significance).

In the alternative periodogram analysis of the time series excluding the first annulus, significant periodicity was detected for oscillations of Mg, Ba, Mn, and P at the hypothesized 1 cycle per annulus at high normalized power (Fig. 4, bottom set of panels). Magnesium deposition periodicity remained at 1 cycle per annulus after truncation of the time series. The periodogram for oscillations of Sr again failed to indicate a dominant period. In the truncated series, oscillations of Co had multiple peaks, all of which deviated from the expected frequency of 1 year.

## Discussion

The hypothesis of aligned optical and chemical oscillations across all annuli (not excluding the first annulus) was confirmed for the element Mg and alignment across age estimates >1 year was confirmed for the microconstituents

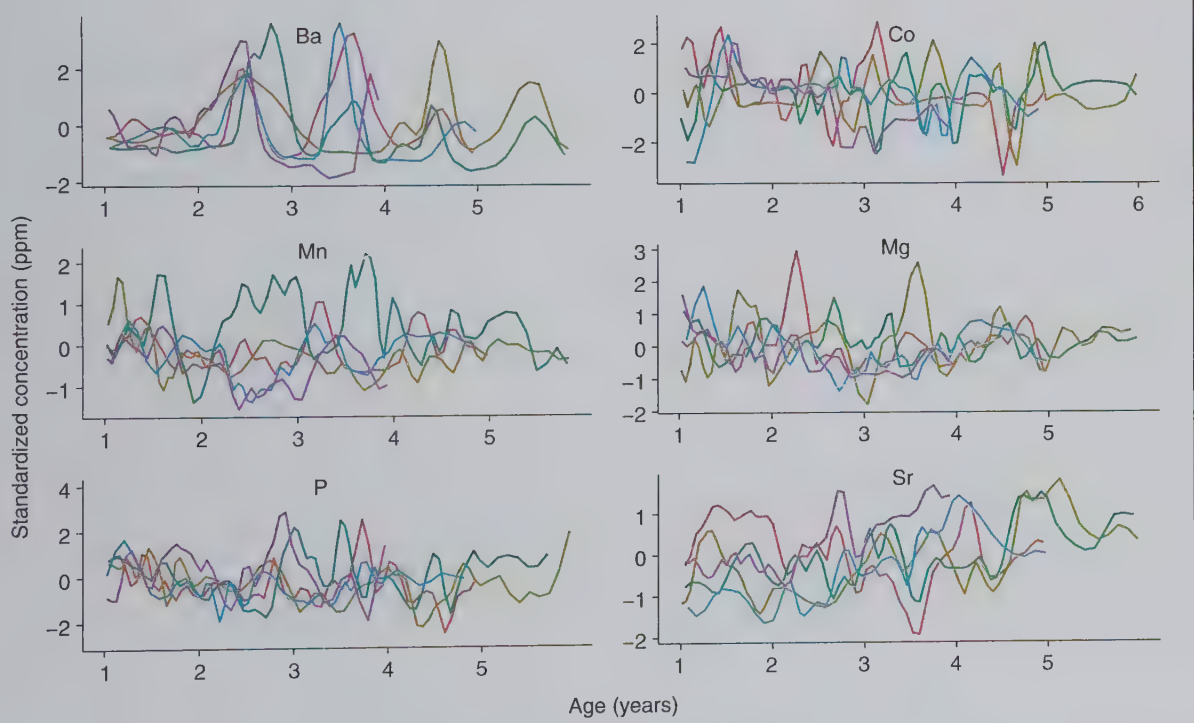


**Figure 3**

Profiles of microconstituent concentrations, smoothed by using consecutive moving median and average filters, in 5 of the 34 otoliths examined through laser ablation inductively coupled plasma mass spectrometry. Otoliths were taken from black sea bass (*Centropristis striata*) caught off Ocean City, Maryland, in October and July 2018. The microconstituents are barium (Ba), cobalt (Co), manganese (Mn), magnesium (Mg), phosphorus (P), and strontium (Sr). The lines for the individual otoliths are depicted in different colors for readability.

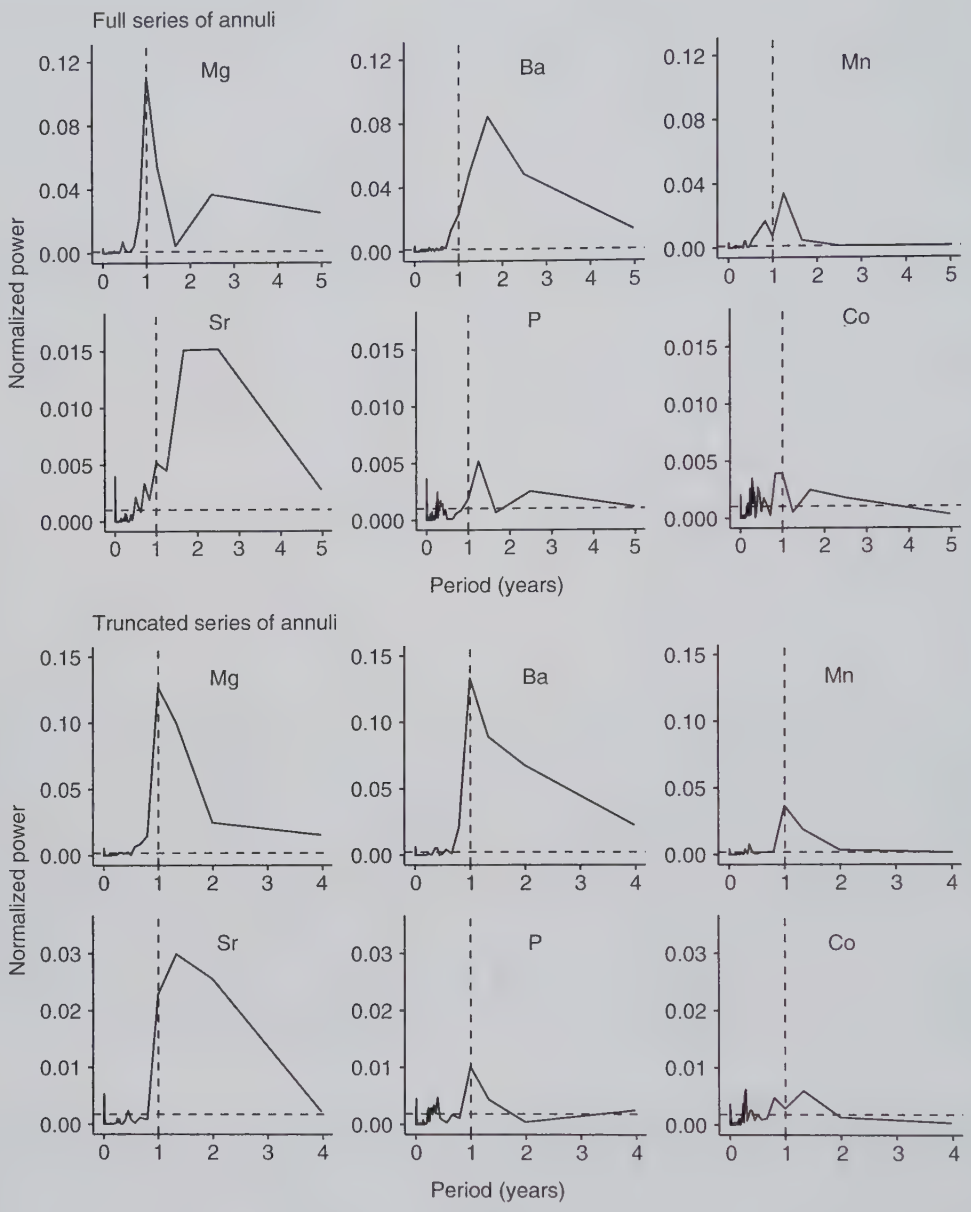


**Figure 4**

Lomb–Scargle periodograms based on elemental profiles for all otoliths examined through microchemical analysis ($n$=34) combined, with the top set of panels including data for the full series of all annuli on each otolith and the bottom set of panels including data for only the series of annuli after the first one. Otoliths were taken from black sea bass (*Centropristis striata*) caught off Ocean City, Maryland, during the summer and fall of 2016 and 2018. The horizontal dashed lines indicate the significance level of 0.001. The vertical dashed line indicates the hypothesized frequency of 1 cycle per annulus. Note the difference in scales between the top and bottom rows in each set of panels.

Ba, Mg, P, and Mn through the Lomb–Scargle periodogram analyses. The periodicity we observed for deposition of Mg in otoliths through the analysis that included data for all annuli supports recent work by Koob et al. (2021) and the conventions used by the Northeast Fisheries Science Center for first annulus assignments. Because the dominant period was 1 year, rather than for instance 1.2 years, the influence of the assumption that otolith growth is linear on the estimated period was negligible. The 2D maps show that chemical zonation corresponded with optical zonation for all annuli in each otolith (in the case of Mg) or for the annuli after the first one in each otolith (in the cases of Ba, P, and Mn). Concentrations of other elements were below detection thresholds (Cu and Zn), had no zonation (Co), or

had patterns that were inconsistent with optical annuli (Sr). Patterns of Sr oscillations are weak in 2D maps and in standardized profiles. This lack of annual periodicity in Sr explains why X-ray dispersive spectroscopy of Sr deposition in otoliths was inconclusive in past work (Richards, 2016; Frey, 2022).

Both periodogram analysis results and 2D maps indicate a lack of consistent chemical zonation associated with the first optical annulus. The inclusion and removal of the first annulus in periodogram analysis had a large influence on the periodicity of Sr, Ba, and Mn oscillations. The shifts in Sr, Ba, and Mn concentrations could be explained by habitat changes occurring during the juvenile life stage. Nursery habitats in estuarine and nearshore environments for black sea bass (Dery and Mayo, 1988) are heterogenous in ambient concentrations of Sr, Ba, and Mn. Strontium is conservatively mixed with and is often positively associated with salinity (Kraus and Secor, 2004), observations that are consistent with the lower otolith concentrations of Sr deposited during the first year of life than the levels deposited during later years in otoliths analyzed in our study (Fig. 2). Barium becomes less available in eutrophic waters of estuaries and coastal waters (Hüssy et al., 2021b), a finding that aligns with the lower otolith concentrations of Ba around the first optical annulus compared to the levels around the rest of the annuli beyond the first annulus in otoliths analyzed in our study. How Mn is associated with ambient exposure remains unsettled in the literature, although higher than normal concentrations of Mn in otoliths have been associated with hypoxic waters (Limburg and Casini, 2018). Early elemental oscillations could also reflect a change in reproductive state for black sea bass (maturation is achieved at ages ≥2 years) or early habitat transitions (Drohan et al., 2007). Understanding the lack of expected periodicity for age-1 black sea bass requires a deeper consideration of otolith composition during the first year of life.

Seasonal changes in otolith composition with regard to the elements Mg, Sr, and Mn have been found to conform to expectations of environmental and physiological influences (Grammer et al., 2017; Hüssy et al., 2021a). In their scheme, Hüssy et al. (2021a) proposed that otolith uptake of Ba, K, and Sr, versus that of P, Cu, and Zn, was respectively under environmental versus physiological controls. Further, Mg and Mn uptake was influenced jointly by the environment and physiology (Hüssy et al., 2021a). Concentration of Mg in otoliths is known to be linked to growth (Grammer et al., 2017), possibly explaining the strength of the periodogram analyses and the visibility of chemical annuli in the 2D maps created in our study. Results of recent work by Brophy et al. (2021) indicate that seasonal variation in deposition of Sr in otoliths is detectable in anglerfish (*Lophius piscatorius*), but in our analysis, Sr oscillations were weak and no yearly periodic fluctuations were apparent. Concentrations of Ba in otoliths, like those of Sr, may reflect seasonal temperature cycles (Barnes and Gillanders, 2013; Reis-Santos et al., 2013; Stanley et al., 2015).

A central premise of aligning otolith microconstituent cycles with annulus zone formation is that black sea bass are exposed to seasonal changes in temperatures. Moser and Shepherd (2008) placed archival tags in black sea bass released off coastal states from Massachusetts to Virginia. These and conventionally tagged black sea bass made offshore migrations during winter months, cued by cooling temperatures in near-shelf regions. Off the coast of Maryland, black sea bass migrate to inner shelf regions in spring and reside in bottom waters that have stable thermal conditions until fall, when turnover or seasonal mixing causes a rapid increase in water column temperatures (Wiernicki et al., 2020). These conditions are then followed by cooling in late fall, cueing winter migrations of black sea bass to offshore waters (Moser and Shepherd, 2008). Off the coast of Maryland, where this study's samples originated, this pattern of residency in the spring and fall and offshore migration in winter would be associated with exposure to a seasonal amplitude in temperature of 12–17°C, with most of that change in temperature occurring during August–November (based on observed bottom temperatures in near- and mid-shelf waters off Deleware, Maryland, and Virginia; Rothermel et al. 2020). During a single, long-term (more than 3 years) mark-recapture study in which archival tags were used, Moser and Shepherd (2008) observed temperatures experienced by tagged fish that were consistent with this seasonal cycle and that ranged between 6°C (in winter) and 25°C (from late summer to fall). As reviewed in the "Introduction" section, seasonal temperature was expected to influence concentrations of Mg, Mn, Sr, and Ba—the elements that are incorporated into an otolith's aragonitic structure.

For temperate species, such as the black sea bass, changes in composition of an otolith are thought to relate to the formation of organic-rich (winter) and Ca-rich (spring, summer, and fall) zones in an otolith (Secor and Piccoli, 1996; Hüssy et al., 2021b). These optical zones are also associated with seasonal changes in temperature, with the translucent zone forming during high growth seasons of summer and fall and the narrow opaque zone forming during winter and early spring (Zlokovitz et al., 2003). For example, variation in the level of Sr in hard parts can serve as a proxy for oscillations in temperature: in cooler temperatures, higher levels of Sr are substituted for Ca in the lattice structure of a hard part (Engstedt et al., 2012). Such oscillations across the optical zones of otoliths have been observed for the temperate species red emperor (*Lutjanus sebae*) (Seyama et al., 1991) and bluefin tuna (*Thunnus thynnus*) (Siskey et al., 2016). Therefore, the variations in microchemical composition of otoliths across optical zones can validate the seasonal frequency of these chemical annuli.

## Conclusions

In addition to their use in validation of microconstituent composition in otoliths, one could directly age individuals on the basis of chemical annuli rather than optical annuli. Such an approach would have application for species like the goosefish (*Lophius americanus*), for which optical

annuli are not easily interpreted (Bank et al., 2020). For black sea bass, optical annuli are well aligned with chemical annuli in the 2D maps created in our study (Fig. 2), especially those for Mg, indicating that age can be assigned through direct interpretation of the 2D maps of element deposition in otoliths. The high-contrast visualizations of such analysis of otoliths from black sea bass can provide improved precision in age validation for optical annuli interpretation (Limburg et al., 2018; Heimbrand et al., 2020; Hüssy et al., 2021b). On the other hand, for even moderate sample sizes ($n$>50), reliance on 2D maps could be cost-prohibitive and demand greater investment in time than standard aging approaches. Further, 2D map interpretations are subjective and not supported by objective time-series analyses, such as the periodogram approach applied in our study.

Validation of direct aging through hard-part analysis provides the foundation for strong stock assessments. The results from our use of a chemical aging approach for black sea bass support the findings of recent marginal increment validation studies and optical annulus interpretations. Still, the variable interpretations of the first optical annulus in otoliths merit additional examination given the 1) varying results across the candidate elements Mg, Ba, P, and Mn and 2) past uncertainty in assignment of the first annulus. Chemical validation of optical annulus formation in otoliths of black sea bass further strengthens the confidence in accurate age data for age-structured black sea bass stock assessments.

## Resumen

En este estudio, examinamos si los microconstituyentes de los otolitos se depositan estacionalmente de forma similar a la formación del anillo óptico y, por tanto, pueden utilizarse para validar las interpretaciones de la edad. En las especies templadas, los cambios estacionales de temperatura impulsan la formación de anillos ópticos, y suponemos que de la misma manera causan oscilaciones en la deposición de microconstituyentes. Utilizando análisis de espectrometría de masas con plasma de acoplamiento inductivo por ablación láser, comprobamos la periodicidad en la deposición de bario (Ba), calcio, cobre, magnesio (Mg), manganeso (Mn), fósforo (P), estroncio y zinc en los otolitos y comparamos esa periodicidad con la periodicidad de la zona anular (zonas ópticas opacas y translúcidas). Para esta investigación de la periodicidad de los anillos químicos, utilizamos serrano estriado (*Centropristis striata*), una especie para la que se ha validado la formación anual de anillos ópticos. Se detectaron periodicidades en los perfiles de los elementos de otolitos de lobina negra mediante análisis de periodogramas de Lomb-Scargle. La formación de anillos ópticos se alineó con los perfiles de Mg, pero la periodicidad en la deposición de anillos de otros elementos, Ba, Mn y P, se observó sólo después del primer anillo óptico, un resultado que es indicativo de los cambios ontogenéticos en el hábitat (de aguas costeras a aguas cercanas a la plataforma) que se sabe ocurren durante la etapa de vida juvenil de esta especie. Ciertos elementos, como el Mg, identificados mediante este análisis de otolitos y el análisis del periodograma podrían aplicarse a especies para las que no existe un procedimiento de validación de la edad.

## Acknowledgments

This work was made possible by the NOAA Office of Education Educational Partnership Program (NOAA EPP) (award no. NA16SEC4810007) and through a NOAA EPP Living Marine Resources Cooperative Science Center Fellowship to the senior author.

## Literature cited

Armbruster, D. A., and T. Pry.
2008. Limit of blank, limit of detection and limit of quantitation. Clin. Biochem. Rev. 29:S49–S52.

Arslan, Z., and D. H. Secor.
2005. Analysis of trace transition elements and heavy metals in fish otoliths as tracers of habitat use by American eels in the Hudson River estuary. Estuaries 28:382–393.

Bank, C. M., K. Oliveira, S. J. Sutherland, M. P. Armstrong, J. Landa, and S. X. Cadrin.
2020. Age validation for goosefish (*Lophius americanus*) in the northeastern United States. Fish. Bull. 118:8–20.

Barnes, T. C., and B. M. Gillanders.
2013. Combined effects of extrinsic and intrinsic factors on otolith chemistry: implications for environmental reconstructions. Can. J. Fish. Aquat. Sci. 70:1159–1166.

Bradford, M. J.
1991. Effects of ageing errors on recruitment time series estimated from sequential population analysis. Can. J. Fish. Aquat. Sci. 48:555–558.

Brophy, D., S. Pérez-Mayol, R. Duncan, K. Hüssy, A. J. Geffen, H. D. Gerritsen, M. C. Villanueva, and B. Morales-Nin.
2021. Elemental composition of illicia and otoliths and their potential application to age validation in white anglerfish (*Lophius piscatorius* linnaeus [sic], 1758). Estuar. Coast. Shelf Sci. 261:107557.

Campana, S. E.
1997. Use of radiocarbon from nuclear fallout as a dated marker in the otoliths of haddock *Melanogrammus aeglefinus*. Mar. Ecol. Prog. Ser. 150:49–56.
1999. Chemistry and composition of fish otoliths: pathways, mechanisms and applications. Mar. Ecol. Prog. Ser. 188:263–297.
2001. Accuracy, precision and quality control in age determination, including a review of the use and abuse of age validation methods. J. Fish Biol. 59:197–242.

Casselman, J. M.
1983. Age and growth assessment of fish from their calcified structures—techniques and tools. *In* Proceedings of the international workshop on age determination of oceanic pelagic fishes: tunas, billfishes, and sharks; Miami, 15–18 February 1982 (E. D. Prince and L. M. Pulos, eds.), p. 1–17. NOAA Tech. Rep. NMFS 8.

Chale-Matsau, J. R., A. Govender, and L. E. Beckley.
2001. Age, growth and retrospective stock assessment of an economically extinct sparid fish, *Polysteganus undulosus*, from South Africa. Fish. Res. 51:87–92.

Dery, L. M., and J. P. Mayo.
1988. Black sea bass, *Centropristis striata*. *In* Age determination methods for Northwest Atlantic species (J. Penttila and L. M. Dery, eds.), p. 59–69. NOAA Tech. Rep. NMFS 72.

Drohan, A. F., J. P. Manderson, and D. B. Packer.
2007. Essential fish habitat source document: black sea bass, *Centropristis striata*, life history and habitat characteristics, 2nd ed. NOAA Tech. Memo. NMFS-NE-200, 68 p.

Dwyer, K. S., S. J. Walsh, and S. E. Campana.
2003. Age determination, validation and growth of Grand Bank yellowtail flounder (*Limanda ferruginea*). ICES J. Mar. Sci. 60:1123–1138.

Elvarsson, B. Þ., P. J. Woods, H. Björnsson, J. Lentin, and G. Thordarson.
2018. Pushing the limits of a data challenged stock: a size- and age-structured assessment of ling (*Molva molva*) in Icelandic waters using Gadget. Fish. Res. 207:95–109.

Engstedt, O., P. Koch-Schmidt, and P. Larsson.
2012. Strontium (Sr) uptake from water and food in otoliths of juvenile pike (*Esox lucius* L.). J. Exp. Mar. Biol. Ecol. 418–419:69–74.

Frey, B. A.
2022. Validation of age and growth using microconstituent analysis of fish hardparts. [sic] M.S. thesis, 89 p. Univ. Md., College Park, MD. [Available from website.]

Grammer, G. L., J. R. Morrongiello, C. Izzo, P. J. Hawthorne, J. F. Middleton, and B. M. Gillanders.
2017. Coupling biogeochemical tracers with fish growth reveals physiological and environmental controls on otolith chemistry. Ecol. Monogr. 87:487–507.

Heimbrand, Y., K. E. Limburg, K. Hüssy, M. Casini, R. Sjöberg, A.-M. Palmén Bratt, S.-E. Levinsky, A. Karpushevskaia, K. Radtke, and J. Öhlund.
2020. Seeking the true time: exploring otolith chemistry as an age-determination tool. J. Fish Biol. 97:552–565.

Hunt, J. J.
1980. Guidelines for age determination of silver hake, *Merluccius bilinearis*, using otoliths. J. Northwest Atl. Fish. Sci. 1:65–80.

Hüssy, K., M. Krüger-Johnsen, T. B. Thomsen, B. D. Heredia, T. Næraa, K. E. Limburg, Y. Heimbrand, K. McQueen, S. Haase, U. Krumme et al.
2021. It's elemental, my dear Watson: validating seasonal patterns in otolith chemical chronologies. Can. J. Fish. Aquat. Sci. 78:551–566.

Hüssy, K., K. E. Limburg, H. de Pontual, O. R. B. Thomas, P. K. Cook, Y. Heimbrand, M. Blass, and A. M. Sturrock.
2021. Trace element patterns in otoliths: the role of biomineralization. Rev. Fish. Sci. Aquac. 29:445–477.

Jensen, A. C.
1970. Validation of ages determined from otoliths of Gulf of Maine cod. Trans. Am. Fish. Soc. 99:359–362.

Jensen, A. C., and J. P. Wise.
1962. Determining age of young haddock from their scales. Fish. Bull. 61:439–450.

Jochum, K. P., U. Nohl, K. Herwig, E. Lammel, B. Stoll, and A. W. Hoffman.
2005. GeoReM: a new geochemical database for reference materials and isotopic standards. Geostand. Geoanal. 29:333–338.

Jolivet, A., J.-F. Bardeau, R. Fablet, Y.-M. Paulet, and H. de Pontual.
2008. Understanding otolith biomineralization processes: new insights into microscale spatial distribution of organic and mineral fractions from Raman microspectrometry. Anal. Bioanal. Chem. 392:551–560.

Kohler, A. C.
1964. Variations in the growth of Atlantic cod (*Gadus morhua* L.). J. Fish. Board Can. 21:57–100.

Koob, E. R., S. P. Elzey, J. W. Mandelman, and M. P. Armstrong.
2021. Age validation of the northern stock of black sea bass (*Centropristis striata*) in the Atlantic Ocean. Fish. Bull. 119:261–273.

Kraus, R. T., and D. H. Secor.
2004. Incorporation of strontium into otoliths of an estuarine fish. J. Exp. Mar. Biol. Ecol. 302:85–106.

Limburg, K. E., and M. Casini.
2018. Effect of marine hypoxia on Baltic Sea cod *Gadus morhua*: evidence from otolith chemical proxies. Front. Mar. Sci. 5:00482.

Limburg, K. E., M. J. Wuenschel, K. Hüssy, Y. Heimbrand, and M. Samson.
2018. Making the otolith magnesium chemical calendar-clock tick: plausible mechanism and empirical evidence. Rev. Fish. Sci. Aquac. 26:479–493.

Lomb, N. R.
1976. Least-squares frequency analysis of unequally spaced data. Astrophys. Space Sci. 39:447–462.

Lux, F. E., and F. E. Nichy.
1969. Growth of yellowtail flounder, *Limanda ferruginea* (Storer), on three New England fishing grounds. Int. Comm. Northwest Atl. Fish., ICNAF Res. Bull. 6:5–25.

Machias, A., N. Tsimenides, L. Kokokiris, and P. Divanach.
1998. Ring formation on otoliths and scales of *Pagrus pagrus*: a comparative study. J. Fish Biol. 52:350–361.

Massmann, W. H.
1963. Annulus formation on the scales of weakfish, *Cynoscion regalis*, of Chesapeake Bay. Chesap. Sci. 4:54–56.

Mayo, R. K.
1981. Age validation of redfish, *Sebastes marinus* (L.), from the Gulf of Maine-Georges Bank region. J. Northwest Atl. Fish. Sci. 2:13–19.

Mills, K. H., and R. J. Beamish.
1980. Comparison of fin-ray and scale age determinations for lake whitefish (*Coregonus clupeaformis*) and their implications for estimates of growth and annual survival. Can. J. Fish. Aquat. Sci. 37:534–544.

Morin, R., S. G. LeBlanc, and S. E. Campana.
2013. Bomb radiocarbon validates age and long-term growth declines in American plaice in the southern Gulf of St. Lawrence. Trans. Am. Fish. Soc. 142:458–470.

Moser, J., and G. R. Shepherd.
2008. Seasonal distribution and movement of black sea bass (*Centropristis striata*) in the Northwest Atlantic as determined from a mark-recapture experiment. J. Northwest Atl. Fish. Sci. 40:17–28.

Musick, J. A., and L. P. Mercer.
1977. Seasonal distribution of black sea bass, *Centropristis striata*, in the Mid-Atlantic Bight with comments on the ecology and fisheries of the species. Trans. Am. Fish. Soc. 106:12–25.

NEFSC (Northeast Fisheries Science Center).
2020. Operational assessment of the black sea bass, scup, bluefish, and monkfish stocks, updated through 2018. Natl. Mar. Fish. Serv., Northeast Fish. Sci. Cent. Ref. Doc. 20–01, 160 p. [Available from website.]

Paton, C., J. Hellstrom, B. Paul, J. Woodhead, J., and J. Hergt.
2011. Iolite: freeware for the visualisation and processing of mass spectrometric data. J. Anal. At. Spectrom. 26:2508–2518.

Penttila, J., and L. M. Dery (eds.).
1988. Age determination methods for Northwest Atlantic species. NOAA Tech. Rep. NMFS 72, 132 p.

Powles, P. M.
1966. Validity of ageing young American plaice from otoliths. Int. Comm. Northwest Atl. Fish., ICNAF Res. Bull. 3:103–105.

Rajaković, L. V., D. D. Marković, V. N. Rajaković-Ognjanović, and D. Z. Antanasijević.
2012. Review: the approaches for estimation of limit of detection for ICP-MS trace analysis of arsenic. Talanta 102:79–87.

Reis-Santos, P., S. E. Tanner, T. S. Elsdon, H. N. Cabral, and B. M. Gillanders.
2013. Effects of temperature, salinity and water composition on otolith elemental incorporation of *Dicentrarchus labrax*. J. Exp. Mar. Biol. Ecol. 446:245–252.

Richards, R. A.
2016. 2016 monkfish operational assessment. Northeast Fish. Sci. Cent. Ref. Doc. 16–09, 109 p. [Available from website.]

Rothermel, E. R., M. T. Balazik, J. E. Best, M. W. Breece, D. A. Fox, B. I. Gahagan, D. E. Haulsee, A. L. Higgs, M. H. O'Brien, M. J. Oliver, et al.
2020. Comparative migration ecology of striped bass and Atlantic sturgeon in the US Southern mid-Atlantic bight [sic] flyway. PLoS ONE 15(6):e0234442.

Ruf, T.
1999. The Lomb–Scargle periodogram in biological rhythm research: analysis of incomplete and unequally spaced time-series. Biol. Rhythm Res. 30:178–201.

Scargle, J. D.
1982. Studies in astronomical time series analysis. II. Statistical aspects of spectral analysis of unevenly spaced data. Astrophys. J. 263:835–853.

Secor, D. H., and P. M. Piccoli.
1996. Age- and sex-dependent migrations of striped bass in the Hudson River as determined by chemical microanalysis of otoliths. Estuaries 19:778–793.

Seyama, H., J. S. Edmonds, M. J. Moran, Y. Shibata, M. Soma, and M. Morita.
1991. Periodicity in fish otolith Sr, Na, and K corresponds with visual banding. Experientia 47:1193–1196.

Siskey, M. R., V. Lyubchich, D. Liang, P. M. Piccoli, and D. H. Secor.
2016. Periodicity of strontium: calcium across annuli further validates otolith-ageing for Atlantic bluefin tuna (*Thunnus thynnus*). Fish. Res. 177:13–17.

Stanley, R. R. E., I. R. Bradbury, C. DiBacco, P. V. R. Snelgrove, S. R. Thorrold, and S. S. Killen.
2015. Environmentally mediated trends in otolith composition of juvenile Atlantic cod (*Gadus morhua*). ICES J. Mar. Sci. 72:2350–2363.

Thomas, R. M.
1983. Back-calculation and time of hyaline ring formation in the otoliths of the pilchard off South West Africa. South Afr. J. Mar. Sci. 1:3–18.

Vitale, F., L. A. Worsøe Clausen, and G. N. Chonchúir.
2019. Handbook of fish age estimation protocols and validation methods. ICES Coop. Res. Rep. 346, 180 p. [Available from website.]

Watson, J. E.
1964. Determining the age of young herring from their otoliths. Trans. Am. Fish. Soc. 93:11–20.

Wiernicki, C. J., M. H. O'Brien, F. Zhang, V. Lyubchich, M. Li, and D. H. Secor.
2020. The recurring impact of storm disturbance on black sea bass (*Centropristis striata*) movement behaviors in the Mid-Atlantic Bight. PLoS ONE 15(12):e0239919.

Wilhelm, M. R., M. D. Durholtz, and C. H. Kirchner.
2008. The effects of ageing biases on stock assessment and management advice: a case study on Namibian horse mackerel. Afr. J. Mar. Sci. 30:255–261.

Yule, D. L., J. D. Stockwell, J. A. Black, K. I. Cullis, G. A. Cholwek, and J. T. Myers.
2008. How systematic age underestimation can impede understanding of fish population dynamics: lessons learned from a Lake Superior cisco stock. Trans. Am. Fish. Soc. 137:481–495.

Zlokovitz, E. R., D. H. Secor, and P. M. Piccoli.
2003. Patterns of migration in Hudson River striped bass as determined by otolith microchemistry. Fish. Res. 63:245–259.

National Marine
Fisheries Service
NOAA

*Fishery Bulletin*
established in 1881

Spencer F. Baird
First U.S. Commissioner
of Fisheries and founder
of *Fishery Bulletin*

# Distribution, abundance, and habitat associations of young of the year of rockfish species (*Sebastes* spp.) in deep waters along the central coast of California

**Thomas E. Laidig (contact author)**
**Diana L. Watters**

Email for contact author: tom.laidig@noaa.gov

Fisheries Ecology Division
Southwest Fisheries Science Center
National Marine Fisheries Service, NOAA
110 McAllister Way
Santa Cruz, California 95060

**Abstract**—The distribution and abundance of demersal young of the year (YOY) of rockfish species (*Sebastes* spp.) were investigated over a 17-year period along the central coast of California at depths of 19–326 m. More than 87,000 YOY rockfish were counted during surveys of 1292 transects on the seafloor. The 3 most abundant species were the pygmy (*S. wilsoni*), halfbanded (*S. semicinctus*), and shortbelly (*S. jordani*) rockfish. Young of the year of many rockfishes were found at greater depths than have been previously reported. The highest densities of all species combined occurred in shallow and intermediate depths (≤100 m). Most YOY rockfish occupied rock or mixed substrata, except the greenstriped (*S. elongatus*) and stripetail (*S. saxicola*) rockfish, which were associated primarily with soft substrata. Statistically significant ($P$<0.01) hot spots of YOY rockfish densities were located throughout the region, but only Soquel Canyon, a known refuge for large adult rockfish (>50 cm in total length), was a significant ($P$<0.01) cold spot. Biological processes (e.g., ontogenetic movement and predation) and environmental characteristics (e.g., seafloor habitat and oceanographic conditions) are potential influences on the distribution of YOY of rockfishes. The results of our study provide insights into the distributions of YOY of rockfishes in deep, complex seafloor habitats and can help improve estimation of year-class strength through targeted surveys of preferred habitats.

Manuscript submitted 10 May 2023.
Manuscript accepted 5 December 2023.
Fish. Bull. 121:199–213 (2023).
Online publication date: 15 December 2023.
doi: 10.7755/FB.121.4.5

The views and opinions expressed or implied in this article are those of the author (or authors) and do not necessarily reflect the position of the National Marine Fisheries Service, NOAA.

Over 70 rockfish species (*Sebastes* spp.) occur in the northeast Pacific Ocean from Alaska to Baja California, Mexico, and many of them are important to commercial and recreational fisheries. Rockfish species have long lifespans (from decades to more than 100 years for certain species), are slow growing, and mature late (Love et al., 2002), making them slow to recover from high levels of fishing mortality. In studies of the distribution and abundance of young of the year (YOY) of rockfishes, large interannual fluctuations in abundance have been found (Woodbury and Ralston, 1991; Sakuma et al., 2006; Ralston et al., 2013). Such variation in abundance is a contributor to variable year-class strength, which is largely determined within the first year of life (Ralston and Howard, 1995; Hobson et al., 2001; Laidig et al., 2007). Annual indices of YOY abundance are used in stock assessments for several rockfish species (He et al., 2011; Dick et al., 2017; Field et al., 2017; He and Field, 2018).

Young-of-the-year rockfish begin as pelagic larvae, transform to pelagic juveniles, and settle to a variety of benthic habitats generally after 3–6 months, typically at shallower depths than those occupied by conspecific adults (Boehlert, 1977; Love et al., 2002). In nearshore areas (depths <30 m), species-specific habitat associations of settled YOY rockfish have been identified with kelp beds, estuaries, and man-made structures, such as piers and jetties (Anderson, 1983; Hallacher and Roberts, 1985; Carr, 1991; Gallagher and Heppell, 2010). In offshore areas, large numbers of YOY rockfish have been found in high-relief rocky habitats at depths of 30–100 m off central California and Oregon (Stein et al., 1992; Yoklavich et al., 2002), and newly settled YOY of 3 rockfish species were commonly found in a study on soft sediments at depths of 40–100 m in Monterey Bay, located south of the San Francisco Bay Area in California (Johnson et al., 2001).

Relatively few surveys of settled YOY rockfish have been conducted in high-relief, rocky habitats at depths >30 m compared to the number of surveys conducted in shallow nearshore areas (depths ≤30 m). The latter are often conducted by scuba divers or with small trawl nets deployed from small boats or from shore, and the former require large, specialized survey vehicles (such as human-occupied and remotely operated vehicles) and support vessels, as well as skilled equipment operators

(Yoklavich et al., 2015). The researchers that have conducted the few surveys that have been carried out in rocky habitats at depths >30 m have reported on YOY rockfish in general rather than on individual species, because of difficulties in identifying young fish to species. As a result, our understanding of the abundance and habitat use of YOY rockfish is lacking for those species that inhabit depths deeper than 30 m.

In our study, a manned submersible was used to conduct visual surveys of YOY of deep-living, demersal rockfishes along a 140-km section of the central coast of California from the seaward edge of kelp beds (depths ~30 m) to depths >300 m. Survey data were used 1) to characterize species composition, 2) to determine associations of YOY rockfish with seafloor substrata by species and for all species combined, and 3) to examine spatial patterns of density, as a measure of abundance, relative to depth. The resultant data on YOY rockfish distributions will help to unravel the complex life history strategies of many commercially important rockfish species and to discover vital rockfish nursery areas in deep waters that are not often surveyed.

## Material and methods

Visual surveys of demersal fish were conducted along the central coast of California from Big Creek (36°00′N, 121°35′W) to Ascension Canyon (37°02′N, 122°25′W) (Fig. 1) by using the 4.6-m-long *Delta* manned submersible (Delta Oceanographics[1], Torrance, CA). A total of 11 research expeditions were completed over the 17-year period from 1992 through 2009 (Table 1) during late summer and fall (typically the time of the calmest waters along this coastline) at depths from 19 to 326 m (the maximum depth to which the submersible can travel safely is 365 m). All surveys were conducted during daylight hours from 0700 to 1700.

The submersible had space for 1 pilot and 1 scientific observer and was equipped with an external color video camera (fabricated by Delta Oceanographics) mounted on the starboard side above the observer viewports. Before 2002, tapes in the Hi8 format were used in the external camera, and in 2002, the tape format changed to MiniDV to improve video resolution. Also, in 2002, a handheld MiniDV video camera (DCR-VX1000, Sony Group Corp., Tokyo, Japan) was placed in the lowest viewport inside the submersible and angled down to document the fish that could be seen close to the submersible, along the inside edge of a transect. Two parallel lasers were mounted on either side of the external color camera about 20 cm apart (except during the research expedition in 1992, when the lasers were spaced 39.5 cm apart). These lasers were used to estimate fish length and as a tool to help in determining the width of transects. A conductivity, temperature, and depth instrument (SBE 19plus SeaCAT, Sea-Bird Scientific, Bellevue, WA) was attached to the submersible to accurately measure depth. From 2007 through 2009, a ring laser gyro and Doppler velocity log were affixed to the submersible to measure the distance travelled.

Strip-transect surveys were conducted to quantify the fish within a 2-m-wide swath along the seafloor and from the seafloor to a height 2 m above it. During transect surveys, the submersible transited approximately 1 m above the bottom at rates of 0.4–0.9 kt (depending on bottom topography). The surveys were conducted for either 10 or 15 min (depending on the year), with 2–6 transects surveyed during each submersible dive. The start position and direction of travel on transects were directed to the submersible pilot by a scientist aboard the support vessel who tracked the submersible's position using an ultra-short baseline acoustic system (ORE Trackpoint II, EdgeTech, West Wareham, MA) and WinFrog software (vers. 3.1; Fugro Pelagos Inc., San Diego, CA). During transect surveys, the submersible followed the depth contour with minor course corrections (e.g., for obstacle avoidance) left to the submersible pilot's discretion.

The scientific observer (all of whom were biologists experienced in fish identification) in the submersible identified (to the lowest possible taxon), enumerated, and estimated the length (to the nearest 5 cm in total length [TL] using the lasers spaced 20 cm apart) of all fish observed within the 2-m-wide transects and ≤2 m above the seafloor, verbally recording this information on an audio channel of each video tape (for more details, see Yoklavich et al., 2002, 2007). Few YOY rockfish were observed >2 m above the seafloor, and most were within 0.5 m of the seafloor. The 2-m width of transects was determined by using a combination of the distance of the laser spots from the submersible and measurements with a handheld sonar.

Young-of-the-year rockfish were identified to species by their body shape, length-specific pigment patterns, and physical characteristics (e.g., the bocaccio, *S. paucispinis*, has a large mouth; Butler et al., 2012). However, many of these patterns and characteristics were not easily observed from the submersible or in video footage because of the small size of some fish and their orientation, and these fish remained classified as unidentified YOY rockfish. All rockfish that were ≤5 cm TL were considered YOY, as were fish ≤10 cm TL that were identified as bocaccio, olive rockfish (*S. serranoides*), and shortbelly rockfish (*S. jordani*). These 3 species are relatively fast growing during their first year and can attain lengths >10 cm TL by the end of summer and fall of their first year (Anderson, 1983; Love et al., 2002).

All video footage was reviewed back in the laboratory. Data from the observer's verbal recordings were entered into a database, and fish identifications and counts were confirmed. Sections of seafloor observed in video footage for at least 5 s in duration along transects were characterized as a combination of primary and secondary substratum types. Primary substratum types covered at

[1] Mention of trade names or commercial companies is for identification purposes only and does not imply endorsement by the National Marine Fisheries Service, NOAA.

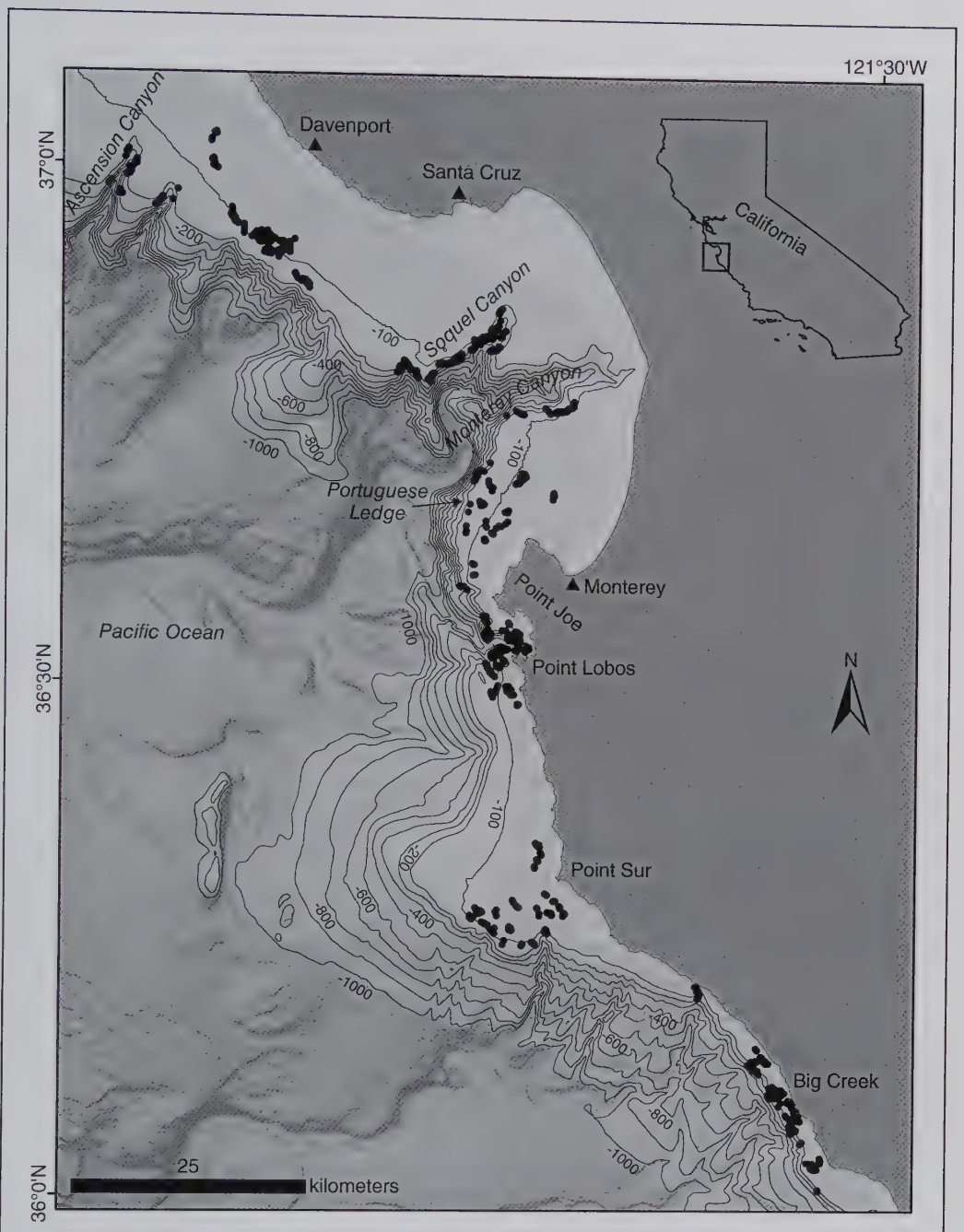


**Figure 1**

Map of the study area along the central coast of California showing locations where dives (black dots) of the *Delta* manned submersible were made to conduct surveys of transects during 1992–2009. Depth contours are shown at intervals of 100 m.

least 50% of the seafloor, and secondary types represented at least 20% of the remaining seafloor. We used these substratum types, following Greene et al. (1999): rock outcrop (bedrock outcrops), rock pinnacle (vertical bedrock pinnacles), continuous flat rock (flat-topped bedrock), boulder (individual rocks >25 cm in diameter), cobble (stones 6–25 cm in diameter), pebble (stones <6 cm in diameter), sand, and mud. Combinations of primary and secondary substrata were further classified as hard, mixed, or soft. Any combination of cobble, pebble, boulder, flat rock, rock outcrop, or rock pinnacle was considered hard, and a combination of mud and sand was deemed soft. For the mixed category, hard and soft substratum types each composed either the primary (≥50%) or the secondary (≥20%) portion of the observed substratum.

**Table 1**

Year, month or period, location, number of transects surveyed, total duration in minutes of all transect surveys, area surveyed, depth range surveyed, and total number of young-of-the year (YOY) rockfish (*Sebastes* spp.) observed for each of the 11 research expeditions conducted with the *Delta* manned submersible off the central coast of California from 1992 through 2009.

| Year | Period | Location | Transects | | Area ($m^2$) | Depth range (m) | No. of YOY observed |
|---|---|---|---|---|---|---|---|
| | | | Number | Minutes | | | |
| 1992 | Aug | Soquel Canyon | 42 | 420 | 14,142 | 95–305 | 3 |
| 1993 | Oct | Monterey Bay | 90 | 900 | 48,772 | 62–296 | 4557 |
| 1994 | Sep | Ascension and Carmel Canyons | 78 | 1170 | 49,872 | 79–316 | 8833 |
| 1997 | Sep–Oct | Big Creek | 64 | 640 | 25,768 | 19–222 | 20,119 |
| 1998 | Sep | Big Creek | 81 | 810 | 29,567 | 22–250 | 9827 |
| 2002 | Oct | Soquel Canyon | 10 | 115 | 5066 | 110–292 | 550 |
| 2003 | Sep | Soquel Canyon | 30 | 300 | 12,794 | 113–296 | 139 |
| 2004 | Aug–Sep | Davenport and Monterey Bay | 172 | 1880 | 104,630 | 66–260 | 2606 |
| 2007 | Sep–Nov | Big Creek to Soquel Canyon | 317 | 3170 | 162,694 | 23–325 | 21,617 |
| 2008 | Sep–Nov | Big Creek to Soquel Canyon | 391 | 3910 | 176,856 | 19–326 | 19,221 |
| 2009 | Sep–Oct | Soquel Canyon | 17 | 170 | 7972 | 99–288 | 215 |
| Total | | | 1292 | 13,485 | 638,133 | | 87,687 |

Transect length was estimated by using 1 of 3 methods: 1) counting intervals of paired laser spots end-to-end in the video footage as it advanced (in 1992–1994, 1997, and 1998), 2) plotting transect lines in ArcGIS (vers. 10.3; Esri, Redlands, CA) with edited and smoothed latitudes and longitudes from the ultra-short baseline acoustic system (in 2002–2009), or 3) using distances travelled measured with a ring laser gyro and Doppler velocity log (in 2007–2009). Transect area was estimated by multiplying the transect length by the 2-m transect width. Densities of YOY rockfish on each transect were calculated by dividing the total number of YOY rockfish by the total transect area.

For analyses, data from all years were combined. We analyzed all YOY rockfish grouped together and YOY of the most common species that had overall densities ≥0.01 fish/100 $m^2$ (with a minimum of 64 individuals counted on all transects) and that occurred on at least 15 transects (Table 2). We excluded fish identified to species in the subgenus *Sebastomus* from analyses because multiple species (e.g., the rosy rockfish, *S. rosaceus*, and the greenspotted rockfish, *S. chlorostictus*) in this group had varied distributions that would confound these analyses. A Kruskal–Wallis (KW) test, a nonparametric method of one-way analysis of variance, was conducted for each species and for all rockfishes combined to determine if there was a statistically significant difference in overall YOY density with depth (average depths of transects were grouped in 10-m depth bins). A canonical correlation analysis was used to examine the relationships between densities of the most common species and environmental factors (i.e., average depth of transects [grouped in 10-m bins] and substratum type). We examined which substrata were used by YOY rockfish by using a chi-square test to test the null hypothesis that YOY of all species combined were distributed proportionately to the relative availability of the substratum types.

We examined the spatial distribution of YOY rockfish densities on transects, using ArcMap in ArcGIS. We conducted hot-spot analyses (with the Spatial Analyst extension in ArcGIS), employing the Getis–Ord Gi* statistic (Getis and Ord, 1992) to identify statistically significant spatial clusters of transects with high (hot spots) or low (cold spots) densities of YOY rockfish. Hot-spot analyses of YOY densities were conducted for each rockfish species, for all rockfishes and depths combined, and for all rockfishes combined within 50-m depth strata.

To calculate the Getis–Ord Gi* statistic for each feature (i.e., transect) relative to its neighbors, inputs that define the spatial relationships among features and the size of the neighborhood are required. For each analysis, we chose the input of 3000 m as a fixed distance band that provided a reasonable spatial scale relative to the seafloor topography and the input of 8 or more neighbors for most transects (or a minimum of 6 neighbors for some transects). The input of a false discovery rate correction was also applied to adjust critical thresholds of *P*-values from analysis with the Gi* statistic to account for multiple testing and spatial dependency issues (Caldas de Castro and Singer, 2006). As a local statistic, the Gi* tests each feature in a data set (i.e., allows multiple testing), and the identification of some statistically significant hot or cold spots may actually be driven by random spatial processes (i.e., some results may falsely reject the spatial randomness null hypothesis). Spatial dependency is caused by the tendency of features near each other to be similar and can artificially inflate statistical significance. We considered *Z*-scores with *P*-values, adjusted with a false discovery rate procedure, at the 99% confidence level to be statistically significant; at this level, we rejected the

**Table 2**

Total number, overall density (the total number of fish observed per total area surveyed), and minimum, maximum, and mean depths of observed young of the year for all rockfish species (*Sebastes* spp.) identified during or in video footage from transect surveys conducted with the *Delta* manned submersible off the central coast of California from 1992 through 2009. An asterisk (*) after a common name indicates that the species is one of the most abundant species that were used in analyses. A dagger (†) after a common name indicates that the species belongs to the subgenus *Sebastomus*. Some of the fish identified as blue rockfish (*S. mystinus*) may have been deacon rockfish (*S. diaconus*) because these species have not been differentiated at small sizes. Mean depths are rounded to the nearest 10 because 10-m depth bins were used in analyses. SD=standard deviation. N/A=not applicable because only 1 individual was observed.

| Common name | Scientific name | Number | Density (fish/100 $m^2$) | Depth | | | |
|---|---|---|---|---|---|---|---|
| | | | | Min | Max | Mean | SD |
| Aurora rockfish | *Sebastes aurora* | 1 | <0.01 | 241 | 241 | 240 | N/A |
| Pinkrose rockfish† | *Sebastes simulator* | 1 | <0.01 | 209 | 209 | 210 | N/A |
| Swordspine rockfish† | *Sebastes ensifer* | 1 | <0.01 | 90 | 90 | 90 | N/A |
| Yelloweye rockfish | *Sebastes ruberrimus* | 1 | <0.01 | 72 | 72 | 70 | N/A |
| Chameleon rockfish | *Sebastes phillipsi* | 2 | <0.01 | 244 | 275 | 260 | 22.5 |
| Gopher rockfish | *Sebastes carnatus* | 2 | <0.01 | 36 | 38 | 30 | 4.7 |
| Black rockfish | *Sebastes melanops* | 3 | <0.01 | 39 | 45 | 40 | 2.9 |
| Copper rockfish | *Sebastes caurinus* | 3 | <0.01 | 44 | 51 | 50 | 5.0 |
| Vermilion rockfish | *Sebastes miniatus* | 4 | <0.01 | 29 | 48 | 40 | 11.2 |
| Bank rockfish | *Sebastes rufus* | 6 | <0.01 | 140 | 249 | 210 | 52.2 |
| Canary rockfish | *Sebastes pinniger* | 9 | <0.01 | 44 | 52 | 40 | 3.4 |
| Rosethorn rockfish† | *Sebastes helvomaculatus* | 12 | <0.01 | 152 | 200 | 170 | 14.6 |
| Bocaccio | *Sebastes paucispinis* | 13 | <0.01 | 28 | 78 | 50 | 11.6 |
| Olive rockfish | *Sebastes serranoides* | 17 | <0.01 | 30 | 83 | 40 | 15.7 |
| Darkblotched rockfish | *Sebastes crameri* | 26 | <0.01 | 89 | 262 | 220 | 46.1 |
| Splitnose rockfish | *Sebastes diploproa* | 35 | 0.01 | 159 | 302 | 200 | 32.8 |
| Greenspotted rockfish*† | *Sebastes chlorostictus* | 86 | 0.01 | 81 | 151 | 120 | 18.6 |
| Stripetail rockfish* | *Sebastes saxicola* | 112 | 0.02 | 41 | 257 | 130 | 41.5 |
| Yellowtail rockfish* | *Sebastes flavidus* | 147 | 0.02 | 28 | 50 | 50 | 3.7 |
| Starry rockfish*† | *Sebastes constellatus* | 150 | 0.02 | 44 | 131 | 80 | 17.7 |
| Rosy rockfish*† | *Sebastes rosaceus* | 174 | 0.03 | 33 | 126 | 60 | 16.0 |
| Greenstriped rockfish* | *Sebastes elongatus* | 236 | 0.04 | 82 | 203 | 120 | 19.5 |
| Squarespot rockfish* | *Sebastes hopkinsi* | 402 | 0.06 | 44 | 113 | 70 | 16.2 |
| Widow rockfish* | *Sebastes entomelas* | 533 | 0.08 | 30 | 81 | 40 | 6.9 |
| Blue rockfish* | *Sebastes mystinus/diaconus* | 541 | 0.08 | 24 | 81 | 40 | 11.1 |
| Unidentified *Sebastomus* | *Sebastes* spp. | 1359 | 0.21 | 32 | 227 | 90 | 32.1 |
| Shortbelly rockfish* | *Sebastes jordani* | 3656 | 0.57 | 38 | 181 | 70 | 27.7 |
| Halfbanded rockfish* | *Sebastes semicinctus* | 4143 | 0.65 | 39 | 149 | 60 | 10.1 |
| Pygmy rockfish* | *Sebastes wilsoni* | 11,292 | 1.77 | 43 | 177 | 70 | 14.7 |
| Unidentified YOY | *Sebastes* spp. | 64,720 | 10.15 | 22 | 314 | 70 | 21.8 |
| Total | | 87,687 | 13.76 | | | | |

null hypothesis that the density of YOY rockfish is completely spatially random.

## Results

Surveys of 1292 transects were conducted, resulting in >220 h of observations (Table 1). The depths of transects ranged from 19 to 326 m (from roughly the outer edge of the kelp bed to near the maximum depth to which the submersible can travel safely). The total area surveyed was 638,133 $m^2$, and the mean transect area (with all transects included regardless of YOY presence) was 494 $m^2$ (standard deviation [SD] 151.6). The mean transect area for 10-min transects (sample size [$n$]=1203) was 480 $m^2$ (SD 137.9) and for 15-min transects ($n$=89) was 647 $m^2$ (SD 137.1).

A total of 87,687 YOY rockfish from at least 28 different species were counted, with an overall density of 13.8 fish/100 $m^2$ (Table 2). Young-of-the-year rockfish were observed on nearly two-thirds of all transects (822 of 1292 transects). Approximately one-quarter (26%) of YOY were identified to a taxon lower than the genus *Sebastes* ($n$=22,967), with 94% of them identified to species. The most abundant identified species were as follows: the pygmy rockfish (*S. wilsoni*), with 11,292 individuals observed at a density of 1.8 fish/100 $m^2$; the halfbanded rockfish (*S. semicinctus*), with 4143 individuals counted at a density of 0.7 fish/100 $m^2$; and the shortbelly rockfish, with 3656

individuals observed at a density of 0.6 fish/100 $m^2$. Individuals were also identified to the subgenus *Sebastomus*, a group of 11 similar-looking rockfishes characterized by 5 large white spots along the dorsal half of their body (Love et al., 2002; Butler et al., 2012). Species in this subgenus are difficult to identify as adults and even more so as YOY; however, in our study, rockfish were identified to 6 species in this group, and 3 of these species are among the most commonly identified (Table 2).

Young-of-the-year rockfish were found at depths from 22 to 314 m. Overall, the highest densities of all taxa combined within 10-m depth bins (i.e., the total number of fish divided by the total area sampled, for each 10-m depth bin) were found on transects at depths between 40 and 90 m (Figs. 2 and 3), and the densities in this depth range were significantly higher than they would have been if the depth distribution had been uniform as expected (KW test: $P<0.0001$). Most species had depth distributions of YOY that were significantly different from a uniform depth distribution (KW test: $P<0.0001$), except the stripetail rockfish (*S. saxicola*), which had a broad distribution ranging from 41 to 257 m. For the blue (*S. mystinus*), widow (*S. entomelas*), and yellowtail (*S. flavidus*) rockfish, YOY were found at the relatively shallow depths of 40 or 50 m. Young-of-the-year rosy, halfbanded, squarespot (*S. hopkinsi*), shortbelly, starry (*S. constellatus*), and pygmy rockfish were observed at mean depths ranging between 60 and 100 m, and greenspotted and greenstriped (*S. elongatus*) rockfish were found at mean depths >100 m (Table 2). The species for which YOY occurred at the greatest depths, such as the splitnose rockfish (*S. diploproa*) and the chameleon rockfish (*S. phillipsi*), were too scarce to include in our analyses. Sampling effort (measured as the area surveyed) for each 10-m depth bin varied from >30,000 $m^2$ at a depth of 90 m to <1000 $m^2$ at the depths of 10–20 m (the submersible could not sample kelp beds safely; therefore, few transects within this depth stratum were surveyed) and depths >330 m (Fig. 2).

Results from the canonical correlation analysis indicate that YOY are separated by depth in 3 groups of rockfish species (Fig. 4). The group with the negative second canonical coefficient includes the greenstriped rockfish, greenspotted rockfish, and stripetail rockfish. These species occurred at the deepest average depths (120–130 m) and had generally high densities (0.3–0.4 fish/100 $m^2$) on soft substrata. The group with high second canonical and low first canonical coefficients includes the fishes that occupied average mean depths between 60 and 100 m (i.e., pygmy, starry, rosy, squarespot, and halfbanded rockfish), and YOY of all rockfishes combined (mean depth for all

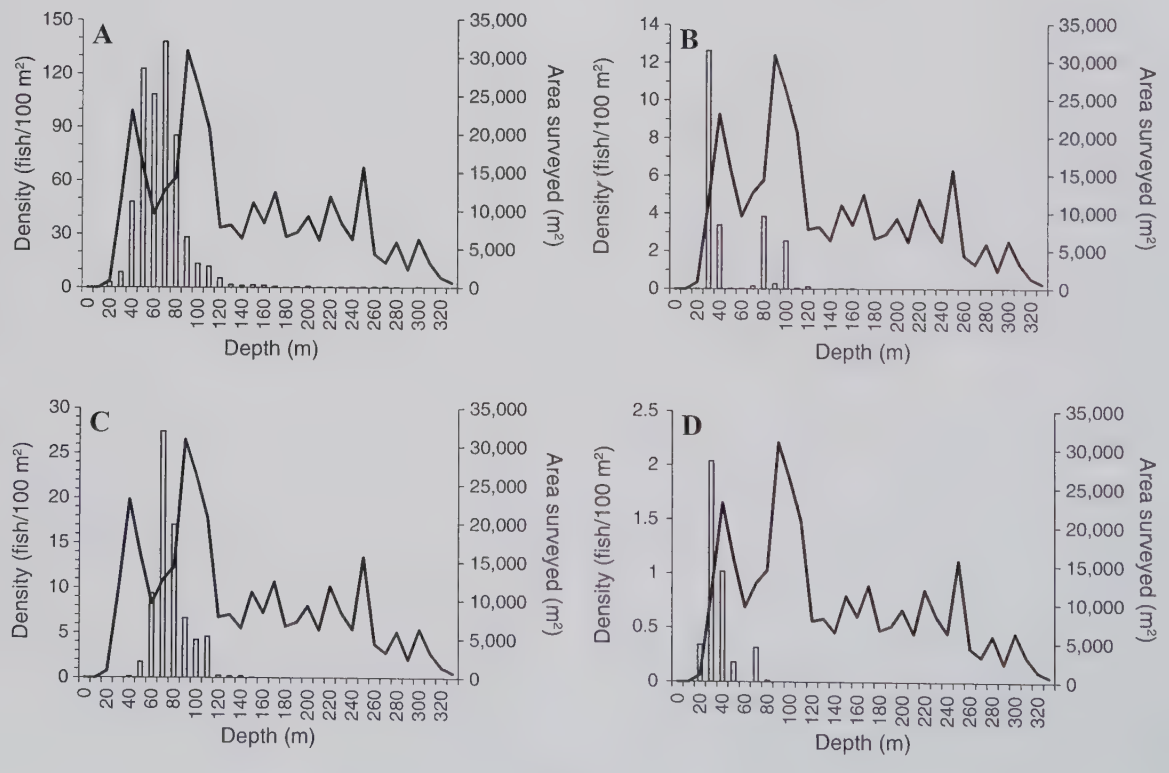


**Figure 2**

Densities of young-of-the-year (YOY) rockfish (*Sebastes* spp.) by depth (grouped in10-m bins), for (**A**) all YOY rockfish combined, (**B**) shortbelly rockfish (*S. jordani*), (**C**) pygmy rockfish (*S. wilsoni*), and (**D**) blue rockfish (*S. mystinus*), from surveys conducted with the *Delta* manned submersible off central California from 1992 through 2009. The black line in each graph indicates the total area surveyed for each depth.

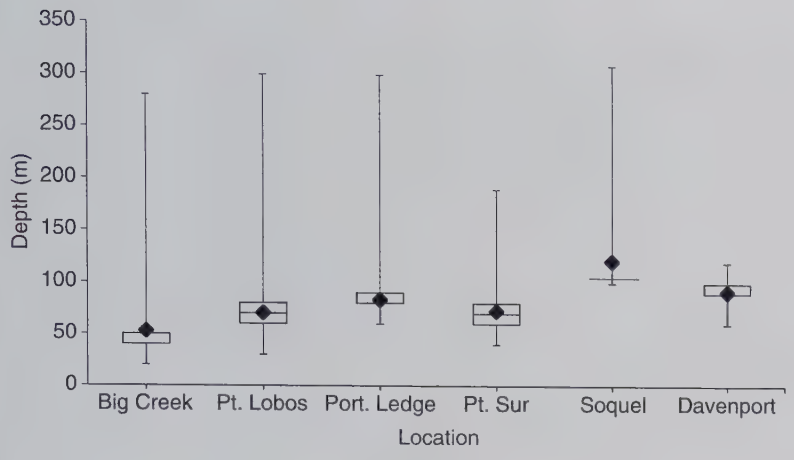


**Figure 3**

Box plots of the mean depth at which all young-of-the-year (YOY) rockfish (*Sebastes* spp.) were observed at the 6 locations along the coast of central California that were surveyed the most during 1992–2009. Each box shows the mean depth (diamond), the distribution between the first and third quartile (top and bottom lines), and the median depth (horizontal line). The whiskers indicate the maximum and minimum depths at which YOY rockfish were observed. Port. Ledge=Portuguese Ledge, a marine protected area located at the southern end of Monterey Bay.

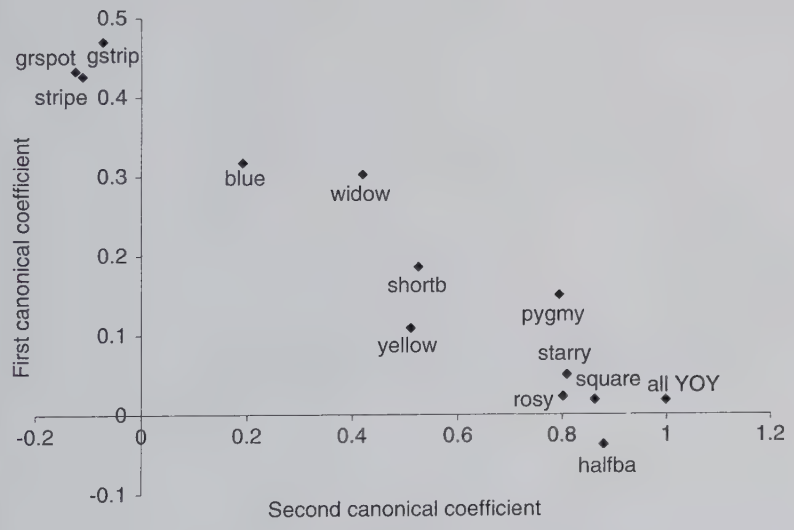


**Figure 4**

Comparison of first and second canonical correlation coefficients for densities of young of the year (YOY) of the 12 most abundant rockfish species (*Sebastes* spp.) and of all rockfishes combined from surveys conducted with the *Delta* manned submersible along the central coast of California during 1992–2009. The species with abbreviated common names are the greenstriped rockfish (*Sebastes elongatus*) (gstrip), greenspotted rockfish (*S. chlorostictus*) (grspot), stripetail rockfish (*S. saxicola*) (stripe), shortbelly rockfish (*S. jordani*) (shortb), yellowtail rockfish (*S. flavidus*) (yellow), squarespot (*S. hopkinsi*) (square), and halfbanded rockfish (*S. semicinctus*) (halfba).

YOY was 67 m) had similar results in this analysis. The remaining species grouped in the middle of Figure 4 (i.e., blue, widow, yellowtail, and shortbelly rockfish) occurred at mostly shallow depths in high densities on hard substrata. Although shortbelly rockfish were found at a mean depth equal to that of the mid-depth group, over 2000 individuals of this species were found at shallow depths of 50 m or less (Fig. 2B).

The breakdown of seafloor substrata types for all transects combined (over the entire survey area of 638,133 $m^2$), is as follows: 43% hard, 27% mixed, and 30% soft (Fig. 5). Most YOY rockfish occupied hard and mixed substrata (Fig. 5). The frequency of occurrence of YOY for each of 7 species was disproportionally greater on hard substrata relative to its availability (chi-square test: $P<0.0001$), with frequencies varying from 58% (greenspotted rockfish) to 96% (squarespot rockfish). For 4 of these species, the squarespot, widow, yellowtail, and blue rockfish, YOY were never observed on soft substrata. Each of 3 species, the halfbanded, pygmy, and rosy rockfish, occurred disproportionally more on mixed substrata relative to its availability (chi-square test: $P<0.0001$), with 75% of halfbanded rockfish occurring on this substrata. Each of 2 species, the greenstriped and stripetail rockfish, occurred disproportionally more on soft substrata relative to its availability (chi-square test: $P<0.0001$).

Although YOY of rockfish species were present throughout the study area at densities ranging from 0.1/100 $m^2$ to 3236/100 $m^2$, density hot spots for all but greenstriped rockfish were located within the southern region from Point Joe to Big Creek. For all taxa combined, there was a statistically significant ($P<0.01$) hot spot at Big Creek (Table 3, Fig. 6), where hot spots of YOY densities were found for individual species, including the stripetail, blue, shortbelly, and halfbanded rockfish, and for unidentified rockfish. Point Sur was a statistically significant hot spot for 7 taxa: greenspotted, yellowtail, starry, rosy, widow, and pygmy rockfish and unidentified rockfish (hot spots for pygmy rockfish are shown in Figure 6, as an example). Three species, the starry, squarespot, and pygmy rockfish, had a hot spot at Point Lobos. Point Joe,

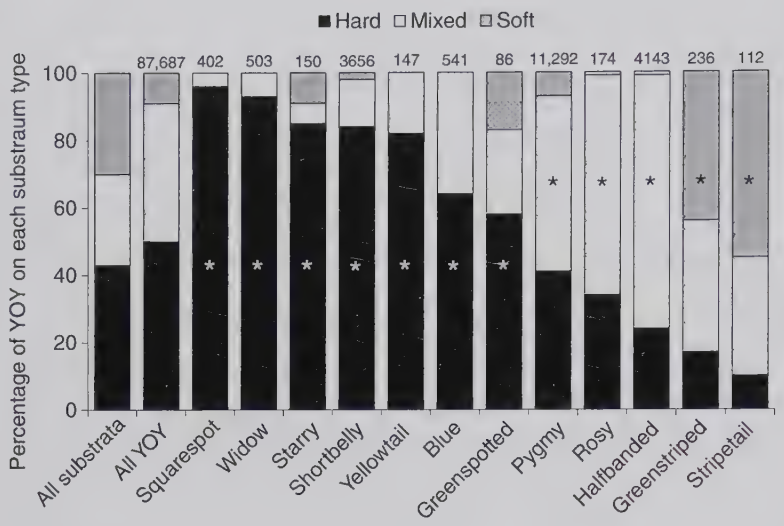


**Figure 5**

Frequency of occurrence on substratum types occupied for young of the year (YOY) of each rockfish species (*Sebastes* spp.) and for YOY of all rockfishes combined during surveys conducted with the *Delta* manned submersible off the central coast of California from 1992 through 2009. Percentages of surveyed area classified as each substratum type, combined over the entire study period, are given in the first bar. The number at the top of each bar is the number of individuals observed for that species. The total area surveyed during this study was 638,133 $m^2$. An asterisk (*) indicates that YOY were observed significantly more on this substratum type relative to what was expected.

Davenport, and Monterey Canyon were statistically significant hot spots for YOY pygmy, greenstriped, and stripetail rockfish, respectively. The greenstriped rockfish was the only species that had a cold spot, which was a statistically significant ($P<0.01$) cluster of transects with low densities located in Soquel Canyon inside Monterey Bay.

In the spatial examination of the density at depth for YOY of all rockfishes combined, no statistically significant hot spots were found at depths ≤50 m, depths of 150–200 m, or depths of 250–300 m. Statistically significant ($P<0.01$; Table 4) hot spots were located at Big Creek at depths of 50–100 m, Point Sur at depths of 100–150 m, and Point Lobos at depths of 200–250 m. A statistically significant cold spot was located at Soquel Canyon at depths of 200–250 m.

## Discussion

In most previous studies, YOY of all rockfish species have been categorized into a single group. In this study, we were able to identify individuals of 28 species, because of recent progress in

**Table 3**

Results from hot-spot analysis with the Gi* statistic for young of the year (YOY) of rockfish species (*Sebastes* spp.) along the central coast of California from 1992 through 2009. This analysis was used to identify locations of statistically significant ($P<0.01$) clusters of survey transects with high (hot spots) and low (cold spot) densities of YOY rockfish, by species.

| | Location | |
|---|---|---|
| Species | Cold spot | Hot spots |
| All rockfishes | None | Big Creek |
| Blue rockfish | None | Big Creek |
| Greenspotted rockfish | None | Point Sur |
| Greenstriped rockfish | Soquel Canyon | Davenport |
| Halfbanded rockfish | None | Big Creek |
| Pygmy rockfish | None | Point Sur, Point Lobos, Point Joe |
| Rosy rockfish | None | Point Sur |
| Shortbelly rockfish | None | Big Creek |
| Squarespot rockfish | None | Point Lobos |
| Starry rockfish | None | Point Sur, Point Lobos |
| Stripetail rockfish | None | Big Creek, Monterey Canyon |
| Widow rockfish | None | Point Sur |
| Yellowtail rockfish | None | Point Sur |
| Unidentified rockfish | None | Point Sur, Big Creek |

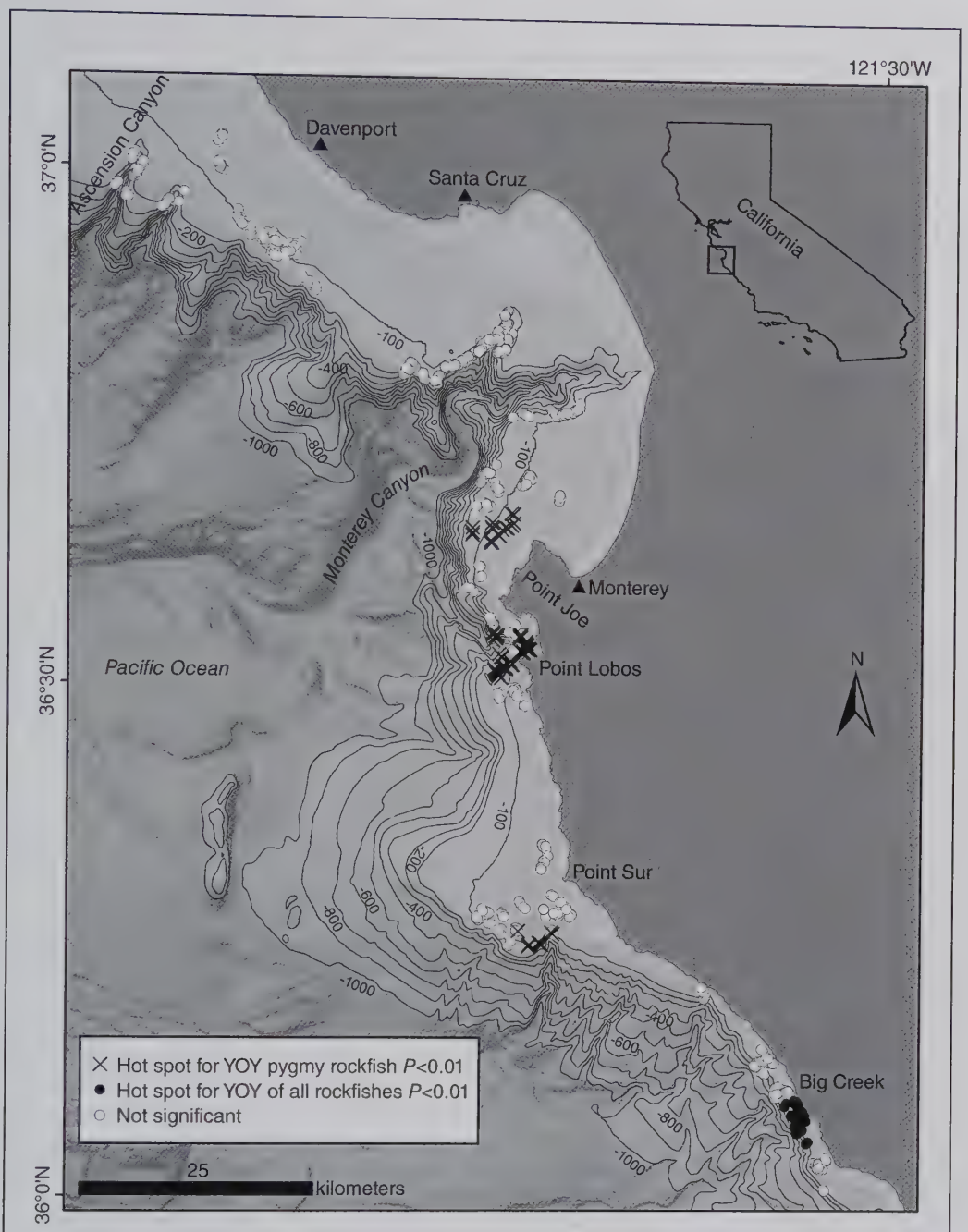


**Figure 6**

Map showing the results from hot-spot analysis with the Gi* statistic for young-of-the-year (YOY) pygmy rockfish (*Sebastes wilsoni*) and for YOY of all rockfish species combined from surveys conducted with the *Delta* manned submersible off the central coast of California from 1992 through 2009. This analysis was used to identify hot spots, or statistically significant ($P<0.01$) clusters of survey transects, with high YOY densities.

the identification of rockfishes for individuals at the YOY stage along the West Coast of the United States (Butler et al., 2012). In 2002, YOY were identifiable for less than 30 species (Love et al., 2002); currently, about 40 of the over 70 rockfish species have detailed, descriptive developmental series of the larval and juvenile stages, allowing for more accurate identifications (Anderson, 1983; Love et al., 2002; Butler et al., 2012).

Most of the rockfishes that occur along the central coast of California have had their juvenile pigment patterns identified and documented, and many of these species (i.e., pygmy, halfbanded, shortbelly, and squarespot

**Table 4**

Results from hot-spot analysis with the Gi* statistic for young of the year (YOY) rockfish (*Sebastes* spp.) along the central coast of California from 1992 through 2009. This analysis was used to identify locations of statistically significant ($P<0.01$) clusters of survey transects with high (hot spots) and low (cold spot) densities of YOY rockfish, by 50-m depth bin. The number of transects in the >300-m depth bin was insufficient for analysis.

| | Location | |
|---|---|---|
| Depth (m) | Cold spot | Hot spots |
| ≤50 | None | None |
| >50 and ≤100 | None | Big Creek |
| >100 and ≤150 | None | Point Sur |
| >150 and ≤200 | None | None |
| >200 and ≤250 | Soquel Canyon | Point Lobos |
| >250 and ≤300 | None | None |

rockfish) are among the most numerous that we observed. Many of them, such as the halfbanded rockfish with its large, dark, diamond-shaped pigment spot on the side of its body and the blue rockfish with its blue coloration, are quite distinctive. Young-of-the-year blue rockfish have not been positively differentiated from the more northerly distributed deacon rockfish (*S. diaconus*) (Butler et al., 2012). Therefore, some of the YOY rockfish identified as blue rockfish in our study may be deacon rockfish. Bizzarro et al. (2020) found that, as adults, blue rockfish were more frequently observed from Monterey Bay south with from two-thirds to three-quarters of the catch identified as blue rockfish. Further studies are needed to determine the identification and distribution of YOY blue and deacon rockfish. It is more difficult to differentiate between species in a few groups, including species in the subgenus *Sebastomus*, the yellowtail and olive rockfish, and a group consisting of the widow, pygmy, squarespot, and shortbelly rockfish. The species in the latter group are all tan-colored and, even though their pigment patterns are distinctive as large individuals, they have only subtle differences at small sizes (e.g., shortbelly rockfish are more elongated than the other species in this group).

Advances in high-definition camera systems that take high-resolution images allow researchers to see the definitive characters needed for identification of YOY in video and still images. Despite these advances, species identification for YOY rockfish during visual surveys remains difficult, and we were able to identify to species only one-quarter of the total number of individuals observed on transects in our study. Most of the unidentified rockfish were small individuals (≤5 cm TL), partially obstructed from view, or not observed with enough resolution in video images to get a positive identification. However, on the basis of the number of individuals of each species that we identified, their tan color, and lack of obvious pigment patterns, we believe that most of the unknown YOY rockfish were probably pygmy, squarespot, or shortbelly rockfish. The number of YOY rockfish that can be identified to species can only be expected to increase in the future, along with increases in camera quality and resolution. With these improvements in identification and image quality and with the advent of emerging technologies (i.e., environmental DNA and light-field cameras), it may be possible in the future to identify most YOY rockfish to species during visual surveys.

Rocky substrata have been shown to be important habitats for YOY rockfishes living in shallow water (depths <30 m) (Anderson, 1983; Carr, 1991; Laidig et al., 2007). In our study, we observed the highest densities of YOY rockfish on hard or mixed substrata at depths between 40 and 90 m and the lowest densities at depths >160 m or over soft bottom habitat. Love et al. (2006) found the highest densities of YOY bocaccio on oil platforms (hard man-made substrate) and on shell mounds near platform bases in Southern California at depths between 25 and 80 m. High abundances of YOY rockfish have also been seen in rocky substrata at depths <100 m in southeast Alaska and in Oregon, with low numbers of YOY rockfish observed in soft sediments (Carlson and Straty, 1981; Stein et al., 1992). Although densities were not available from these studies, these results indicate that rocky substrata at these depths may be important to YOY of rockfishes along the West Coast.

For many rockfish species, YOY had statistically significant associations with rocky areas, but soft sediments served as a habitat for YOY greenstriped and stripetail rockfish. Not surprisingly, the highest densities of these 2 species were located in areas with high amounts of muddy seafloor (at Monterey Canyon and Davenport), at the deep average depths of 120 m for greenstriped rockfish and 130 m for stripetail rockfish. Soft sediments are also the common habitats of conspecific adults, but adults have been found at deeper depths than YOY (Love et al., 2002). Young-of-the-year stripetail rockfish have been observed in large numbers on soft sediments off Big Creek in central California at depths of about 70 m and in Southern California at depths of 18–150 m (Mearns et al., 1980; Yoklavich et al., 2002), and, for YOY, both the greenstriped rockfish and the stripetail rockfish have been found to be the most abundant rockfishes surveyed on the soft sediments of Monterey Bay from the depth of 60 m to the 100-m limit of their sampling (Johnson et al., 2001).

Most settled YOY of rockfishes live at shallower depths than their adult counterparts. Ontogenetic shifts in depth are most obvious in the deepwater species that recruit initially to kelp beds (e.g., the shortbelly and yellowtail rockfish; Anderson, 1983; Love et al., 1991, 2002, 2009; Butler et al., 2012). The YOY of a handful of kelp-bed-settling species remain in shallow depths (e.g., kelp rockfish, *S. atrovirens*, and black-and-yellow rockfish, *S. chrysomelas*), and YOY of most species either remain for only a short time (days to a month; e.g., halfbanded and shortbelly rockfish) or for many months until the first big storms of winter hit in October or November (e.g., copper rockfish, *S. caurinus*;

stripetail rockfish; and yellowtail rockfish; Anderson, 1983). Most YOY blue and olive rockfish move to deeper water in fall, but some individuals remain in kelp beds throughout the winter.

Although these ontogenetic habitat movements have been recorded in nearshore areas, the movements of only a few species that recruit to deeper waters have been observed. Johnson et al. (2001) used a size-frequency analysis to document the ontogenetic movement to deeper waters for cowcod (*S. levis*), greenstriped rockfish, and stripetail rockfish in Monterey Bay. Love et al. (1991) found that bocaccio move successively deeper as they mature, with a shallow-water-dwelling juvenile taking around 5 years to move to deeper adult habitats. In our study, YOY rockfish were observed living in habitats similar to, but shallower than, habitats utilized by conspecific adults, according to data on depth distributions from Love et al. (2002).

The average depth at which YOY of most rockfishes were found was over 50 m shallower than the average depth at which adults have been found. For example, YOY widow and yellowtail rockfish in our study were found at average depths of 40 and 50 m, respectively, and in contrast the average depth of adults has been reported as well over 100 m (Love et al., 2002). However, some species make an ontogenetic depth change of well over 100 m; for example, stripetail rockfish can settle in depths as shallow as 15 m but as adults live at 200 m (Love et al., 2002).

Some rockfish species recruit to nearshore kelp beds, but many of these same species also recruit to deeper depths. Young-of-the-year blue, widow, and yellowtail rockfish have been recorded in large numbers in nearshore kelp beds (Anderson, 1983; Carr, 1991; Laidig et al., 2007). These beds reach maximum depths of 20–30 m depending on water clarity (Schiel and Foster, 2015). The highest densities of blue rockfish in our study occurred at depths around 30–40 m, and widow and yellowtail rockfish were most abundant at depths of 40–50 m. These species utilize both shallow nearshore areas (depths <30 m) and deeper rocky habitats. Carr (1991) counted YOY blue rockfish in kelp beds and estimated densities of 180–400 fish/100 $m^2$ over a 2-year period. Laidig et al. (2007) surveyed YOY of rockfishes in the kelp beds off Northern California and found large interannual fluctuations in abundance for YOY blue and yellowtail rockfish with densities varying from 0.07 to 655 fish/100 $m^2$. In this study, the density of blue rockfish at the depth of 30 m was 2 fish/100$m^2$, and the density of yellowtail rockfish at the same depth was 0.1 fish/100 $m^2$. The submersible could not survey within the kelp bed; therefore, a substantial proportion of each of the populations of blue and yellowtail rockfish may have been missed.

The differences in densities may also be explained through the interannual variation in recruitment strength realized in all rockfishes (Carr, 1991; Ralston et al., 2013). Some species that recruit to the kelp bed, including the bocaccio and the black (*S. melanops*), gopher (*S. carnatus*), olive, and vermilion (*S. miniatus*) rockfish, were rarely seen at deeper depths in this study. The YOY of these species may be more restricted to shallow depths than YOY of other rockfish species. Other species have more protracted distributions that stretch from the kelp bed to depths >100 m. Stripetail, halfbanded, and shortbelly rockfish all occasionally recruit to kelp beds (Anderson, 1983), but distributions of their YOY occur at much deeper depths. Love et al. (2009) surveyed rockfishes in Southern California and found YOY halfbanded rockfish in areas ranging from the kelp bed (<30 m) to depths over 200 m. Therefore, recruitment numbers for many species in kelp bed environments provide only a relative measure of their abundance, and the numbers of these species living in deeper waters should be considered.

The abundance of YOY pygmy, halfbanded, and shortbelly rockfish in our study reflects the dominance of adults of these dwarf species in the fish assemblages of deepwater rocky habitats off California (Yoklavich et al., 2002; Baskett et al., 2006). Love et al. (2009) found that the 4 most abundant species in Southern California at depths between 19 and 365 m were the squarespot, halfbanded, shortbelly, and pygmy rockfish. In a study of marine protected areas (MPAs) along the central coast of California, Starr and Yoklavich (2008) observed that at most depths between 100 and 200 m, the dominant species group was dwarf rockfishes. In another study at the Big Creek Ecological Reserve also along the central coast of California, Yoklavich et al. (2002) observed that the halfbanded and shortbelly rockfish were the 2 dominant fish species as adults within the reserve.

Although dwarf species dominate many reefs, some protected areas harbor many old fish of larger species. An example of a relatively pristine refuge is Soquel Canyon. There, considerable numbers of large (>50 cm TL), old individuals of piscivorous rockfishes have been reported, but, not surprisingly, few adults of dwarf rockfishes have been observed there (Yoklavich et al., 2000). As expected, with so many large predators there, few YOY rockfish were observed in Soquel Canyon during this study. Much of the deep rocky habitat off the U.S. West Coast has been heavily fished, and fishing has disproportionately removed rockfish of large, slow-growing, piscivorous species that prey on small, fast-growing dwarf rockfish species (O'Farrell et al., 2009). With the decline in abundance of larger species, populations of dwarf species have increased in abundance. The recovery of large rockfish species may be slowed by competition with these highly abundant dwarf rockfish species (an outcome referred to as the *cultivation effect*; Walters and Kitchell, 2001).

Initial settlement of pelagic juvenile rockfish to benthic areas is dependent on many factors, including upwelling, fronts, depth, available habitat, and temperature (Anderson, 1983; Love et al., 2002; Laidig, 2010). Upwelling has been suggested as a settlement mechanism for winter-spawned rockfish off California, with pelagic juveniles actively descending through the water column into the deeper shoreward currents that transport them to the appropriate shallow habitats (Lenarz et al. 1991; Larson et al., 1994; Johnson et al., 2001). Markel and Shurin (2020) observed high recruitment of black rockfish off Canada during a year with strong upwelling. Conversely, they

ascertained that periods of downwelling were correlated to higher settlement of other species: the copper, quillback (*S. maliger*), and brown (*S. auriculatus*) rockfish. Woodson et al. (2012) found that ocean fronts in the California Current Large Marine Ecosystem were positively correlated with recent settlement of winter-spawned fish of *Sebastes* species. Larson et al. (1994) found an unusually shallow distribution of late-stage pelagic juvenile rockfish above the thermocline in Monterey Bay and suggested that this behavior may contribute to shoreward transport of these large juveniles. They also described a multistage settlement process, with moving to shore as the first stage and finding suitable settlement habitat as the second stage.

The distribution of settled YOY rockfish is determined by the availability of food and shelter, mortality, the number of rockfish that initially settled there, or the redistribution of YOY rockfish on different substrata (Love et al., 1991). Once settled, predator avoidance (West et al., 1994; Hobson et al., 2001; Love et al., 2002) and food availability (Hallacher and Roberts, 1985; Love et al., 1991) are likely factors affecting distribution. Stein et al. (1992) observed clouds of YOY rockfish near the top of a rocky bank (at depths of 60–80 m) and larger adults in deeper areas (at depths of 100–150 m), indicating that predation is a potential cause for this distribution. The tops of rocky banks have more ambient light than deeper areas, aiding in predator detection and avoidance. In a laboratory study, predator avoidance by YOY black rockfish was higher when the predator was visible to the YOY rockfish than when they had only chemical cues (Giger, 2015).

In a study of artificial reefs, West et al. (1994) determined that abundance of demersal YOY rockfish was greatest on the most complex reefs, with aggregations near crevices. Small rockfish near the top of reefs may also be feeding on planktonic organisms in open waters above the reef more than from the reef itself (Carlson and Haight, 1976; Singer, 1985). Love et al. (1991) found evidence that food resources were less abundant in deeper, offshore areas than in shallow reefs. Besides food resources, temperature may be a factor in determining YOY rockfish distributions. Boehlert and Yoklavich (1983) studied YOY black rockfish in the laboratory and determined that growth rates increased at warmer temperatures. The YOY rockfish that settle in shallow zones may have an advantage by growing faster than deeper-living conspecifics.

The spatial distribution of settled YOY rockfish varied by species within our study area. Big Creek was the hot spot for YOY of all rockfishes combined, with the identification of this hot spot driven by high densities of half-banded and shortbelly rockfish and of unidentified YOY rockfish there during 1997 and 1998. These taxa along with the blue and stripetail rockfish also each had statistically significant hot spots at this location. For several species (i.e., the greenspotted, pygmy, rosy, starry, widow, yellowtail rockfish) and unidentified rockfish, hot spots of high densities were found at Point Sur, a major upwelling center (Traganza et al., 1981).

Four other locations were also hot spots for 1 or 2 species: Davenport, Point Joe, Point Lobos, and Monterey Canyon. None of these locations was a hot spot for all rockfish species combined (Table 3), and the oceanographic currents differ between locations. Therefore, it is unlikely that ocean current transport alone is the basis for these distributions because many of these species aggregate together as pelagic juveniles before settling to the seafloor (Lenarz et al., 1991; Larson et al., 1994; Field et al., 2021). If they had all settled together and not migrated after settlement, we would expect hot spots to be populated by the species that aggregated together in the planktonic environment, and that is not the case. In a study of pelagic juveniles of rockfishes off central California during 2001–2019, only the shortbelly rockfish was in the top ten of the most abundant rockfish species over the 19-year study (Field et al., 2021). If ocean currents brought fish to these locations, we would expect the most abundant species of settled YOY rockfish to be proportional to the abundances of pelagic juvenile rockfish in the same areas, and they are not. It is more likely that the fish migrated after settlement to specific regions of high food availability or of low predation at appropriate species-specific depths and seafloor habitats (Love et al., 1991; Hobson et al., 2001; Auster et al., 2003). Those individual YOY rockfish that remain in the less desirable areas may perish or experience reduced growth rates.

Some of the areas of highest abundance of YOY rockfish were located within or near an MPA. The fish living in these areas receive increased protection from fishing and other human activities, leading to increased numbers of rockfish that can translate into greater larval production and greater numbers of YOY rockfish settling there. Most of the MPAs in our study area were established in 2007 (information on the MPAs in California are available on the website of the California Department of Fish and Wildlife); therefore, they were too new to have a significant effect on larval production. However, 2 MPAs were established prior to 2007, the Point Lobos and Big Creek Ecological Reserves in 1973 and 1994, respectively (McArdle, 1997). There may have been some additional contribution of larval rockfish from within these 2 reserves, but these reserves are small and their contribution may have been minimal. Also, high numbers of YOY were observed at Big Creek in 1997, only 3 years after the reserve was established, likely not enough time for rockfish abundance to increase enough to result in a substantial increase in the number of larvae produced. In the future, the added larval production from these MPAs should increase the numbers of YOY rockfish recruiting along the coast of central California.

A better understanding of the habitats and areas of importance to YOY rockfish can improve estimates of year-class strength and management measures to protect them. Marine protected areas, gear restrictions, and other protective measures can be employed to reduce human effects in these areas, which may prove to be nursery areas where juveniles may be able to thrive and survive to maturity, increasing their contribution to the population. Year-class

strength is a valuable component of assessing the status of fish populations and forecasting future growth. Indices of year-class strength for YOY rockfishes have traditionally been estimated by using catch-per-unit-of-effort data from midwater trawl and scuba surveys (Laidig et al., 2007; Ralston et al., 2013). Visual surveys conducted routinely in deep, complex rock habitats can enhance these traditional indices and provide indices of year-class strength for YOY rockfish species not represented in traditional surveys. Habitat-specific estimates of YOY abundance improve our ability to manage rockfish populations on an ecosystem basis.

## Conclusions

Young-of-the-year rockfish were distributed throughout the central coast of California at depths of 22–314 m. In the visual surveys of YOY in this study, 28 species of rockfish were identified, and for many this study was the first time they were identified in situ, leading to new depth distributions and habitat associations for them. The highest YOY densities for rockfishes were found in hard or mixed habitats at depths of 40–90 m. For YOY, rockfishes fell into 3 groups, the group found on soft substrata in deep water, the mid-depth group, and the shallow-water group. The shallow-water group consisted of many species that also recruit to kelp beds. For 2 of the species that recruit to shallow kelp beds, the blue and yellowtail rockfish, densities were generally higher in these beds than at deeper depths. However, the maximum depths at which these 2 species were observed in this study were 81 and 50 m, respectively, depths that are much deeper than the edge of the kelp beds (depths of ~30 m). Therefore, estimating species densities from surveys of kelp beds alone may result in underestimation of population density for YOY of species that recruit to kelp beds.

The hot spots of YOY rockfish densities coincided with 3 MPAs at Big Creek, Point Sur, and Point Lobos. These MPAs offer protection for these young fish, potentially allowing more individuals to reach maturity. Understanding of the species-specific distributions and habitat preferences of rockfish in these early life stages will improve fisheries management by enhancing 1) the reliability of density estimates with sampling of correct depths and habitats, 2) the protection of potential nursery areas and placement of future MPAs, and 3) estimates of year-class strength for stock assessment models.

## Resumen

Se investigó la distribución y abundancia de juveniles demersales del año de especies de peces de roca (*Sebastes* spp.) durante un periodo de 17 años a lo largo de la costa central de California a profundidades de 19–326 m. Se contaron más de 87,000 juveniles de peces de roca durante los estudios de 1292 transectos en el fondo marino. Las 3 especies más abundantes fueron el rocote pigmeo (*S. wilsoni*), el rocote inspector (*S. semicinctus*) y rocote pancita (*S. jordani*). Los juveniles del año de muchas especies de peces de roca se hallaron a profundidades mayores que las registradas anteriormente. Las mayores densidades de todas las especies combinadas se dieron en profundidades someras e intermedias. La mayoría de los juveniles ocuparon sustratos rocosos o mixtos, excepto el rocote reina (*S. elongatus*) y el rocote cola listada (*S. saxicola*), que se asociaron principalmente con sustratos blandos. En toda la región se localizaron puntos calientes de densidades de juveniles de peces de roca estadísticamente significativos ($P<0.01$), pero sólo el cañón Soquel, un conocido refugio de grandes peces de roca adultos (>50 cm de longitud total), fue un punto frío significativo ($P<0.01$). Los procesos biológicos (ej., el movimiento ontogénico y la depredación) y las características ambientales (ej., el hábitat del fondo marino y las condiciones oceanográficas) pueden influir en la distribución de juveniles del año de peces de roca. Los resultados de nuestro estudio proporcionan información sobre la distribución de juveniles del año de peces de roca en hábitats profundos y complejos del fondo marino, y pueden ayudar a mejorar la estimación de la fuerza de la cohorte anual mediante estudios específicos de los hábitats preferidos.

## Acknowledgments

We thank M. Yoklavich who was instrumental in developing, planning, and securing funding for the research expeditions and in collecting the data used in our analyses. We thank all of the scientific observers, Delta Oceanographics personnel, and the crews of all the support vessels (RVs *Cavalier*, *Jolly Roger*, and *McGaw* and FV *Velero IV*). We thank M. Carr, J. Field, and K. Sakuma for their thoughtful reviews. This study was partially supported by grants from the West Coast and Polar Regions Undersea Research Center of the NOAA National Undersea Research Program and the California Ocean Protection Council.

## Literature cited

Anderson, T. W.
1983. Identification and development of nearshore juvenile rockfishes (genus *Sebastes*) in central California kelp forests. M. A. thesis, 176 p. Cal. State Univ., Fresno, CA. [Available from website.]

Auster, P. J., J. Lindholm, and P. C. Valentine.
2003. Variation in habitat use by juvenile Acadian redfish, *Sebastes fasciatus*. Environ. Biol. Fishes 68:381–389.

Baskett, M. L., M. Yoklavich, and M. S. Love.
2006. Predation, competition, and the recovery of overexploited fish stocks in marine reserves. Can. J. Fish. Aquat. Sci. 63:1214–1229.

Bizzarro, J. J., E. A. Gilbert-Horvath, E. J. Dick, A. M. Berger, K. T. Schmidt, D. Pearson, C. Petersen, L. A. Kautzi, R. R. Miller, J. C. Field, et al.
2020. Genetic identification of blue rockfish (*Sebastes mystinus*) and deacon rockfish (*S. diaconus*) to enable life history analyses for stock assessment. Fish. Bull. 118:37–50.

Boehlert, G. W.
1977. Timing of the surface-to-benthic migration in juvenile rockfish, *Sebastes diploproa*, off southern California. Fish. Bull. 75:887–890.
Boehlert G. W., and M. Yoklavich.
1983. Effects of temperature, ration, and fish size on growth of juvenile black rockfish, *Sebastes melanops*. Environ. Biol. Fishes 8:17–28.
Butler, J. L., M. S. Love, and T. E. Laidig.
2012. A guide to the rockfishes, thornyheads, and scorpionfishes of the northeast Pacific, 185 p. Univ. Calif. Press, Berkeley, CA.
Caldas de Castro, M., and B. H. Singer.
2006. Controlling the false discovery rate: a new application to account for multiple and dependent tests in local statistics of spatial association. Geogr. Anal. 38:180–208.
Carlson, H. R., and R. E. Haight.
1976. Juvenile life of Pacific ocean perch, *Sebastes alutus,* in coastal fiords of southeastern Alaska: their environment, growth, food habits, and schooling behavior. Trans. Am. Fish. Soc. 105:191–201.
Carlson, H. R., and R. R. Straty.
1981. Habitat and nursery grounds of Pacific rockfish, *Sebastes* spp., in rocky coastal areas of southeastern Alaska. Mar. Fish. Rev. 43(7):13–19.
Carr, M. H.
1991. Habitat selection and recruitment of an assemblage of temperate zone reef fishes. J. Exp. Mar. Biol. Ecol. 146:113–137.
Dick, E. J., A. Berger, J. Bizzarro, K. Bosley, J. Cope, J. Field, L. Gilbert-Horvath, N. Grunloh, M. Ivens-Duran, R. Miller, et al.
2017. The combined status of Blue and Deacon Rockfishes in U.S. waters off California and Oregon in 2017, 309 p. Pac. Fish. Manage. Counc., Portland, OR.
Field, J. C., S. G. Beyer, and X. He.
2017. Status of the Chilipepper Rockfish, *Sebastes goodei*, in the California Current for 2015, 185 p. Pac. Fish. Manage. Counc., Portland, OR. [Available from website.]
Field, J. C., R. R. Miller, J. A. Santora, N. Tolimieri, M. A. Haltuch, R. D. Brodeur, T. D. Auth, E. J. Dick, M. H. Monk, K. M. Sakuma, et al.
2021. Spatiotemporal patterns of variability in the abundance and distribution of winter-spawned pelagic juvenile rockfish in the California Current. PLoS ONE 16(5):e0251638.
Gallagher, M. B., and S. S. Heppell.
2010. Essential habitat identification for age-0 rockfish along the central Oregon coast. Mar. Coast. Fish. 2:60–72.
Getis, A., and J. K. Ord.
1992. The analysis of spatial association by use of distance statistics. Geogr. Anal. 24:189–206.
Giger, S.
2015. Anti-predator behavior of juvenile black rockfish, *Sebastes melanops*. Explor. Undergrad. Res. J. 17:1–13.
Greene, H. G., M. M. Yoklavich, R. M. Starr, V. M. O'Connell, W. W. Wakefield, D. E. Sullivan, J. E. McRea Jr., and G. M. Cailliet.
1999. A classification scheme for deep seafloor habitats. Oceanol. Acta 22:663–678.
Hallacher, L. E., and D. A. Roberts.
1985. Differential utilization of space and food by the inshore rockfishes (Scorpaenidae: *Sebastes*) of Carmel Bay, California. Environ. Biol. Fishes 12:91–110.
He, X., and J. C. Field.
2018. Stock assessment update: status of bocaccio, *Sebastes paucispinis*, in the Conception, Monterey, and Eureka INPFC areas for 2017, 181 p. Pac. Fish. Manage. Counc., Portland, OR. [Available from website.]
He, X., D. E. Pearson, E. J. Dick, J. C. Field, S. Ralston, and A. D. MacCall.
2011. Status of the widow rockfish resource in 2011, 174 p. Report to the Pacific Fishery Management Council, Portland, OR. [Available from website.]
Hobson, E. S., J. R. Chess, and D. F. Howard.
2001. Interannual variation in predation on first-year *Sebastes* spp. by three northern California predators. Fish. Bull. 99:292–302.
Johnson, K. A., M. M. Yoklavich, and G. M. Cailliet.
2001. Recruitment of three species of juvenile rockfish (*Sebastes* spp.) on soft benthic habitat in Monterey Bay, California. CalCOFI Rep. 42:153–166.
Laidig, T. E.
2010. Influence of ocean conditions on the timing of early life history events for blue rockfish (*Sebastes mystinus*) off California. Fish. Bull. 108:442–449.
Laidig, T. E., J. R. Chess, and D. F. Howard.
2007. Relationship between abundance of juvenile rockfishes (*Sebastes* spp.) and environmental variables documented off northern California and potential mechanisms for the covariation. Fish. Bull. 105:39–48.
Larson, R. J., W. H. Lenarz, and S. Ralston.
1994. The distribution of pelagic juvenile rockfish of the genus *Sebastes* in the upwelling region off central California. CalCOFI Rep. 35:175–221.
Lenarz, W. H., R. J. Larson, and S. Ralston.
1991. Depth distributions of late larvae and pelagic juveniles of some fishes of the California Current. CalCOFI Rep. 32:41–46.
Love, M. S., M. H. Carr, and L. J. Haldorson.
1991. The ecology of substrate-associated juveniles of the genus *Sebastes*. Environ. Biol. Fishes 30:225–243.
Love, M. S., M. Yoklavich, and L. Thorsteinson.
2002. The rockfishes of the northeast Pacific, 405 p. Univ. Calif. Press, Berkeley, CA.
Love, M. S., D. M. Schroeder, W. Lenarz, A. MacCall, A. S. Bull, and L. Thorsteinson.
2006. Potential use of offshore marine structures in rebuilding an overfished rockfish species, bocaccio (*Sebastes paucispinis*). Fish. Bull. 104:383–390.
Love, M. S., M. Yoklavich, and D. M. Schroeder.
2009. Demersal fish assemblages in the Southern California Bight based on visual surveys in deep water. Environ. Biol. Fishes 84:55–68.
Markel, R. W., and J. B. Shurin.
2020. Contrasting effects of coastal upwelling on growth and recruitment of nearshore Pacific rockfishes (genus *Sebastes*). Can. J. Fish. Aquat. Sci. 77:950–962.
McArdle, D. A.
1997. California marine protected areas, 268 p. California Sea Grant College System, La Jolla, CA.
Mearns, A. J., M. J. Allen, M. D. Moore, and M. J. Sherwood.
1980. Distribution, abundance, and recruitment of soft-bottomed rockfishes (Scorpaenidae: *Sebastes*) on the southern California mainland shelf. CalCOFI Rep. 21:180–190.
O'Farrell, M. R., M. M. Yoklavich, and M. S. Love.
2009. Assessment of habitat and predator effects on dwarf rockfishes (*Sebastes* spp.) using multi model inference. Environ. Biol. Fishes 85:239–250.
Ralston, S., and D. F. Howard.
1995. On the development of year-class strength and cohort variability in two northern California rockfishes. Fish. Bull. 93:710–720.

Ralston, S., K. M. Sakuma, and J. C. Field.
2013. Interannual variation in pelagic juvenile rockfish (*Sebastes* spp.) abundance—going with the flow. Fish. Oceanogr. 22:288–308.

Sakuma, K. M., S. Ralston, V. G. Wespestad.
2006. Interannual and spatial variation in the distribution of young-of-the-year rockfish (*Sebastes* spp.): expanding and coordinating the survey sampling frame. CalCOFI Rep. 47:127–139.

Schiel, D. R., and M. S. Foster.
2015. The biology and ecology of giant kelp forests, 416 p. Univ. Calif. Press, Berkeley, CA.

Singer, M. M.
1985. Food habits of juvenile rockfishes (*Sebastes*) in a central California kelp forest. Fish. Bull. 83:531–541.

Starr, R., and M. Yoklavich.
2008. Monitoring MPAs in deep water off central California: 2007 IMPACT submersible baseline survey, 21 p. California Sea Grant, La Jolla, CA.

Stein, D. L., B. N. Tissot, M. A. Hixon, and W. Barss.
1992. Fish-habitat associations on a deep reef at the edge of the Oregon continental shelf. Fish. Bull. 90:540–551.

Traganza, E. D., J. C. Conrad, and L. C. Breaker.
1981. Satellite observations of a cyclonic upwelling system and giant plume in the California Current. *In* Coastal upwelling (F. A. Richards, ed.), p. 228–241. Am. Geophys. Union, Washington, DC.

Walters, C., and J. F. Kitchell.
2001. Cultivation/depensation effects on juvenile survival and recruitment: implications for the theory of fishing. Can. J. Fish. Aquat. Sci. 58:39–50.

West, J. E., R. M. Buckley, and D. C. Doty.
1994. Ecology and habitat use of juvenile rockfishes (*Sebastes* spp.) associated with artificial reefs in Puget Sound, Washington. Bull. Mar. Sci. 55:344–350.

Woodbury, D., and S. Ralston.
1991. Interannual variation in growth rates and back-calculated birthdate distributions of pelagic juvenile rockfishes (*Sebastes* spp.) off the central California coast. Fish. Bull. 89:523–533.

Woodson, C. B., M. A. McManus, J. A. Tyburczy, J. A. Barth, L. Washburn, J. E. Caselle, M. H. Carr, D. P. Malone, P. T. Raimondi, B. A. Menge, et al.
2012. Coastal fronts set recruitment and connectivity patterns across multiple taxa. Limnol. Oceanogr. 57:582–596.

Yoklavich, M. M., H. G. Greene, G. M. Cailliet, D. E. Sullivan, R. N. Lea, and M. S. Love.
2000. Habitat associations of deep-water rockfishes in a submarine canyon: an example of a natural refuge. Fish. Bull. 98:625–641.

Yoklavich, M., G. Cailliet, R. N. Lea, H. G. Greene, R. Starr, J. deMarignac, and J. Field.
2002. Deepwater habitat and fish resources associated with the Big Creek Marine Ecological Reserve. CalCOFI Rep. 43:120–140.

Yoklavich, M. M., M. S. Love, and K. A. Forney.
2007. A fishery-independent assessment of an overfished rockfish stock, cowcod (*Sebastes levis*), using direct observations from an occupied submersible. Can. J. of Fish. Aquat. Sci. 64:1795–1804.

Yoklavich, M., J. Reynolds, and D. Rosen.
2015. A comparative assessment of underwater visual survey tools: results of a workshop and user questionnaire. NOAA Tech. Memo. NMFS-TM-SWFSC-547, 44 p.

## Acknowledgment of reviewers

The editorial staff of *Fishery Bulletin* would like to acknowledge the scientists who reviewed manuscripts in 2022–2023. Their contributions have helped ensure the publication of quality science.

Robert Ahrens
Scott Alford

Elizabeth Babcock
Henry Bart Jr.
Katherine Bemis
Lee Benaka
Florian Berg
Corinthia Black
Jesper Boje
Randy Brown

Matthew Campbell
Nick Caputi
J. Leonardo Castillo-Géniz
Brandon Chasco
Michael Courtney
Wendell Cropper

Evan D'Alessandro
Simon de Lestang
Lukas DeFilippo
Côme Denechaud
William Driggers III
Claude Dykstra

Jessica Farley
Jayde Ferguson
Lowell Fritz
Rainer Froese
Richard Fulford

Audrey Geffen
Jason Goldstein
Gretchen Grammer
Shane Griffiths
Jongkar Grinang
Benjamin Gutzler

Eric Hoffmayer
Edward Houde

James Ianelli
David Itano

George Jackson
Mattias Johansson
Matthew Johnson
Simon Jones

David Kerstetter
Jeff Kneebone

Tom Laidig
Richard Langton
Kari Lavalli
Cleridy Lennert-Cody

J. Fernando Márquez-Farías
Mary Elizabeth Matta
Richard McBride
Loren McClenachan
Richard Merrick

Richard Methot
Michael Murphy

Lisa Natanson

Krista Oke

Michelle Passerotti
Andrew Pershing
Mark Peterson
John Piatt
Gregg Poulakis
André Punt

Joseph Quattro

Paul Rudershausen
Brendan Runde

Joseph Serafy
Carrie Simmons
Christoph Stransky

Eric Taylor
James Tolan

John Waldman
John Walter III
Phoebe Woodworth-Jefcoats

# Fishery Bulletin

## Guidelines for authors

Contributions published in *Fishery Bulletin* describe original research in marine fishery science, fishery engineering and economics, and marine environmental and ecological sciences (including modeling). Preference will be given to manuscripts that examine processes and underlying patterns. Descriptive reports, surveys, and observational papers may occasionally be published but should appeal to an audience outside the locale in which the study was conducted.

Although all contributions are subject to peer review, responsibility for the contents of papers rests upon the authors and not on the editor or publisher. *Submission of an article implies that the article is original and is not being considered for publication elsewhere.*

All submissions are subject to a double-blind review to remove the identity of author and reviewer during the review process.

Plagiarism and double publication are considered serious breaches of publication ethics. To verify the originality of the research in papers and to identify possible previous publication, manuscripts may be screened with plagiarism-detection software.

Manuscripts must be written in English; authors whose native language is not English are strongly advised to have their manuscripts checked by English-speaking colleagues before submission.

Artificial intelligence (AI), machine learning, or similar algorithmic tools should not be used to write or generate scientific content, including text, tables, and figures, for manuscripts submitted to *Fishery Bulletin*. Although some authors may use such tools to improve the readability or syntax of their manuscript, it must be done with extreme caution, and authors must review and edit the result. If such a tool is used, authors must declare the name of the tool, where it was used, and the purpose for which it was used in an "Artificial intelligence declaration" section after the "Acknowledgments" section. Authors remain accountable for all elements of their manuscript and should state that they take full responsibility for the content of their manuscript in the AI declaration.

Once a paper has been accepted for publication, online publication takes approximately 2 weeks.

There is no cost for publication in *Fishery Bulletin*.

### Types of manuscripts accepted by the journal

**Articles** generally range from 20 to 30 double-spaced typed pages (12-point font) and describe an original contribution to fisheries science, engineering, or economics. Tables and figures are not included in this page count, but the number of figures should not exceed 1 figure for every 4 pages of text. Articles contain the following divisions: abstract, introduction, methods, results, discussion, and conclusions.

**Notes** are generally less than 10 double-spaced typed pages (12-point font), including the Literature cited section. Like articles, notes describe an original contribution to fisheries science. They follow a format similar to that for articles: abstract, introduction, methods, results, and discussion, but the results and discussion sections may be combined and a conclusions section should not be included. They should include no more than 2 figures or tables (2 of each would be too many). They are distinguished from full articles in that they report a noteworthy new observation or discovery—such as the first report of a new species, a unique finding, condition, or event that expands our knowledge of fisheries science, engineering, or economics—and do not require a lengthy discussion. Manuscripts on range extensions will not be considered.

**Companion articles** should be submitted together and are published together as a scientific contribution. Both articles should address a closely related topic and may be articles that result from a workshop or conference.

**Review articles** of exceptional quality may be considered occasionally for publication on a case-by-case basis. They address a timely topic that is relevant to aspects of fisheries science. They should include an abstract, but the format of the article, per se, will be up to the author. Please contact the scientific editor to discuss your ideas regarding a potential review article before embarking on such a project.

**Perspective essays** generally are less than 5 double-spaced typed pages (12-point font) and provide clarification of misused terms or misunderstood topics in fisheries science. Essays are accepted at the discretion of the scientific editor. Opinion pieces on policy will not be considered. They should include an abstract and a list of the literature cited, but no other sections should divide the article. Please contact the scientific editor to discuss your idea before making a submission.

### Preparation of manuscript

**Title page** should include authors' full names, affiliations, mailing addresses, and the senior author's email address.

**Abstract** should be limited to 200 words (one-half typed page), state the main scope of the research, and emphasize the authors' conclusions and relevant findings. Do not review the methods of the study or list the contents of the paper. Because abstracts are circulated by abstracting agencies, it is important that they represent the research clearly and concisely.

**General text** must be typed in 12-point Times New Roman font throughout. A brief introduction should convey the

broad significance of the paper; the remainder of the paper should be divided into the following sections: Materials and methods, Results, Discussion, Conclusions, and Acknowledgments. Headings within each section must be short, reflect a logical sequence, and follow the rules of subdivision (i.e., there can be no subdivision without at least 2 subheadings). The entire text should be intelligible to interdisciplinary readers; therefore, all acronyms, abbreviations, and technical terms should be written out in full and defined the first time they are mentioned. Abbreviations should be used sparingly because they are not carried over to indexing databases and slow readability for those readers outside a discipline. They should never be used for the main subject (e.g., species or method) of a paper.

For general style, follow the U.S. Government Publishing Office *Style Manual* (2016, available at website) and *Scientific Style and Format: the CSE Manual for Authors, Editors, and Publishers* (2014, 8th ed.) published by the Council of Science Editors. For scientific nomenclature, use the current edition of the American Fisheries Society's (AFS) *Common and Scientific Names of Fishes from the United States, Canada, and Mexico* and its companion volumes (*Crustaceans, Mollusks, Cnidaria and Ctenophora*, and *World Fishes Important to North Americans*). For species not found in the previously mentioned AFS publications and for more recent changes in nomenclature, use the Integrated Taxonomic Information System (ITIS, available at website), or, secondarily, the California Academy of Sciences *Catalog of Fishes* (available at website) for species names not included in ITIS. Common (vernacular) names of species should be lowercase. Citations must be given for the identification of specimens. For example, "Fish species were identified according to Collette and Klein-MacPhee (2002); sponges were identified according to Stone et al. (2011)."

Dates should be written as follows: 11 November 2018. Measurements should be expressed in metric units, for example, "58 metric tons (t);" if other units of measurement are used, please make this fact explicit to the reader. Use numerals, not words, to express whole and decimal numbers in the general text, tables, and figure captions (except at the beginning of a sentence). For example, "We considered 3 hypotheses. We collected 7 samples in this location." Use American spelling. Refrain from using the shorthand slash (/), an ambiguous symbol, in the general text.

Cite all software, special equipment, and chemical solutions used in the study within parentheses in the general text, including the version number, company name, and the city and state (or nation) of the company headquarters, for example, "SAS, vers. 9.4 (SAS Institute Inc., Cary, NC)."

**Word usage and grammar** that may be useful are the following:

- *Aging*
  For our journal, the word *aging* is used to mean both age determination and the aging process (senescence). Authors should make clear which meaning is intended where ambiguity may arise.

- *Fish and fishes*
  The plural of the word fish (a collective noun that implies individuals without regard to species) is *fish*.
  *Example*: The *fish* were collected by trawl net.
  *Example*: The numbers of *fish* collected that season were less than the numbers from previous years.

  The plural for *fish species* is *fishes* (a contrived plural used by taxonomists to mean several or more *fish species*) or one can use *fish species* (which is preferred in this journal for clarity across disciplines).
  *Example*: The *fishes* of Puget Sound [biodiversity is implied] or
  *Example*: The *fish species* of Puget Sound [preferred plural for clarity across disciplines].

- *Crab and crabs, squid and squids, etc.*
  The plural of the word *crab* (i.e., many individuals without regard to species) is *crab*.
  *Example*: The crab were sorted by weight.
  *Example*: Many red king *crab* were dying [Many individuals of one species of crab.]

  The plural of *crab species* is *crabs* (a word used by taxonomists) or *crab species* (the latter is preferred in this journal for clarity).
  *Example*: These *crabs* were selected for treatment. [Different crab species are implied.]
  *Example*: These *crab species* were selected for treatment. [Preferred word choice for clarity.]
  *Example*: Snow *crabs* are found throughout the North Pacific Ocean and Bering Sea. [There are 2 species of snow crab; therefore the word *crabs* can be used here.]
  *Example*: *Two species* of snow *crab* are found throughout the North Pacific Ocean and Bering Sea. [Preferred usage for clarity.]
  *Example*: Three crabs were selected for treatment. [3 species of crab are implied.]
  *Example*: Three crab species were selected for treatment. [Preferred word choice for clarity.]

- We use *fisherman* and *fishermen*, not *fisher* and *fishers*, in this journal. One can always use crew member, vessel operator, and angler (the latter for recreational fishing).

- *The definite article with common names of species*
  When the singular common name of a species represents the entire class or group to which it belongs, use the definite article.
  *Example*: Only one species of the genus *Salmo* is found in the Atlantic Ocean—*the* Atlantic salmon (*Salmo salar*).
  *Example*: The sonic emissions of *the* bottlenose dolphin are complex.

  For plural common names, this rule does not apply.
  *Example*: Chinook salmon are found throughout the Pacific Ocean.
  *Example*: Bottlenose dolphins are found in temperate and tropical waters.

- *Sex*
  For the meaning of male and female, use the word *sex*, not *gender*. Do not write, "fish were sexed." Write, "sex was determined."

- *Participles*
  As adjectives, participles must modify a specific noun or pronoun.
  *Example*: Using mark-recapture methods, these scientists determined the size of the population. [Correct. The participle *using* modifies the word *scientists*.]
  *Example*: These scientists, based on the collected data, concluded that the mortality rate of these fish had increased. [Incorrect. The scientists were not based on the collected data.]
  *Example*: These scientists concluded, on the basis of collected data, that the mortality rate of these fish had increased. [Correct. The offending participle has been eliminated and an adverbial phrase modifies the verb *concluded*.]

**Equations and mathematical symbols** should be set from a standard mathematical program (MathType or Equation Editor). Equations formatted in LaTex are not acceptable. For mathematical symbols in the general text ($\alpha$, $\chi^2$, $\pi$, $\pm$, etc.), use the symbols provided by the MS Word program and italicize all variables, except those variables represented by Greek letters and the superscript and subscript parts of variables and expressions. Do not use photo mode when creating these symbols in the general text, and do not cut and paste equations, letters, or symbols from a different software program.

Number equations (if there are more than one) for future reference by scientists; place the number within parentheses at the end of the first line of the equation.

**Literature cited section** comprises published works and those accepted for publication (in press) in peer-reviewed journals. Follow the name and year system for citation format in this section (i.e., citations should be listed alphabetically by the authors' last names, and then by year if there is more than one citation by the same author. A list of abbreviations for citing journal titles can be found on our website.

Authors are responsible for the accuracy and completeness of all citations. Avoid the use of multiple citations when a single citation sufficiently supports a statement; cite the work that first reported the information that supports a statement, not all of the subsequent works. Literature citation format: Authors (last name, followed by initials for first name and, if given, middle name of first author; then list names of additional authors with initials before last names). Year. Title of article. Abbreviated title of the journal in which it was published. Always include either the range of page numbers (for a journal article) or a total number of pages (for a book or other type of publication). List a sequence of citations in the general text chronologically, for example, "(Smith, 1932; Green, 1998; Smith and Jones, 2015)."

**Acknowledgments** should be no more than 6 lines of text. Only those who have contributed in an outstanding way should be acknowledged by name. For recognition of other persons or groups, use a general term, such as *crew*, *observers*, or *research coordinators*, and do not include names with these terms.

**Digital object identifier (doi) code** ensures that a publication has a permanent location online. A doi link (which may include a doi code) should be included at the end of citations of published literature. Authors are responsible for submitting accurate doi links. Faulty links will be deleted at the page-proof stage.

**Footnotes** are used for all documents that have not been formally peer reviewed and for observations and personal communications, but these types of references should be cited sparingly in manuscripts submitted to the journal.

All reference documents, administrative reports, internal reports, progress reports, project reports, contract reports, personal observations, personal communications, unpublished data, manuscripts in review, and council meeting notes are footnoted in 10-point font and placed at the bottom of the page on which they are first cited. Footnote format is the same as that for formal literature citations. A link to the online source (e.g., [Available from http://www..., accessed July 2017.]), or the mailing address of the agency or department holding the document, should be provided so that readers may obtain a copy of the document.

**Tables** are often overused in scientific papers; it is seldom necessary to present all the data associated with a study. Tables should not be excessive in size and must be cited in numerical order in the text. Headings should be short but ample enough to allow the table to be intelligible on its own.

All abbreviations and unusual symbols must be explained in the table legend. Other incidental comments may be footnoted with numeral footnote markers. Use asterisks only to indicate significance in statistical data. Do not put a table legend on a page separate from the table; place the legend above the table. *Do not submit tables in photo mode.*

- Note probability with a capital, italic *P*.
- Provide a zero before all decimal points for values less than one (e.g., 0.07).
- Round all values to 2 decimal points.
- Use a comma in numbers of 5 digits or more (e.g., 13,000 but 3000).

**Figures** must be cited in numerical order in the text. Graphics should aid in the comprehension of the text, but they should be limited to presenting patterns rather than raw data. The number of figures should not exceed 1 figure for every 4 pages of text.

Figure legends should explain all symbols and abbreviations seen in the figure and should be double spaced on a separate page at the end of the manuscript.

Line art and halftone figures should be saved at resolutions >600 dots per inch (dpi) and >300 dpi, respectively. Color is allowed in figures to show morphological differences among species (for species identification), to show stain reactions, to show gradations (such as those of temperature and salinity within maps), and to distinguish between numerous lines and symbols in graphs. Figures approved for color should be saved in CMYK format.

All figures must be submitted as PDF, TIFF, or EPS files.

- Capitalize only the first letter of the first word and proper nouns in all labels within figures.
- Do not use overly large font sizes for labels in maps and for axis labels in graphs.
- Use the same point size for all labels, except for panel labels (e.g., **A**), which should be slightly larger than other labels (e.g., 11 point versus 8 point).
- Use a sans serif font for all labels. Panel labels (e.g., **A**), however, should be in Times New Roman font.
- Do not use bold fonts or bold lines in figures. Do not use italic fonts. Exceptions include use of italic fonts for labels of bodies of water in maps and a bold font for panel labels (e.g., **A**).
- Do not place outline rules around graphs.
- Do not include vertical and horizontal lines in the background of graphs. Ticks for values on the x-axis and y-axis will suffice.
- Place a north arrow and label degrees latitude and longitude (e.g., 170°E) in all maps. If scale of map requires more than degrees, use degrees minutes, not decimal degrees.
- Place panel labels (e.g., **A**, **B**, **C**) within the upper-left area of each graph or photo in a multi-panel figure, from left to right, then top to bottom. If the letter is not visible against a dark background, put a white box behind it. Do not use white labels.
- Avoid placing labels vertically or diagonally. Y-axis labels can be vertical. Words in horizontal labels can be stacked vertically to fit.
- Use symbols, shading, or patterns (not clip art) in maps and graphs.
- For scale bars in maps, use kilometers. Use the label *km* or *kilometers* (lowercased).

**Supplementary materials** that are considered essential, but are too large or impractical for inclusion in a paper (e.g., metadata, figures, tables, videos, and websites), may be provided at the end of an article. These materials are subject to the editorial standards of the journal. A URL to the supplementary material and a brief explanation for including such material should be sent at the time of initial submission of the paper to the journal.

- **Metadata, figures, and tables** should be submitted in standard digital format (MS Word or PDF file) and should be cited in the general text, for example, as ". . . was determined (Suppl. Table 3, Suppl. Fig. 1)."
- **Websites** should be cited with a URL in the general text.
- **Videos** must not be larger than 30 MB to allow a swift technical response for viewing the video. Authors should consider whether a short video uniquely captures what text alone cannot capture for the understanding of a process or behavior under examination in the article. Supply an online link to the location of the video.

**Copyright law** does not apply to *Fishery Bulletin*, which falls within the public domain. However, if an author reproduces any part of an article from *Fishery Bulletin*, reference to source is considered correct form (e.g., Source: Fish. Bull. 117:105).

**Failure to follow these guidelines and failure to correspond with editors in a timely manner will delay publication of a manuscript.**

## Submission of manuscript

Submit a manuscript online at the ScholarOne Manuscripts website for *Fishery Bulletin*. Commerce Department authors must provide proof of internal clearance of their manuscripts with either a completed and signed NOAA Form 25-700 or a copy of the clearance email from the Research Publication Tracking System. For further details on electronic submission, please contact the associate editor, Cara Mayo, at

cara.mayo@noaa.gov.

When requested, the text and tables should be submitted in MS Word format. Each figure should be sent as a separate PDF, TIFF, or EPS file. Send a copy of a figure in the original software if conversion to any of these formats yields a degraded version of the figure.

**Questions?** If you have questions regarding these guidelines, please contact the managing editor, Kathryn Dennis, at

kathryn.dennis@noaa.gov.

Questions regarding manuscripts under review should be addressed to Associate Editor Cara Mayo.

# *Fishery Bulletin*

## Subscription form

Superintendent of Documents **Publications** Order Form

*5178

☐ YES, please send me the following publications:

____ Subscriptions to *Fishery Bulletin*
for $32.00 per year ($44.80 foreign)

The total cost of my order is $ _____ . Prices include regular domestic postage and handling and are subject to change.

_____
(Company or Personal Name) (Please type or print)

_____
(Additional address/attention line)

_____
(Street address)

_____
(City, State, ZIP Code)

_____
(Daytime phone including area code)

_____
(Purchase Order No.)

**Charge your order. IT'S EASY!**

**Please Choose Method of Payment:**

☐ Check payable to the Superintendent of Documents
☐ GPO Deposit Account ☐☐☐☐☐☐☐–☐
☐ VISA or MasterCard Account
☐☐☐☐☐☐☐☐☐☐☐☐☐☐☐☐
☐☐☐☐ (Credit card expiration date)

**To fax your orders (202) 512-2104**

_____
(Authorizing Signature)

Mail to: Superintendent of Documents
P.O. Box 979050, St. Louis, Missouri 63197
Tel. no. (U.S. callers): 866-512-1800
Tel. no. (International callers): 1-202-512-1800

***Thank you for your order!***

Also available online at
https://bookstore.gpo.gov/products/fishery-bulletin
email: ContactCenter@gpo.gov